Processing of titanium-based composite materials with nanosized TiC and TiB reinforcements using different powder metallurgy processes: hydrogenation/dehydrogenation sintering, and severe plastic deformation (Equal Channel Angular Pressing: ECAP)

Matthieu Bardet

université de BORDEAUX

THÈSE EN COTUTELLE PRÉSENTÉE

POUR OBTENIR LE GRADE DE

DOCTEUR DE

L'UNIVERSITÉ DE BORDEAUX

ET DE L'UNIVERSITÉ DE MELBOURNE

ÉCOLE DOCTORALE DES SCIENCES CHIMIQUES (Université de Bordeaux)

ÉCOLE DOCTORALE DE GÉNIE MÉCANIQUE (Université de Melbourne)

SPÉCIALITÉ : PHYSICO-CHIMIE DE LA MATIÈRE CONDENSÉE

Par Matthieu BARDET

Elaboration de matériaux composites à matrice de Titane et à nano-renforts TiC et TiB par différents procédés de métallurgie des poudres : frittage par hydruration/dehydruration et densification par déformation plastique sévère (Equal Channel Angular Pressing : ECAP)

Sous la direction de M. Jean-François SILVAIN, M. Jean-Marc HEINTZ et M. Kenong XIA

Soutenue le 18 Mars 2014

Membres du jury :

M. MAGLIONE Mario	Directeur de Recherche, CNRS, ICMCB, Bordeaux	Président
M. DIRRAS Guy	Professeur, LSPM, Paris XII	Rapporteur
M. DOUIN Joël	Directeur de Recherche, CNRS, CEMES, Toulouse	Rapporteur
M. SILVAIN Jean-François	Directeur de Recherche, CNRS, ICMCB, Bordeaux	Examinateur
M. XIA Kenong	Professeur, Université de Melbourne	Examinateur
M. XU Wei	Chargé de Recherches, Université de Melbourne	Examinateur
M. BOBET Jean-Louis	Professeur, ICMCB, Université de Bordeaux	Invité
M. HEINTZ Jean-Marc	Professeur, ICMCB, ENSCBP	Invité

université de BORDEAUX

THESIS PRESENTED

FOR THE DEGREE OF

DOCTOR OF PHILOSOPHY

THE UNIVERSITY OF BORDEAUX

AND THE UNIVERSITY OF MELBOURNE

DOCTORAL SCHOOL OF CHEMICAL SCIENCES (University of Bordeaux)

DEPARTMENT OF MECHANICAL ENGINEERING (University of Melbourne)

SPECIALTY: PHYSIC AND CHEMISTRY OF CONDENSED MATTER

By Matthieu BARDET

Processing of Titanium-based composite materials with nanosized TiC and TiB reinforcements using different powder metallurgy processes: Hydrogenation/Dehydrogenation sintering, and Severe Plastic Deformation (Equal Channel Angular Pressing (ECAP))

Advisors: Mr. Jean-François SILVAIN, Mr. Jean-Marc HEINTZ and Mr. Kenong XIA

Defence on the 18th of March, 2014

Chair of examiners:

M. MAGLIONE Mario	Research Director, CNRS, ICMCB, Bordeaux	President
M. DIRRAS Guy	Professor, LSPM, Paris XII	Reviewer
M. DOUIN Joël	Research Director, CNRS, CEMES, Toulouse	Reviewer
M. SILVAIN Jean-François	Research Director, CNRS, ICMCB, Bordeaux	Jury
M. XIA Kenong	Professor, University of Melbourne	Jury
M. XU Wei	Senior Research Fellow, University of Melbourne	Jury
M. BOBET Jean-Louis	Professor, ICMCB, University of Bordeaux	Guest
M. HEINTZ Jean-Marc	Professor, ICMCB, ENSCBP	Guest

Abstract

Titanium and its different alloys are widely used due to their intrinsic properties. These properties made those materials very attractive for advanced applications. The demand for increased performance in titanium and titanium alloy materials continued to drive development of another concept of material, the Titanium Matrix Composites (TMC).

The present work will focus on the fabrication of TMC with nanosized reinforcements, in order to enhance the mechanical properties such as the strength, while keeping the ductility of the single phase titanium. Two different types of reinforcement will be used, the particulate TiC and the whisker-shaped TiB. T

o achieve the fabrication of these composites, different and non-conventional powder metallurgy processes will be used. The first is the Equal Channel Angular Pressing (ECAP), a severe plastic deformation process that has the advantage to densify powder material at relatively low temperature, in a really short time (few minutes).

The other powder metallurgy process used is use the hydrogenation/dehydrogenation process. This process is based on the possibility of Ti to by hydrogenated and dehydrogenated, and uses the dehydrogenation as leverage on the densification.

By adding these reinforcements, the objective is to increase the mechanical properties of commercially pure titanium (yield strength, Young's modulus) without affecting its ductility.

Declaration

This is to certify that

(i) The thesis comprises only my original work towards the PhD except where indicated in the Preface,

(ii) Due acknowledgement has been made in the text to all other material used,

(iii) The thesis is less than 100,000 words in length, exclusive of tables, maps, bibliographies and appendices.

Matthieu Bardet

Acknowledgements

I would first like to thank the financial support offer by the “Région Aquitaine” and the University of Melbourne, without which this research study and the travel between France and Australia would not have been possible.

I would also like to deeply thank Dr. Mario Maglione, Director of the ICMCB, to have welcomed me in the laboratory, and accepted to be the president of my PhD jury. I’m also very thankful to Pr. Guy Dirras and Dr. Joël Douin, to have accepted to be the reviewers of my PhD manuscript and member of the chair of examiners.

At the University of Melbourne, I would like to thank my advisor, Pr. Kenong Xia for welcoming me in his laboratory, and for his support and his advices. I would like to thank Dr. Wei Xu, for his advices, and for being a member of the chair of examiners. I am also very thankful to everyone with whom I have work during my time in Australia, Xiaolin, Xianshun, and to the one than became more than co-worker, my friends Morgan, Edward, Shouqie, Cameron and obviously my British pal Dr. Daniel.

My time at the ICMCB has been a very pleasant moment thanks to all the personnel whose are always available, always nice, and always kind to everyone. I would like to thank all of them, and in particular Stéphane, Eric, Alain Largeteau and Sandrine for their help they and their kindness.

Of course, all of this has been possible thanks to my advisors in France, to whom I would like to deeply thank for caring me, advise me and all the good times spent on and off work, Jean-François Silvain, Jean-Marc Heintz and Jean-Louis Bobet. Thank you very much, this thesis would not have been possible without you.

Obviously, a PhD student work in a laboratory is more or less his life, and to succeed in life you have to have good colleagues and moreover good friends. Therefore, I would like to thank all the persons that bear with me in my successive desks and that became good friends of mine, Guillaume, Marion, Thomas, Greghauss and Cécile who were there before me. And all the other one I’ve seen arrived and who became my friends too, Guy-Marie, Marianne, Rudy, Olaia, Pierrick Solange, Johan, Baptiste, Julia and the list in non-exhaustive.

I would also like all the other person I have met at the ICMCB, with whom I haven’t work, but somehow we managed to become good friends, Cédric, Annelise, Lionel, Kévin, Pierre, Delphin and the ones I have known for a long time, Guillaume G., Cinta, Quentin, Lucie and Isabelle.

I would also thank the friend whom I have known long before the thesis and who support me during those years, Paul, whom I would like to thank for his help on the drawing of different figures of this document, Alexis, Margaux, Baptiste and Etienne.

And obviously, nothing of this would have been possible without the support and the love of my family, which I would like to thank deeply.

To my parents and my brothers.

Résumé des travaux de thèse :

Le contexte de ces travaux de recherche se place dans la problématique d'obtenir des matériaux avec de bonnes propriétés, notamment mécaniques, sans accroitre (voire diminuer) le coût de production. Ces travaux ont ciblé les matériaux à base Titane. En effet, le titane et ses alliages sont largement utilisés dans des secteurs de pointe tel que l'aéronautique, l'aérospatiale, ou encore les milieux biomédicaux du fait de leurs remarquables propriétés telles qu'un très bonne contrainte à rupture (et ce à relativement haute température), un faible masse volumique (matériau considéré léger), et une résistance à la corrosion et aux attaques chimiques. Deux grands axes de recherche commun à cette problématique de baisse de coût et d'amélioration des propriétés sont l'élaboration de matériaux composites, afin d'augmenter les propriétés et ainsi de réduire le volume de matière utilisé, et les procédés de fabrication par métallurgie des poudres, afin de réduire le nombre d'étape d'usinage pour la production d'une pièce et par conséquent réduire les coûts. Ce sont donc les deux grands axes qui ont été suivis durant ces travaux de thèse.

La production du Titane et de ses alliages peut être différenciée en 2 voies, solide, ou liquide. Dans le cadre de ses travaux, on s'est intéressé à la voie solide dite de métallurgie des poudres, qui pourrait permettre de réduire les coûts de production, notamment grâce à la possibilité de mettre en forme les pièces produites avant densification, ce qui va considérablement diminuer les pertes de matière incombées à l'usinage, souvent observées lors de production de lingot (par voie liquide).

La demande d'amélioration des performances dans les matériaux à base titane on conduit à développer le concept de matériaux composites à matrice Titane (TMC). Les TMCs représentent les matériaux composites où une matrice de Titane (ou ses alliages) est renforcée par une seconde phase dans le but d'améliorer les propriétés intrinsèques au titane. Deux grands types de matériaux composites existent, où les renforts sont soit continus, soit discontinus. Le premier type, continu, présente des propriétés fortement isotropes, et peut être obtenu par métallurgie classique (forgeage) ou par métallurgie des poudres. De part cette forte anisotropie, seul des applications spécifiques vont être privilégiées. Les matériaux composites discontinus, eux, sont fortement étudiés de par leurs propriétés fortement anisotropes au potentiel d'application prometteur. La plupart des renforts discontinus étudiés sont typiquement de taille micrométrique, et peuvent être sous forme de particules, d'aiguilles ou de courtes fibres, chaque forme ayant ses intérêts et limitations. Cependant, la plupart des TMCs renforcés de manière discontinue souffre des mêmes limitations d'un point de vue mécanique, l'augmentation des propriétés mécaniques telles que la limite d'élasticité se fait au détriment de la ductilité.

Récemment, des recherches ont montré que l'utilisation de renforts nanométriques en lieu et place des renforts micrométriques ont permis la combinaison de propriétés considérées exclusive l'une par rapport à l'autre, comme la ductilité et la limite d'élasticité. L'utilisation de renforts nanométriques permet d'obtenir les mêmes propriétés mécaniques qu'avec des renforts micrométriques tout en conservant la ductilité du matériau.

Ce travail de thèse a porté sur la fabrication de matériaux composites à matrice de Titane et à renforts nanométriques de borure de Titane (TiB, nano-aiguilles, renfort formé in-situ) et de carbure de Titane (TiC, particules, renfort ex-situ) par deux procédés de métallurgie des poudres non conventionnels. Le premier procédé est le frittage par hydruration/déshydruration du Titane. Les travaux portant sur cette méthode ont tous été effectués à l'ICMCB à Bordeaux. La deuxième

méthode utilisée a été la densification par déformation plastique sévère, via un procédé appelé ECAP (Equal Channel Angular Pressing).

L'obtention de ces matériaux composites utilisant ces différents procédés de métallurgie des poudres a donc pour objectif d'améliorer les propriétés mécaniques du titane pur (limite d'élasticité, module d'Young) sans affecter la ductilité. Une attention particulière a été portée sur différents paramètres qui vont avoir un impact sur les propriétés considérées :

La distribution des renforts

L'interface renfort/matrice

La taille des grains et la microstructure de la matrice

La densité et la pureté des matériaux produits

Ce manuscrit de thèse se divise en trois chapitres. Le premier chapitre explique de manière plus approfondit le contexte à travers une étude de la bibliographie, et introduit les différents matériaux étudiés ainsi que les procédés utilisés, plus en détail. Le second chapitre introduit une étude théorique des matériaux à travers la modélisation des propriétés. Le troisième chapitre concerne les propriétés des matériaux produits et l'influence des différents procédés sur eux.

Le chapitre un, après avoir présenté plus en détail ce qu'était un matériau composite, un matériau composite à de titane et les différents procédés de métallurgie des poudres existants, présente les procédés utilisés dans ce travail de thèse, le frittage par hydruration/déshydruration du Titane, et la densification par déformation plastique sévère via l'ECAP.

Le principe du frittage par hydruration/déshydruration repose sur la possibilité qu'a le Titane de former un hydrure stable, $TiH_{1,92}$ communément appelé TiH_2 et de relâcher l'hydrogène, et d'utiliser ce phénomène comme d'un levier sur les procédés de frittage, comme indiqué sur l'image suivante.

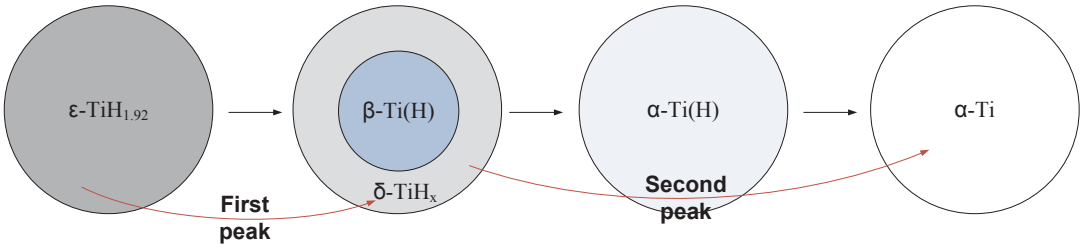

Le TiH_2 étant un matériau fragile, il est possible de contrôler sa taille de particule en utilisant la méthode du broyage planétaire. La taille de particule utilisée est un paramètre important puisque plus cette taille sera petite, plus la température de déshydruratution sera basse. Et plus cette température de déshydruration sera basse, plus les phénomènes de frittage mis en jeu après déhydruration seront efficaces. Dans ces travaux de thèse, la granulométrie de la poudre de TiH_2 utilisée a été de 180 nm – 500 nm. Pour fabriquer les composites, la technique du broyage planétaire est utilisée à plus faible vitesse afin de mélanger efficacement les particules de renforts avec les particules de matrice. Différents composites ont été obtenus utilisant cette technique, in-situ Ti/TiB (1,3 et 10% volumique) et ex-situ Ti/TiC (1,3 et 10 % volumique).

L'autre méthode employée, la densification par déformation plastique sévère, repose sur un phénomène de densification mécanique et non plus chimique. La poudre de départ ne sera donc plus le TiH_2 mais le Ti. Le principe est d'utiliser la déformation d'une poudre métallique afin de briser la couche de passivation et de forcer une densification à une température relativement basse et dans un temps donné relativement court. Dans le cas de l'ECAP, la déformation est induite par un

fort cisaillement. La poudre métallique pré-compactée est insérée dans un canal formant un angle de 90° avec un canal de même diamètre. L'échantillon va être forcé au travers de cet angle, provoquant ainsi un fort cisaillement en son sein. Ce cisaillement provoque la rupture de la couche de passivation des particules de poudre et avant que cette couche n'ait le temps de se reformer, la pression appliquée induit la densification de l'échantillon. De plus, l'équipement d'ECAP utilisé dans ces travaux présente l'avantage d'avoir un contre-piston effectuant une pression constante sur l'échantillon, facilitant le procédé de densification. Le schéma suivant représente la méthode d'ECAP.

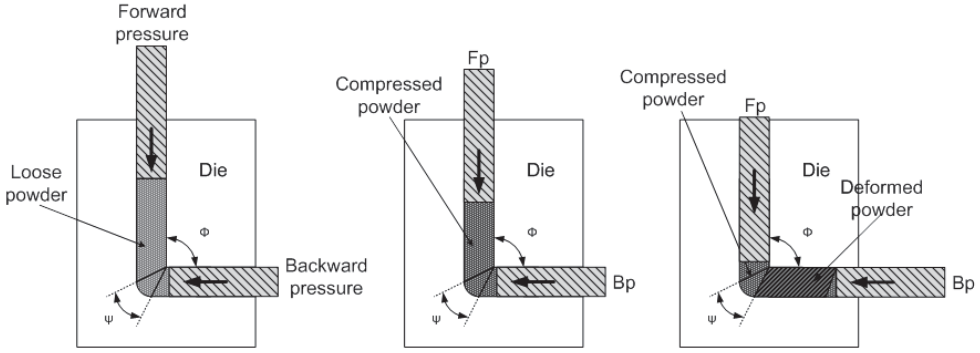

Du fait de la faible température de densification (600°C) seul les composite ex-situ Ti/TiC ont été préparés (1,3 et 10% volumique). Le mélange renfort/matrice a été effectué par broyage planétaire à haute énergie.

Ces deux méthodes très distinctes ont donc été utilisées pour obtenir les matériaux composites envisagés.

Le deuxième chapitre présente une étude théorique des propriétés des matériaux envisagés afin de justifier la pertinence de produire de tels matériaux. Les modèles utilisés pour calculer la limite d'élasticité ou le module d'Young ont été présentés dans le précédent chapitre. Différentes hypothèses sont émises pour que ces modèles soient valables :

- Absence de pores (densité totale)
- Distribution uniforme des renforts dans la matrice
- Interface propre et sans réaction entre les renforts et la matrice
- Interaction forte renfort/matrice

En respectant ces hypothèses, différents effets de différents paramètres sur les propriétés ont pu être analysés et des propriétés théoriques des matériaux envisagés ont pu être calculées, présentées dans le tableau suivant.

		Limite d'élasticité (MPa)		**Module d'Young (GPa)**
		HDH	***ECAP***	
Ti		545	610	105
Ti/TiC	*1%vol.*	632	701	106.7
	3%vol.	699	768	110
	10%vol.	864	936	122.4
Ti/TiB	*1%vol.*	590	N.A	107.7

	3%vol.	662		113.1
	10%vol.	887		132.5

Ce second chapitre a permis de justifier de la pertinence de fabriquer de tels matériaux composites, montrant une augmentation significative des propriétés théoriques envisagées, la limite d'élasticité ou le module d'Young. En effet, qu'il s'agisse de composite in-situ ou ex-situ, à renfort particulaire ou en forme d'aiguille, l'augmentation à faible pourcentage volumique, dans les limites des hypothèses du modèle, sont significatives.

Le troisième chapitre présente les caractérisations des matériaux élaborés par les méthodes présentés dans les chapitres précédents. Les méthodes de caractérisations utilisées sont présentées : Microscopie électronique à balayage (MEB, microscopie électronique en transmission (TEM), Diffraction des rayons X (DRX) ainsi que la diffraction d'électrons rétrodiffusés (EBSD). Il est ainsi possible de relier les différents paramètres des méthodes utilisées avec les propriétés mesurées sur les matériaux produits.

Lors de l'étude des matériaux produits par HDH, les principales conclusions des caractérisations effectuées (DRX, MEB, TEM ou encore EBSD) ont permis de déduire différents effets :

- L'étude par ESBD montre que lors de la densification par frittage HDH (libre ou contraint), il n'y a aucune texturation de la matrice dans le matériau final.
- L'étude MEB et TEM permettre de conclure à une distribution uniforme des renforts dans le composite final.
- L'étude DRX confirme la formation d'aiguille de TiB et la conservation des particules de TiC lors des procédés de densifications.
- Aucune caractérisation mécanique n'a été effectuée du fait de la taille des matériaux produits et de leur fragilité.

Les matériaux obtenus par ECAP ont été caractérisés par les mêmes méthodes, présentant des résultats différents, dû aux principes mis en jeu pour la densification (déformation plastique sévère) :

- Les caractérisations par EBSD ont en effet permis de montrer que, lors de la densification des matériaux par ECAP, une forte texturation est observée. Le cisaillement effectué, ajouté à la compression appliquée par le contre piston vont texturer le matériau final, où la maille de titane hexagonal (matrice) va se retrouver perpendiculaire à l'axe de compression du contre piston, comme indiqué sur le schéma suivant.

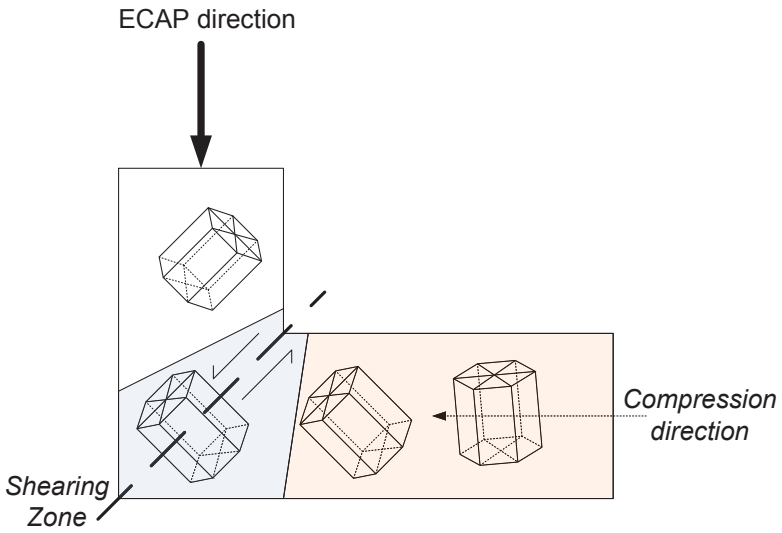

- Les analyses TEM et MEB permettent de conclure quant à la présence de pollution présente dans l'échantillon, probablement dû au procédé de dispersion des renforts (broyage planétaire à haute énergie)
- Ces mêmes analyses permettent cependant de rendre compte du potentiel de dispersion des renforts de façon uniforme dans la matrice que présente cette méthode.
- Une caractérisation mécanique (test par compression) ont permis de montrer que la limite d'élasticité augmenter de manière significative dans le cas du composite (comparé au matériau de Titane pur) mais que cette augmentation se faisait au détriment de la ductilité, comme présenté dans la figure ci-après. Ce phénomène doit encore être expliqué et serait dû à la pollution, la présence de nombreux défauts induits lors de l'ECAP ou encore la diffusion d'oxygène dans le matériau.

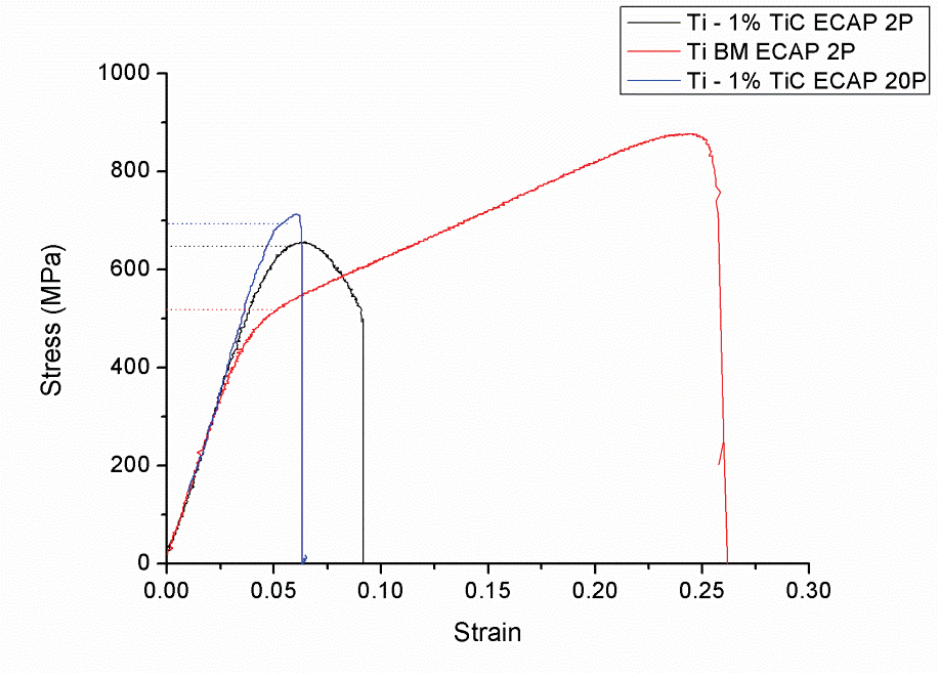

Ces travaux de thèse ont permis de montrer, par l'étude d'un modèle, la pertinence de fabriquer de tels matériaux composite à matrice de Titane (Ti-TiC et Ti-TiB). Des méthodes de métallurgie des

poudres non conventionnelles ont été présentées et ont permis d'obtenir les matériaux envisagés. Les caractérisations effectués sur les matériaux finaux obtenus a permis de montrer l'impact de chaque technique sur les matériaux, et de comprendre les propriétés des matériaux mesurés.

Table of Contents

Introduction

Titanium and its different alloys are widely used due to their intrinsic properties. These properties made those materials very attractive for advanced applications such as aircraft (high strength in combination with low density), aero-engines (high strength, low density, and good creep resistance up to about 550°C), biomedical devices (corrosion resistance and high strength), and components in chemical processing equipment.

The production of titanium and titanium alloys can be differentiate into two distinct ways, liquid and solid. The production starts from titanium ingots that are produced by melting and re-melting of Ti sponge (with the possible addition of alloying elements). These ingots are then transformed into the desired products, using either liquid way (casting, welding) or solid ways (forging, forming, rolling, extrusion). The different ways have their own specificities on the final properties. However, not only the properties, but the cost of titanium is as a concern that has to be taken into consideration for the production. Indeed, the production of titanium materials remains expensive compares to other competing materials. Also, to produce a final component, the products must be machined, often with a high amount of loss. That increases the price not only because of the cost of machining, but also because the weight of the final product can be nearly 30 times smaller than before machining, which represents a lot of loss in scratches. The possibility to produce a component closer to the final configuration will be a big advantage in a cost-reduction perspective. Therefore, the numerous near-net-shape methods that have been developed through the years to produce titanium and titanium alloys using powder metallurgy processes are becoming really attractive. Titanium material from powder metallurgy processes remains relatively more expensive compares to other powder metallurgy materials, but the cost competes effectively with conventional methods of producing titanium materials.

The demand for increased performance in titanium and titanium alloy materials continued to drive development of another concept of material, the Titanium Matrix Composites (TMC). The TMCs designated the composite materials where the titanium (or titanium alloy) matrix is reinforced by a second phase in order to improve its intrinsic properties. The properties of the composite materials are increased compares to the unreinforced matrix material, titanium or titanium alloy. Two main types of TMC exist, the continuously reinforced and the discontinuously reinforced. The first can be obtained using either powder metallurgy or forging techniques. It has reached the industrial status but has only specific application due to its severe anisotropy of its properties (for example strengthening of wires). The discontinuously reinforced TMC are widely investigated because of their promising isotropic properties. Most of the investigated TMC uses micrometric sized reinforcement, which can be particles, short fibres or whiskers, each reinforcement having their own advantages and inconveniences. Even if casting can be used to produce such materials, most of the processes used to fabricate those TMCs are powder metallurgy processes. However, TMCs suffers from limitation in their properties, especially in their mechanical properties, where increasing the strength eventually reduces the ductility.

Recently, researches have shown using nanoscaled reinforcements allow the combination of properties that were mutually exclusive like ductility and high strength. The use of nanosized reinforcements helps to reach the same properties of the microsized reinforced TMC, at an even lower fraction, without affecting properties like ductility.

The present work will focus on the fabrication of TMC with nanosized reinforcements, in order to enhance the mechanical properties such as the strength, while keeping the ductility of the single phase titanium. Two different types of reinforcement will be used, the particulate TiC and the whisker-shaped TiB. To achieve the fabrication of these composites, different and non-conventional

powder metallurgy processes will be used.

The first is the Equal Channel Angular Pressing (ECAP), a severe plastic deformation process that has the advantage to densify powder material at relatively low temperature, in a really short time (few minutes). Segal established this technique in the 70's, as a process that allows intense plastic strain to be introduced into a metal billet by simple shear. Since then, several works have proven its efficiency to obtain dense titanium materials, or dense composite materials, with good mechanical properties due to the effect of the process on the microstructure.

The other powder metallurgy process used is use the hydrogenation/dehydrogenation process. This process is based on the possibility of Ti to by hydrogenated and dehydrogenated, and uses the dehydrogenation as leverage on the densification. Indeed, this process will use titanium hydride (TiH_2) instead of titanium as starting powder. In this work, the HDH will be used in different condition, pressureless sintering and hot pressing. Pressureless sintering will allow the net shape production of material, whereas hot pressing will allow working at lower temperature (about half the one used in pressureless sintering)

The reinforcement used in this work, TiC (particle) and TiB (whiskers) have been chosen for their potential good improvement on mechanical properties of the titanium and their good compatibility with the matrix. Also, the difference between the two reinforcements, beside their shape, is the fact that TiC is an ex-situ reinforcement, which means TiC is introduce into the matrix, whereas TiB is an in-situ reinforcement, growing from TiB_2 powder into whiskers.

By adding these reinforcements, the objective is to increase the mechanical properties of commercially pure titanium (yield strength, Young's modulus) without affecting its ductility.

Considering these parameters, reinforcement and processes, the focus will be on different aspects that will be responsible of the properties of the produced TMC:

- The distribution of the reinforcement within the matrix
- The interface between reinforcements and matrix
- The grains size and microstructure of the matrix and the reinforcement.
- The density and the purity of the produced materials.

The different processes used will have different effects on these aspects. It will be important to understand and control them, because these aspects are directly related to the mechanical properties of the produced material such as Young's modulus, yield strength and ductility.

This PhD thesis has been realised in cooperation between the University of Bordeaux, France, and the University of Melbourne, Australia with an equal time repartition between each university of this three year thesis. The research has been conducted with the knowledge and the facilities of each laboratory. All the ECAP related work have been conducted in the material laboratory of *Mechanical Engineering School* of the University of Melbourne, whereas the work on hydrogenated titanium has been conducted at the *Institut de Chimie de la Matière Condensée de Bordeaux* (ICMCB-CNRS), at the University of Bordeaux.

This work will be presented in 3 chapters. The first chapter will introduce the materials used in this work, along with a background. It will then present the different influence the composite can have on properties. And finally the different processes available for the production of TMCs.

The second chapter will describe the initial materials and processes used during the fabrication of the investigated composites, along with the selected parameters used during those elaborations. But in order to understand the implication of the parameters on the materials, a modelling work is first

presented, showing the influence on different characteristics of the composite properties.

The third chapter will described the effect of the different processes on the produced composites. A characterisation and critical analysis of the composite microstructures, related to their properties, will be done.

Chapter I - Background research and literature review

I. Introduction

High strength, low density, and excellent corrosion resistance make titanium attractive for a variety of applications. Nonetheless, improving its properties has been and still is a main field of study. Alloying, processing and fabrication of composite materials are the three main methods to improve final properties.

To understand the properties of a newly designed titanium materials, it is important to fully understand the implication of methods used to fabricate the materials. Alloying has led to controlled structures, increased strength, improved physical properties, and corrosion resistance. Processing has led to altered microstructure in a desired way. The fabrication of a composites material has led to a combination of properties that are not intrinsic of titanium, such as the stiffness and high strength of a ceramic, with the inherent properties of titanium.

Understanding and fabrication of desired titanium based material will require fully understanding of the implication of the three methods on the material properties. In this chapter, a brief introduction of the materials used during this thesis work is done, in order to be aware of the different characteristic of such materials. Then, a presentation of the different tools that are available to anticipate and model the properties of the presented materials is given. With these tools, a modelling of the investigated materials properties will be done on the next chapter. And finally, the presentation of the different methods available, and the one used to obtain the investigated materials is done. This chapter will set a background of the context this work is set, and highlight the different points that will be studied and explained in this thesis.

II. Material

The materials studied are what it is called multiphase materials, which means they are a combination of different phases. To have a better view of what compose the studied materials, this paragraph will present generalities about multiphase materials, starting with the component of the main phase, the matrix, made of titanium, and then the possibility of different combinations in order to obtain the materials. Following that is presented the different tools used to determine the theoretical benefit of such materials, applied on mechanical properties.

II-1. Titanium and titanium alloys

Titanium can crystallize in various crystal structures that are stable within particular temperature range. Pure titanium crystallizes at low temperatures in a hexagonal closed pack structure (hcp), called α-titanium. At high temperature, the titanium crystallize in a body-centered cubic structure (bcc), called β-titanium. The complete transformation from one into another crystal structure is called allotropic. The β-transus temperature – temperature for which the pure titanium transforms from one phase into another – is 882±2°C. [LUT2003] The Figure 1 shows the atomic unit cells of the hcp α-titanium and the bcc β-titanium. The hatched plans shown on the figure are the most densely packed planes that are {1011}, {1010} and {0001} for the HCP phase and {110} for the BCC phase.

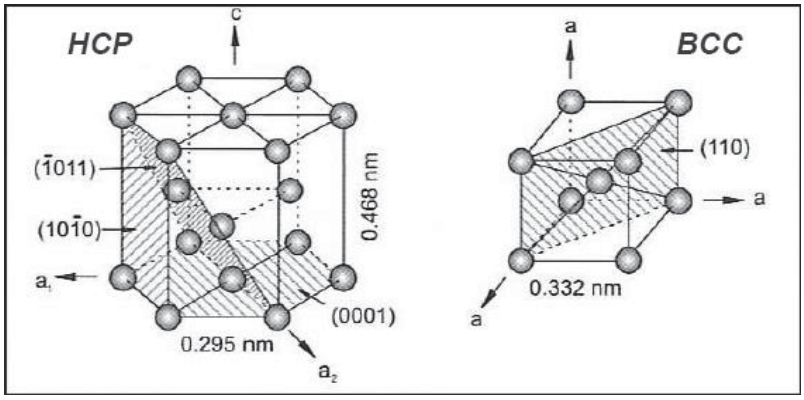

Figure 1: Crystal structure of α-titanium (left) and β-titanium (right) [LEY2003]

The values of lattice parameters display on the figure for the α-titanium are the ones at room temperature (a = 0.295 nm and c = 0.468 nm). The values for β-titanium are the ones at 900°C (a = 0.332 nm). The anisotropic character of the α-titanium has an influence on the mechanical properties of a single crystal, as shown on Figure 2. Nevertheless, a pronounced anisotropy of properties is usually not desired. That is why most of the materials properties reported in literature are usually polycrystalline textured-free. However, that anisotropy can be deliberately used to increase properties such as stiffness. Specific processing for the crystallisation or re-crystallisation of α-titanium can be used to texture the orientation of the crystals and enhances the anisotropy of the materials. [JIA2011] [NIX2010] [KNE2013]

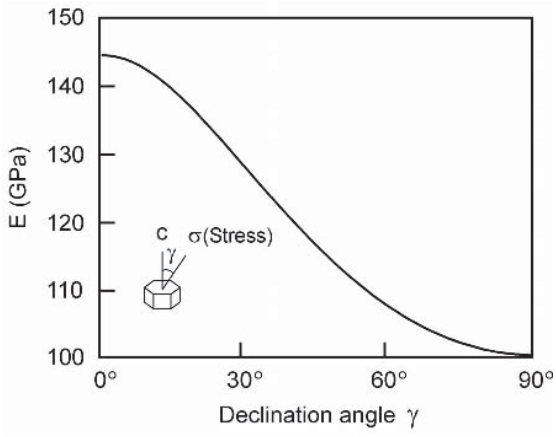

Figure 2: Modulus of elasticity E of α-titanium single crystals as function of declination angle γ [LUT2003]

The β/α phase transformation causes a slight atomic reorganisation due to the difference in their crystal structure. In some case, where the β-transus lead to a α+β zone, passing from BCC to HCP leads to a martensitic phase transformation. This transformation corresponds to a diffusionless transformation of the phase, only induce by movement of the atoms that results in a change of the crystal structure. This transformation leads to a fine needle-like microstructure. Indeed, during the cooling, within the β-grains, individual α lamellar packets nucleates and grow. The cooling rate has an effect on the final lamellar structure of the materials. When titanium is cooled at low rates from the β-phase, the α-phase nucleates preferentially at β-grain boundaries, and grows into the β-grains as parallel plates. A faster cooling rate, such as quenching, leads to a complete transformation of the β-phase to the α-phase in a metastable fine acicular martensitic microstructure (very fine needle-like microstructure).

However, these microstructures are mostly observed when some elements are added to the titanium, to influence the microstructure. These elements, called alloying elements, have an influence on the β-transus temperature. As shown on the Figure 3, these alloying elements are classified in different category, neutral, α-stabiliser, or β-stabilizer. The α-stabilizers allow the α-phase to exist at higher temperatures, while the β-stabilizers allow the β-phase to exist at lower temperatures, and consequently, to coexist with α at room temperature. The neutral elements have nearly no influence on the β/α phase boundary, and are used to increase the strength in the α-phase. This fact forms the basis for the creation of titanium alloys that can be strengthened by heat treatment.

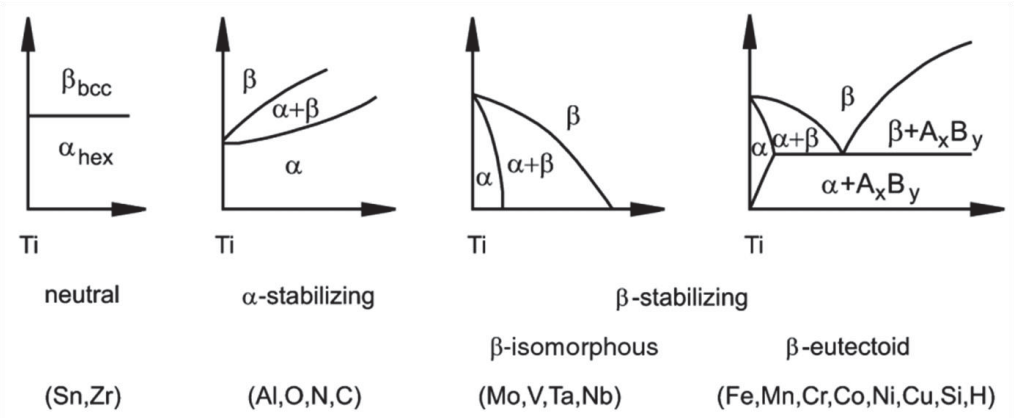

Figure 3: Influence of alloying elements on phase diagrams of Ti alloys [LEY2003]

Usually, titanium alloys are classified as α, α+β and β alloys, with subdivision in the β alloys, the near-α, and the metastable β. The comportment of the alloys regarding the added elements is schematically represented on the Figure 4. This figure represents a schematic 3 dimensional phase diagram composed of α-stabilising and β-stabilising elements phase diagram when added to Ti. The α alloys are the ones with α-stabilising or neutral elements, and it also includes commercially pure titanium. These elements are represented on the scheme by the Al percentage. When a low fraction of β-stabilising elements (represented by V) is added, the alloys are referred to as near α. The α+β alloys have a β-stabilising elements volume fraction ranging from 5 to 40%. Increasing the fraction of β-stabilising element leads to metastable β alloys, where the β phase no longer transforms to martensite, but they remain 2 phase alloys. When the amount of β-stabilising element is high enough, the alloys become single phase β alloys.

Properties of the titanium alloys are mainly determined by the arrangement and the volume fraction of each phase. Because the hcp phase is denser, and limited in deformation, α-alloys are less ductile compared with the β-alloys. But because the hcp is denser than the bcc, the diffusion rate in it is lower. This means the resistance oxidation increases in the α-alloys, when the ductility and deformability deteriorate. Compares with the β-phase, the α-phase is characterised by higher resistance to plastic deformation, anisotropic mechanical and physical properties, higher creep resistance, and a lower diffusion rate. The following table lists the essential differences between the three main alloy classes α, α+β and β on the basis of physical and mechanical properties [LEY2003]

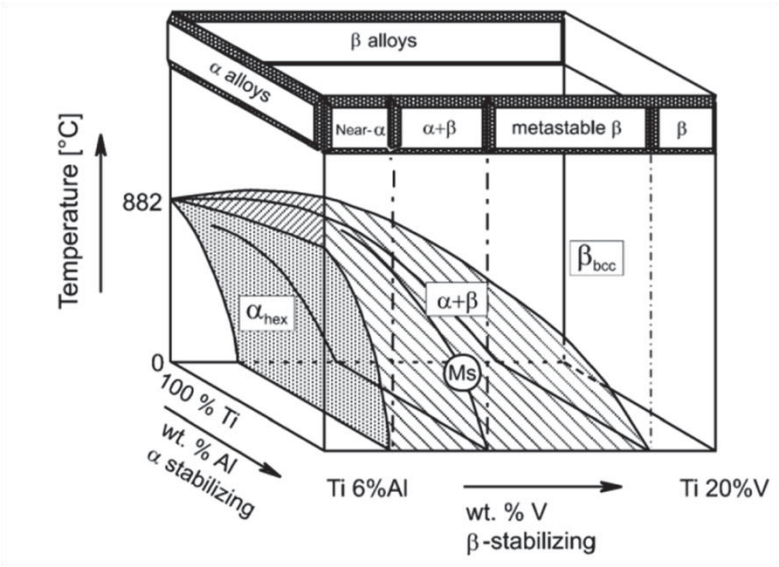

Figure 4: 3D phase diagram of Ti alloys classification [LEY2003]

	α	α + β	β
Density	+	+	-
Strength	-	+	++
Ductility	-/+	+	+/-
Fracture toughness	+	-/+	-
Corrosion behaviour	++	+	+/-
Oxidation behaviour	++	+/-	-

Table 1: Properties of α, α+β and β Ti alloys

- α alloys have an excellent corrosion behaviour, made them a preferable choice in chemistry and process engineering industry, when high strength is not the critical criteria.
- Near α alloys are the classical high temperature alloys. It combines the creep behaviour of α alloys and the high strength of α+β alloys.
- α+β alloys are widely used in industry due to excellent balanced properties, between corrosion behaviour, high strength and high ductility.
- Metastable β alloys are mainly used for their really high strength levels that can be reached.

More than 100 alloys are known today, but only 20 to 30 have reached the commercial status. Among them, considered to be in the α-alloys class, the most used and most commons are the commercially pure titanium alloys (cp-Ti), with different grades that indicate the quantity of interstitial alloying elements (mainly oxygen and irons). As well, in the α+β alloys, the Ti-6%Al-4%V, also named TA6V, covers more than 50% of the commercial usage of titanium. These two types of alloys are a good representation of the commercial titanium. The alloys that have reached a commercial status are usually produced through casting techniques, alloying elements being added during the liquid phase. The previous and following characteristics of the alloys discussed concerned the ones produced through this process, except if it is specified otherwise.

Alloying the titanium has for main purpose to increase the properties of it. The chemical composition of the titanium alloys determines the volume fraction of the phases α and β. However, the interstitial oxygen in the cp-Ti increases strength. From there, each grade refers to a different amount of oxygen, and to a different tensile strength level. This chemical composition determines most of the physical properties (density, elastic modulus, coefficient of thermal expansion) and has an influence on the corrosion and oxidation of the materials, but it is not the only factor that has an influence on the microstructure. Post-production processing of titanium and titanium alloys can be used to optimise the microstructure, regardless the way of production, liquid or solid, as long the material is dense.

The microstructure of alloys is described by the size and the arrangement of the different phase. The two extreme cases of phase arrangement are equiaxed microstructure and lamellar microstructure. The first is obtained through a recrystallization process, whereas the second is obtained upon cooling from the β phase. Obviously, each microstructure can be either coarse of fine arrangement. These different microstructures are generally generated by thermomechanical treatments. One major aspect to consider in these treatments is the β-transus temperature that separate the β phase from the α+ β phase. Lamellar microstructures are obtained by cooling the material from temperature above the β-transus temperature. Once the temperature is below the β-transus temperature, α nucleates at grain boundaries and then grow as lamellae into the former β grain (Figure 5). The cooling rate will have an influence on the thickness of the lamellar microstructure. A slow cooling rate from the β phase results in pure lamellar microstructure, with an increase in the lamellae thickness while reducing this rate. One the other hand, rapid quenching leads to a martensitic transformation of β, resulting in a very fine needle-like microstructure.

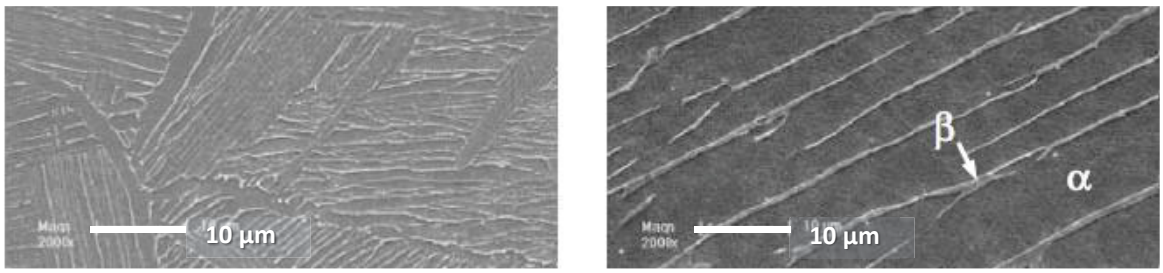

Figure 5: Lamellar α+β microstructure from the β-phase at a slow cooling rate. Air cooled on the left (slow) and furnace cooled on the right (very slow) [KIM2008]

Unlike lamellar microstructures, equiaxed microstructures are the result of recrystallization process, that is subsequent to the heat treatment at temperatures into the α+ β phase. The equiaxed microstructure is generated at temperature below the β-transus temperature, and extended heat treatment will increase the grain size. The coarsening of equiaxed microstructure is the result of the heat treatment solution carried out. Heat treatment at temperature just below the β-transus temperature results in bimodal microstructures that consist partly of equiaxed α in a lamellar α+ β matrix (Figure 6).

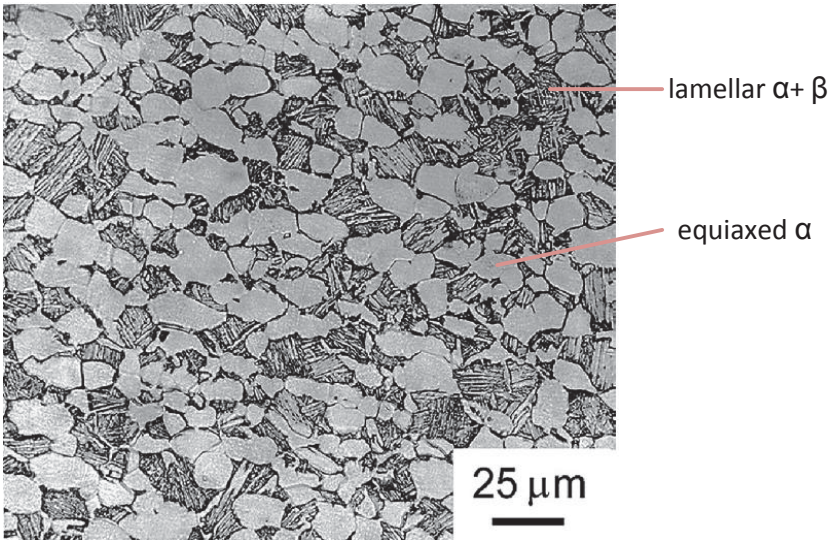

Figure 6: Bimodal microstructure of Ti-6Al-4V (SEM) [NAL2002]

The influence of the various microstructures on the mechanical behaviour of Ti alloys has been resumed in the Table 2 comparing the coarse and fine microstructures on one hand, and the lamellar and equiaxed on the other.

Fine	Coarse	Property	Lamellar	Equiaxed
o	o	Elastic Modulus	o	+/- (texture)
+	-	Strength	-	+
+	-	Ductility	-	+
-	+	Fracture toughness	+	-
+	-	Fatigue crack initiation	-	+
-	+	Fatigue crack propagation	+	-
-	+	Creep strength	+	-
+	-	Oxidation behaviour	+	-

Table 2: Influence of the microstructure of Ti alloys on different properties

The different microstructures have a strong influence on the mechanical behaviour of the alloys. Fine microstructures increase the strength and the ductility, and they also delay the crack nucleation. Coarse microstructures are nonetheless more resistant to creep and fatigue crack growth. Equiaxed microstructures tends to have better ductility as well as better fatigue strength, while lamellar microstructures show superior resistance creep and fatigue crack growth.

But alloying are not the only possibilities to obtain a titanium material with superior properties. Indeed, in the continuity of the metal matrix composites [MOR2010], the idea is to combine the inner properties of titanium and titanium alloys with the properties of a second phase dispersed within the Ti matrix, to obtain Titanium Matrix Composites (TMCs)

II-2. Titanium matrix composites (TMC)

The studied materials in this work are multiphase material, titanium matrix composites. In this part, generalities on what makes a metal matrix composite are presented. From there, the different kind of TMC that exists will be discussed, the continuously reinforced and the discontinuously reinforced

titanium matrix composite. Finally, the different specificities of reinforcements are presented, whether they are ex-situ added to the matrix, or in-situ obtained.

II-2.1 Metal Matrix Composites

Metal matrix composite (MMC) materials are composed of at least two chemically and physically distinct phases, the metallic matrix, and the reinforcements, that can be for example ceramic, glass, or metallic. The main goal of the MMCs is to provide properties not obtainable with the individual metallic phases. For most of composites, it is generally two phases. The reinforcement phases can be either continuous, in a form of fibres, or discontinuous, in a form of whiskers, short fibres or particles. This phase is distributed within the matrix. The metallic matrix can be either pure metal or alloy. The most common MMCs are classified in three different types, represented schematically on Figure 7:

(i) particle reinforced MMCs

(ii) short fiber or whisker reinforced MMCs

(iii) continuous fiber or sheet reinforced MMCs

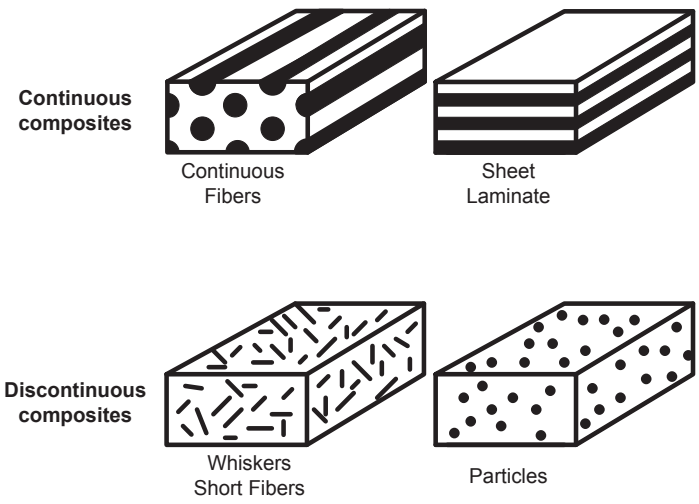

Figure 7: Types of metal matrix composites [CHA2006]

The continuous fibres composites are the most anisotropic kind of MMCs. On the contrary, the particulate composites will be the most isotropic in term of properties. The properties of the MMCs can be tailored and designed according to specific applications. For example, the continuous Al_2O_3-fibre reinforced Al matrix composites that are used in power transmission lines. In this case, the fibres are used to improve the mechanic properties of the lines, and therefore, are oriented along the direction of the lines. [MCC1994] [US Patent 6723451] Other examples are 1) Tungsten carbide (WC)/cobalt (Co) particulate composites used as cutting tool and oil drilling inserts 2) SiC particle reinforced Al matrix composites used in aerospace, automotive, and 3) thermal management applications like the Cu/Carbon discontinuous composites. [CHA2006] [SIL2012] [WEI2012]

In general, the discontinuous MMCs offer these advantages:

- Lower cost compares to the continuous MMCs.

The price of the particulate reinforced MMCs is quite lower. Cost is an important parameter in applications where large volumes are required.

- Conventional fabrication techniques.

Conventional metallurgical processing techniques as such as casting or powder metallurgy, followed by conventional secondary processing (rolling, forging, and extrusion) can be used.

- Higher use temperatures than the unreinforced metal.
- Enhanced mechanical properties.
- Increased thermal stability.
- Better wear resistance.
- Relatively isotropic properties compared to fibre reinforced composites.

The main parameters that will have influence on the mechanical properties of the composite will be obviously the nature of the matrix and the reinforcement, but also the distribution of the reinforcement, the interface between matrix and reinforcements, and the size of the reinforcement. A longer review on MMCs has been done with more detail the various microstructure types and processing techniques. [VIS2007] [SRI2006] [SOB1994]

One kind of MMCs relevant in this study are the one having titanium or titanium alloys as a matrix metal: the titanium matrix composites (TMCs). Same as any kind of MMC, continuous and discontinuous reinforcements can be found for the TMCs.

II-2.2 Continuously reinforced TMC

In the continuous reinforcements, individual monofilaments have been distinguished from the ones in form of tows. The tows are the ones with multiples fibres (carbon fibre-like) with an average diameter of 10-20 µm and the monofilaments such as SiC, with a diameter usually larger, in order of 100-150 µm [GAR2006]. If the tows-like reinforcements are less expensive than the monofilaments, they are more sensitive to chemical attack by the matrix. Therefore, the fibres are usually coated to be protected, because only few defects can decrease the composites mechanical properties. However, due to the difficulty to produce, their high cost and their high chemical reactivity with titanium, the two-based fibres are not really common in continuous TMCs. The most common fibres used are the SiC-based fibres (monofilaments). Reinforcing titanium alloys with continuous SiC fibres combines the high strength, stiffness and creep resistance of the ceramic SiC fibre with the damage tolerance of titanium alloys.

To avoid any compounds to be formed at the matrix-reinforcement interface, which could drastically decrease the mechanical properties, the reaction zone has been reduced by the incorporation of pyrocarbon coating. The production of such reinforcements has reached a commercial status, and continuous TMCs reinforced with SiC fibres is used as an industrial scale for aeronautic applications (Nozzle and piston rod in F-16 aircraft [MIR2005]). Different kinds of SiC fibres used nowadays are differentiated by their cores (carbon or tungsten) and by their mechanical properties. [CHO2005]

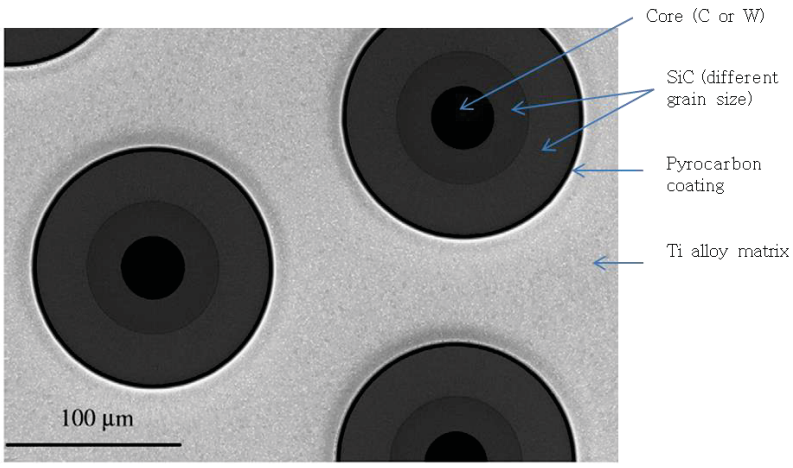

Figure 8: SEM-micrograph of Ti/SiC fibre composite [BET2007]

The continuous Ti/SiC fibre composite really improve the tensile strength of the material compares to titanium alloy itself, but only in the direction of the fibres. Moreover, a major loss of the ductility is observed in such composites as shown on the Figure 9 (tested to fracture for the TMC, interrupted at 6% and 10% for the alloy) [BET2007]

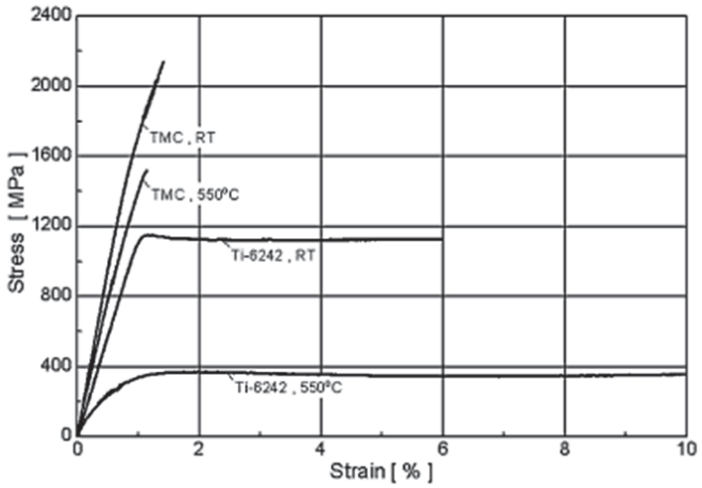

Figure 9: Stress-strain for Ti-62642 (near α) and the TMC Ti-62642/SiC fibres 35%vol. [BET2007]

II-2.3 Discontinuously reinforced TMC

Discontinuously reinforced TMCs present as an obvious advantage the fact they have isotopic properties, in comparison with the continuously ones that are clearly oriented. But, it has the other advantage to be easier to produced, considering the use of secondary processing can be also considered on them (that cannot be used on fibres reinforced composite; otherwise the fibres would be damaged). In this category of composites, two sub classes can be established: the *in-situ* composites and the *ex-situ* composites. The last ones represent the composites where the reinforcement were prepared prior to the composite fabrication and added to the titanium in. The in-situ reinforcements are the ones synthesized inside the titanium matrix by chemical reactions during the composite fabrication step.

Most of the discontinuous reinforcements are ceramic or intermetallic particles, such as SiC, Al_2O_3, Si_3N_4, TiC or TiB. But the most compatible with the titanium matrix are TiC and TiB, because they will

not form reaction products at the interface that could affect the composite properties. [KON1989] [GOR1989]

In this work, both in-situ (Ti-TiB) and ex-situ (Ti-TiC) composites has been investigated.

a/ Ex-situ (micrometric)

The processes used for the fabrication of TMCs are detailed later in this chapter, but it remains the most important parameter for the production of TMCs, *in-situ* or *ex-situ*. Indeed, processes control the aspects of the composites that have the strongest influence on the final properties of the TMCs. These aspects are for example the final density, distribution of the reinforcements or the microstructure of the metallic matrix.

However, ex-situ routes to prepare composites give interesting results, especially with the TiC particles reinforcement. The elastic modulus, tensile strength and hardness of titanium alloys can be increased by the addition of a low volume fraction of micrometer sized TiC particles. [POL2012] [TJO2007] [FRU2012] [WAG2003]

Figure 10 shows the improvement made on Ti alloy by the addition of TiC particles, prepared by different powder metallurgy processes (solid way).

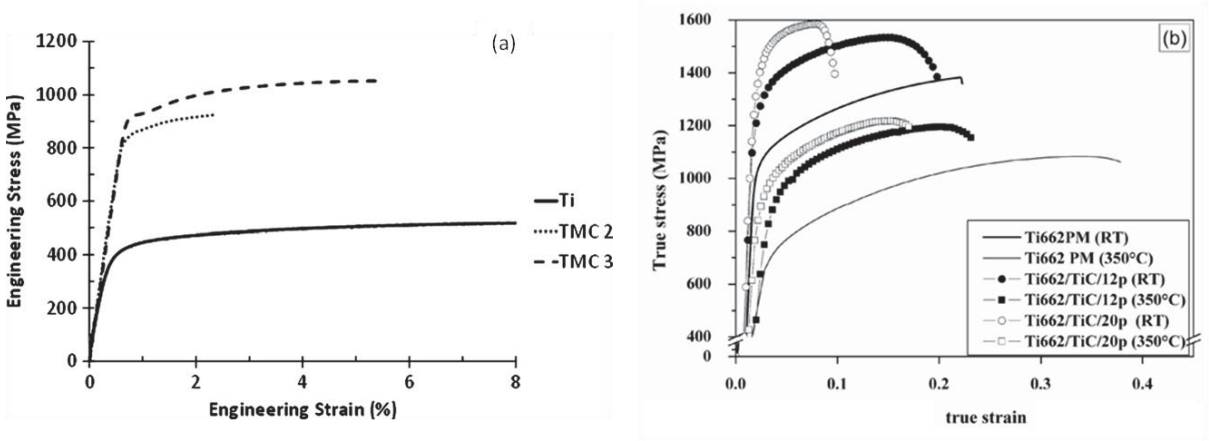

Figure 10: a) Engineering tensile test curves for cp-Ti (grade 2)/15%vol. TiC (2.6 µm) at room temperature [FRU2012] and b) Tensile test curves of a Ti-6Al-6V-2Sn reinforced with 12 and 20 vol.% of TiC particles (10 µm) at RT and 350°C [POL2012]

It appears clear that the tensile strength of the a) cp-Ti and b) Ti662 alloys are improved by the addition of the TiC particles. The difference on a) between TMC 2 and TMC 3 is the powder metallurgy processing method used for the fabrication of the composites, and are a good example of how the processing itself can have an influence on the final properties of the same TMC. TMC 2 is prepared by hot isostatic pressing and TMC 3 is prepared by powder extrusion.

The limitations of this kind of composites are usually related to the interface reinforcement/matrix that can drastically decrease the composites properties if impurities or reaction between reinforcement and matrix form another phase at the interface (called interphase). This interphase can be an issue if their properties are the opposite of the composite properties sought (typically a brittle interphase within a metallic composite)

b/ In-situ (micrometric)

To limit the surface (or interface) contamination sometimes observed in the ex-situ composites, the

reinforcements can be synthesised in-situ in titanium or titanium alloys, via reaction of the matrix with a selected element. Consequently, the interface between the reinforcements and the matrix will be free from contamination. However, few in-situ reinforcement species can be formed. One of the most studied in-situ reinforcement, and the one selected in this work, for TMCs, is the TiB-whisker reinforcement (TiB_w).

From the Ti-B phase diagram [CAL2008], titanium reacts with boron to form several titanium boride compounds, TiB_2, Ti_3B_4 or TiB at respectively 18, 22 and 31 wt.%.

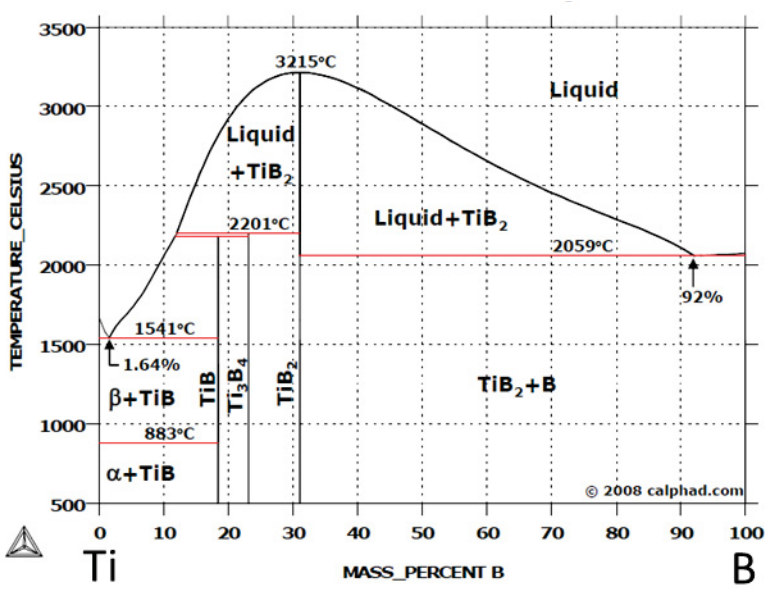

Figure 11: Titanium-Boron Phase Diagram [CAL2008]

Boron can therefore be used to produce in situ TiB, as shown on reaction 1.1. Moreover, the formation of TiB is highly exothermic (-160 kJ/mol [YAM2007]).

$$\mathrm{Ti} + \mathrm{B} \rightarrow \mathrm{TiB} \qquad (1.1)$$

Different starting elements for the formation of TiB_w have been studied such as TiB_2, or B_4C. If the temperature of the processing is high enough (over 1200°C [SHE2011]), TiB_2 reacts with Ti according to the reaction 1.2 to form TiB_w. TiB_w phase is thermodynamically more stable than TiB_2 phases when excess moles of titanium exist. Therefore, TiB_2 phase is transformed into TiB phase during the fabrication, as long as there is an excess of Ti and enough time for the diffusion. [PAN2003] The formation of the whiskers occurs as growth of TiB crystal within the Ti matrix in a hexagonal cross-section (Figure 12). [LU2008]

$$\mathrm{Ti} + \mathrm{TiB_2} \rightarrow 2\mathrm{TiB_w} \qquad (1.2)$$

TiC can also be synthesized inside titanium matrix using carbon as starting elements. The reaction 1.3 occurs [MA2000] [THR2009a] [THR2009b]

$$\mathrm{Ti} + \mathrm{C} \rightarrow \mathrm{TiC} \qquad (1.3)$$

where the source for the carbon can be carbon black [WAN2008] carbon nanotubes, diamonds [MON2011] or even methyl gas [TJO2008]

Another *in-situ* TMCs widely studied are the ones combining TiC and TiB as reinforcements. To

achieve that, B_4C is used as starting element, according to the reaction 1.4 and 1.5. [QIN2003]

$$3Ti + B_4C \rightarrow TiC + 2TiB_2 \quad (1.4)$$

$$5Ti + B_4C \rightarrow TiC + 4TiB \quad (1.5)$$

According to the thermodynamic data, the Gibbs free energy for the reaction 1.5 is more negative than the one for the reaction 1.4. [ZHA2007] From there, it is more likely to observe the formation of TiC + TiB.

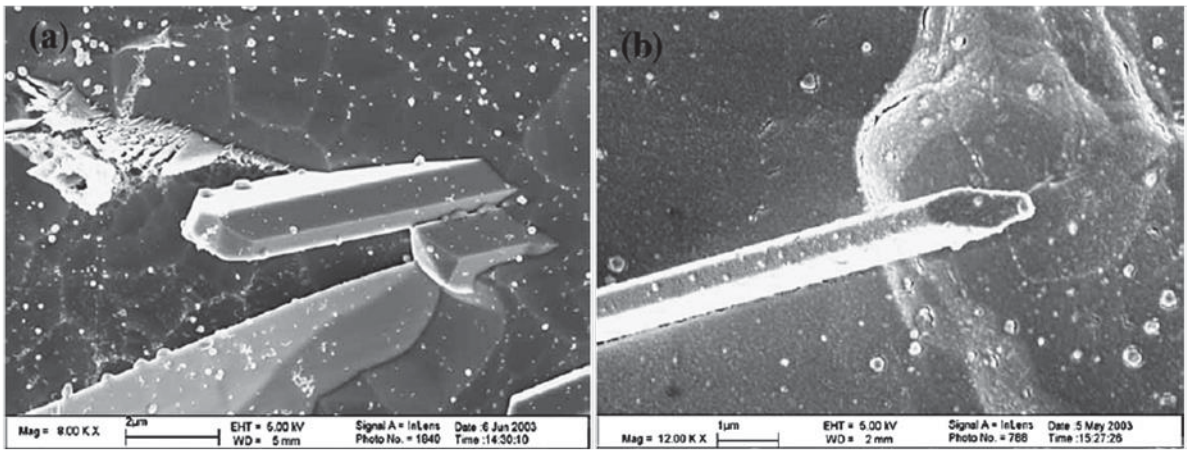

Figure 12: Typical shape of TiB whiskers in Ti matrix [LU2008]

c/ Comparison between in-situ and ex-situ reinforcements

Each of the previously presented reinforcement has some advantages and inconvenient. For example, in-situ composite offers:

- Optimised interface (no porosity)
- Optimised dispersion
- Use of metastable phase

However, some limitation can be encounters using in-situ reinforcements:

- Difficulty to control the size or the shape of the reinforcement
- Only few possible reinforcement for each matrix
- Limitation in some processes, or need of several processes to obtain the desired reinforcement

On the other hand, ex-situ reinforcement offers some advantage in regards of the limitation encounter with in-situ:

- No limitation in the nature of the reinforcement
- Perfect control of the reinforcement phase

Nonetheless, ex-situ reinforcements have some limitations:

- Difficulty to obtain a uniform distribution
- Reaction at the interface that can create non desirable interphase

In regards of these advantages and problem, the choice of the reinforcement has to be made depending on the process used and the properties sought.

d/ Nanosized reinforcements

Despite their really better properties in term of hardness, yield and tensile strength or even Young's modulus, the TMCs, and more generally the MMCs suffers of a major inconvenience, the lack of ductility. Indeed, regardless the nature of the discontinuous reinforcements, if their size is micrometric, it results that the MMC will not have ductility as good as the unreinforced matrix metal. However, reducing the size of the reinforcement at a nanometric size can provide an increase of mechanical properties without sacrificing the ductility. These composite are known as the metal matrix nanocomposites (MMnCs). [KAN2004] [ALE1998a] [VIS2007]

In-situ nanosized second phase precipitates have been successfully introduced into an aluminium alloy resulting in simultaneous increase in both the yield strength and ductility. [ZHA2006a] [CHE2007] Ex-situ nano-sized particles can also be dispersed in a metal matrix. Different examples of Al matrix reinforced with carbon [GOU2009], Al_2O_3 [HOR2005], Cu matrix reinforced by nanosized SiO_2 [ALE1998a], and Mg based matrix reinforced with SiC [FER2001] nanoparticles can be found. In the same idea, titanium can be used as a matrix to produce titanium matrix nanocomposites (TMnCs). One example of TMnC has been synthesized with Y_2O_3 and using different processing [CAS2005] [CAS2006]. The effect of nanosized reinforcement on the ductility can be considerably less significant compares with the microsized reinforcement. As well, another advantage of the use of the nanoparticles is the volume fraction needed to improve mechanical properties is considerably reduced, in respect of the size and the nature of the reinforcement particles. [ZHA2012a] [ZHA2012b]

Whether the reinforcement is *in-situ, ex-situ,* micrometric or nanometric, it will have an effect of the composite properties. However, the process used to obtain these composites is the source of many aspects that have an influence on the properties (particularly the mechanical properties). These aspects are the microstructure, the dispersion of the reinforcements, or the nature of the interface. They are intrinsically linked with the processed used. That is why the process has to be controled and understood.

III. Processing

Titanium is obtained after the transformation of mineral ores (composed of titanium dioxide) to sponge. This process, called Kroll Process, consists in transforming the TiO_2 into Ti sponge. To do so, the TiO_2 is treated with Cl_2 and carbon in order to form $TiCl_4$ and CO_2. Then this $TiCl_4$ is treated with Mg salt (Mg^{2+}; $2Na^{+}$) in order to form Ti sponge, the sponge aspect coming from the extraction of the magnesium chloride compound. The purity of this sponge varies and depends on the purity of the ores used, and the quality of the process [DON2000] [SUB1993]. Ti sponge is usually not interesting for industrial purposes, and therefore, is consequently transformed into ingots, through a melting process.

This is during the melting process that the alloying elements are added. Several melting techniques exist such as vacuum arc remelting (VAR) electron beam or plasma-arc melting, but will not be discussed in this work. The main idea is that it is the control of the atmosphere and the thermal or mechanical conditions that will influence the properties of the titanium ingot. These ingots will be converted into general mill product -bar, rode, plate, etc...- through primary fabrication process. The mill products will be then subjected to secondary transformation where the microstructure will be taken into consideration and controlled to fulfil the desired application requirements. However, primary process such as rolling or extrusion can produce usable mill product, without the need of

secondary process. A detailed discussion about all the processes, primary and secondary (forging, forming, casting…), would not be relevant due to the fact it is only applicable on Ti or Ti alloys bulks only.

The main process used in the fabrication of titanium based composite and titanium alloy based composite are the powder metallurgy processes. Indeed, most of the MMCs are obtained through powder metallurgy because of its simplicity of application, and its wide range of processes having several parameters that can be adjusted. In this work, different powder metallurgy processes presented below have been investigated.

III-1. Powder metallurgy

III-1.1 Generalities

Powder metallurgy designated all the production processes to obtain material starting from metal powders. It is usually associated with cost reduction for the production of net shape material, or with the obtaining of better properties than the cast or wrought material. In the fabrication of titanium, titanium alloys and moreover titanium-based composites materials, PM is widely used and for the TMCs, almost the only way to obtain desired structure and properties. The starting powders in titanium PM can be pure Ti, named blended element (BE) in the form of fine milled sponge, of prealloyed powder (PA) that are produced from alloyed ingots, using different atomization processes to obtain powder. One can note that BE can be obtain through the same way of getting PA, but the cost of such method would be irrelevant.

III-1.2 Ball Milling

Powder metallurgy is obviously dependent on the nature of the starting powder. One of the properties of the starting powder that has influence on the final material will be the particle size. In order to have a control on this aspect, the most used technique is ball milling (BM). This process can also be used to produce alloys, starting with powders of different elements that are milled together to obtain a homogeneous compounds. It is often referred as mechanical alloying (MA) in opposition to mechanical milling. In this work, alloying through BM has not been done, therefore, BM refers only to mechanical milling.

The principle of the MA process, well explained and summarized in Suryanarayana's publication [SUR2001], is roughly the same in the different variations of BM.

The milling medium, usually balls, is inserted in a jar with the powder, and the milling takes place for a set time until the desired state is reached. During this step, the powder is subject to high deformation by the impact generated between the ball-particle-ball or ball-particle-jar's wall collision. These deformations can lead to flattening, cold welding, fracturing and re-welding. And these deformations will act on the particle as work-hardening phenomena. The ductile materials (metals, alloys...) will be subjected to all the previous deformations whereas the brittle material (ceramic, intermetallic...) will not be subjected to any welding. The effect of early stage of ball milling on each kind of powder (ductile or brittle) is given on the following figure. (Figure 13)

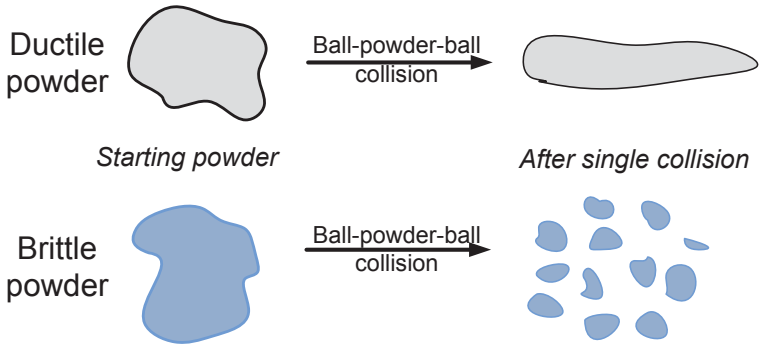

Figure 13: Deformation characteristics during early stage of BM of different starting powders [BEN1974]

In order to control the rate between fracturing and cold welding, process control agents (PCAs) are often added.

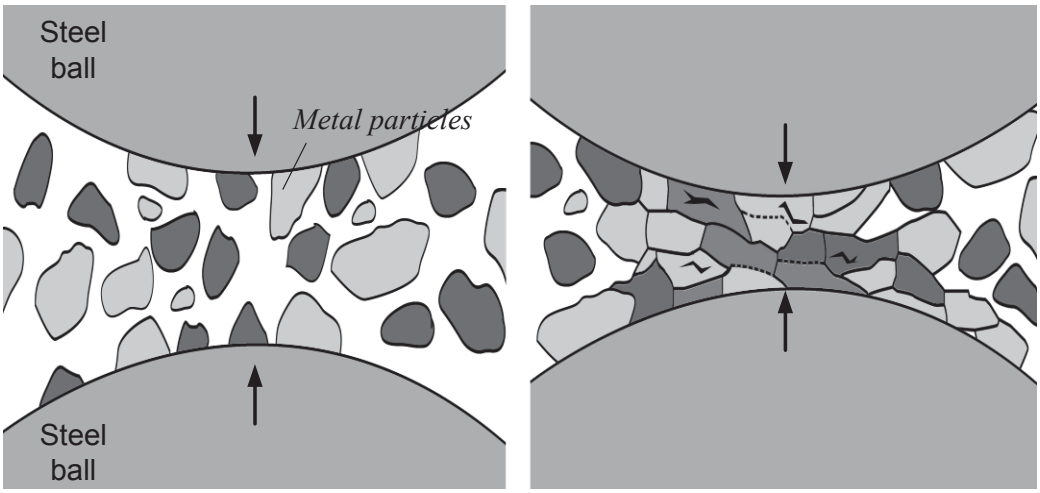

Figure 14: Ball-powder-ball collision during BM of metal material (similar to ball-powder-wall phenomena) [BEN1974]

As presented on the Figure 14, the ball-powder-ball collision plastically deforms the particles, fracturing them into smaller fragments due to the work hardening. The dot lines represent the freshly exposed surface after fragmentation that will favour welding between ductile particles. The milling behaviour, regarding the particles size, is quite different between brittle and ductile materials. Due to the fact brittle powders are not subject to any welding, the ball-powder-ball collision will only lead to increase the defect into the material and consequently lead to fracturing.

Concerning ductile powders, the early stage of BM when the particles are still soft will lead to the formation of large particles because of the welding. Later, when continuing the deformation and work hardening, BM particles will get them fractured by fatigue. At this stage, a balance is reach between the rate of cold welding phenomena and the rate of fracturing one. Indeed, smaller particles will be deformed during the collision without fracturing, and will be weld into larger particles, and large particles are more likely to fracture during collision. The general tendency is illustrated in the Figure 15.

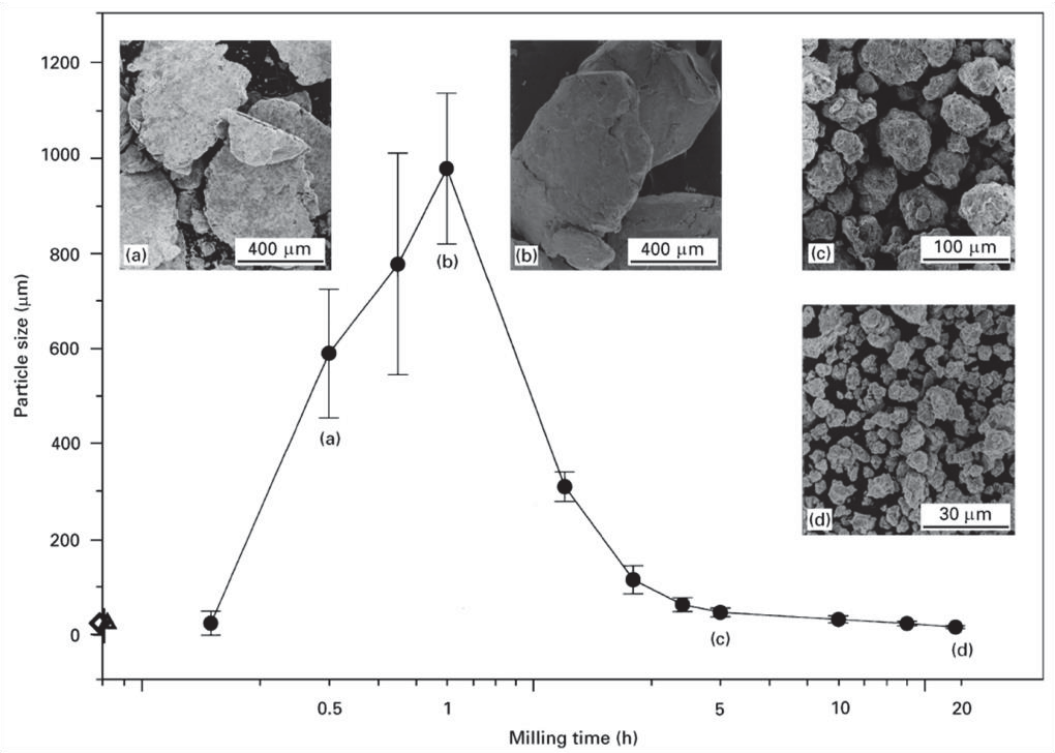

Figure 15: Particle size and SEM observations at different milling time (Ni-Ta alloys) [LEE1998]

Another interesting effect of the BM is the grain refinement (coherent crystal domain) within the particles, due to the high plastic deformation inflicted. During the early stage of BM, the grain size of the particles will decrease rapidly until it reaches a constant value. The following figure (Figure 16) illustrates the rapid grain refinement during the early stage of ball milling, and the reaching of a constant grain size.

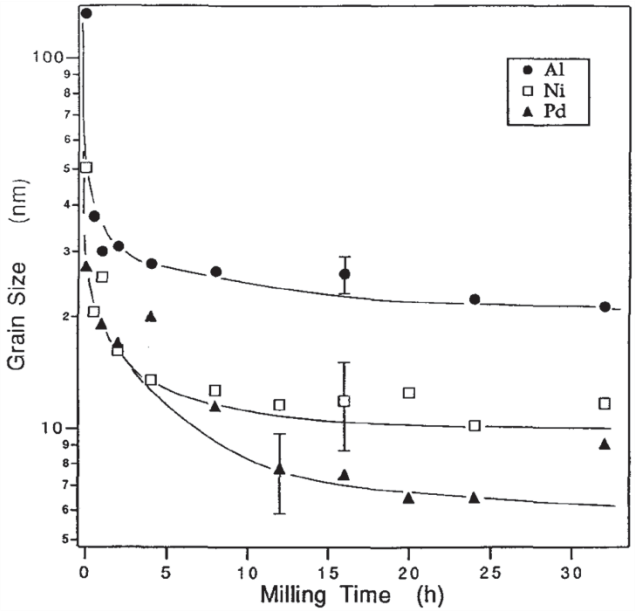

Figure 16: Average grain size evolution of Al, Ni and Pd powders depending on BM time [ECK1992]

The structural evolution during the ball milling of two or more powders, like in composites, is slightly different to the one of a single phase particles. The different combinations of powder are ductile-ductile, ductile-brittle and brittle-brittle.

The ductile-ductile concerns mainly the alloy formation, through mechanical alloying. Indeed, the ductile particles will be first flattened and then cold-welded together, to form lamellar particles of composite. The later stage of BM will work hard and fracture these particles. Eventually, the BM will lead to the alloying of the two phases, due to the increase of crystal defect, that enhance the diffusion [SUR2001].

The brittle-brittle combination will not affect the nature of the powder since there is no cold-welding. Depending on the BM conditions, a size reduction or just a mixing phenomenon will be observed.

The brittle-ductile combination will show an interesting phenomenon, especially for the production of composites. During the early stage of BM, the brittle particle might be fractured when the ductile particles will be work hardened and flattened. And the brittle particles will be trapped in between the ductile lamellar particles. After a longer time of BM, the lamellar particles now formed will be refined, meaning the interlamellae spacing decreases and the brittle particles are more homogeneously dispersed. The following figure illustrates this mechanism with metal (ductile) and oxide (brittle) particles (Figure 17).

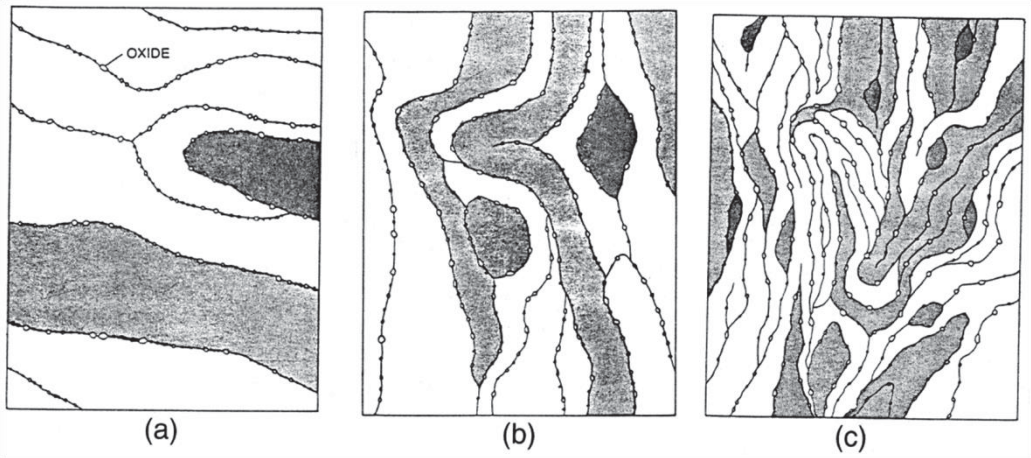

Figure 17: Evolution of brittle-ductile powders during different stage of ball milling a) Early stage; Oxide is trapped between lamellar particles b) and c) Evolution of the system and dispersion of the brittle particles after longer time of BM [SUR2001]

The dispersion of the reinforcement within the matrix is the key problem during the production of TMCs. In a brittle-brittle combination, such as TiH_2-TiC or TiH_2-TiB_2 targeted in this work, the dispersion inside the matrix will happen during the sintering stage. Before, the distribution of the reinforcement particles will be on the surface of the matrix powder. After parameters optimisation, the BM stage will lead to a uniform distribution of the reinforcement and matrix brittle particles one from each other. In the Ti-TiC ductile-brittle combination, also studied in this work, the distribution of the reinforcement within the matrix is an important factor. Following the theory, Gu *et al.* [GU2010] have proposed and observed a mechanism of structural evolution. The first stage is the fracturing stage (0-10 h of BM), where the brittle micrometric TiC will be fragmented into nanometric particles and be trapped in between Ti flattened, work hardened and fractured particles, leading to the formation of Ti/TiC composite fine powder. The second stage (10-15 h of BM) is the cold welding stage, where the newly formed particles will undergo heavy plastic deformation until the cold welding phenomenon prevails. This forms coarsened Ti/TiC particles, and meanwhile the TiC particles get more uniformly dispersed within the matrix. The third stage is the re-fracturing stage

(15-25 h of BM) where the composite powder undergoes more work hardening. Consequently, the particles, that cannot accept more plastic deformation, will fracture reaching the state where cold welding and fracturing are balanced phenomena, as represented on Figure 18.

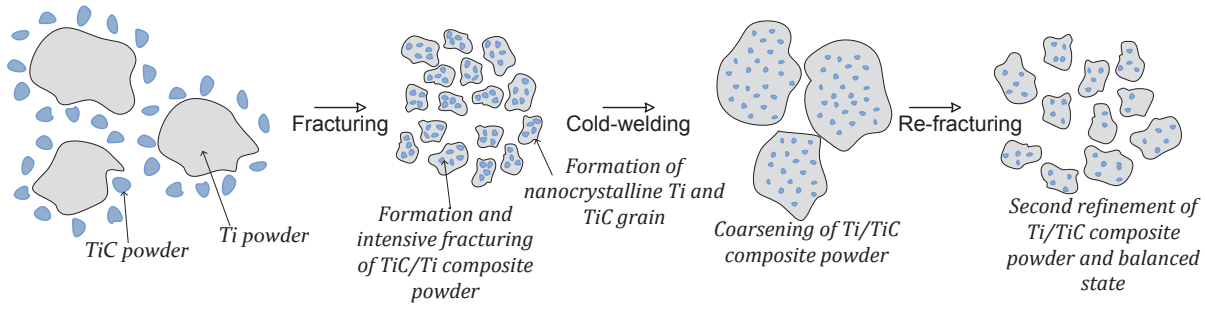

Figure 18: Schematic evolution of brittle-ductile Ti-TiC composite during BM [GU2010]

The preparation of composite powders using ball milling is an essential step during the production of TMCs. The milled powders become the starting powder of the different PM methods used to produce one's composite.

III-1.3 Cold compaction

In order to obtain dense materials, numerous PM methods require a shaping prior densification processes. It is referred as the cold compaction, and the compacted material is referred as the green compact. The goal of the cold compaction is to create contact points between particles, to reduce as much as possible the porosity and to obtain desired forms. Those contact points lead to the creation of surface contact between particles, needed for densification processes such as sintering. The effect of the cold compaction on powders is measured by the relative density D_R of the green compact. The green density, or apparent density ρ, when linked to the apparent volume V, is compared to the theoretical density and volume of the material ρ_m and V_m in order to obtain the relative density. This relative density gives information on the residual porosity p ($p = 1 - D_R$) (Figure 19) In practice, the relative green density is the ratio between measure density of a material and its theoretical density.

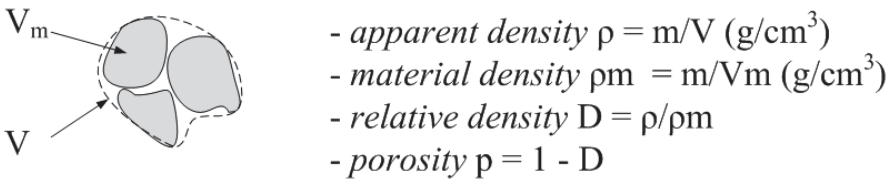

Figure 19: Schematic representation of densities [BOU2002]

The green compaction happens following two phenomena, the particles rearrangement, and their deformation and possible fracturing. The second phenomenon depends on the particles nature, if they are hard or soft. The rearrangement phase occurs early during the compaction, under low pressure. Its efficiency depends on the shape of the powder (spherical, angular, dendritic...). Spherical shape makes the rearrangement easier due to the fact particles can slide against each other. At higher pressure, the particles, which cannot move more, will go under strain. Soft powders will go under deformation that will increase the contact surface between particles. Hard powder, on

the other hand, will not be able to deform much. However, in the case of brittle material, cold compaction can induce fracturing into particles, which leads to a better compaction, considering the fractured parts will then move into a previous pore.

In order to process cold compaction, two main processes are used, the uniaxial pressing, and the cold isostatic pressing (CIP).

The uniaxial pressing consists in the compaction the powder into a close mould, typically a cylinder, by applying pressure following a single direction. The pressure apply on the powder sample during the process will reach an equilibrium state where it is distributed on the sample, with the creation of a gradient at half of the height. Figure 20 a) represents this gradient in the applied pressure on the powder with arrows, where their length is a schematic representation of the pressure applied; long arrows represent high pressure and short arrows represent low pressure. This gradient is usually compensated by the deformation of the particles. To avoid the creation of this gradient, that can be a problem, CIP is a method that will equally distribute the applied pressure on the sample, through the use of liquid medium, usually oil, by increasing the pressure of it (Figure 20 b). Uniaxial pressing is usually preferred to CIP because of its simplicity and its quickness, but CIP is sometimes required to achieve desired green density.

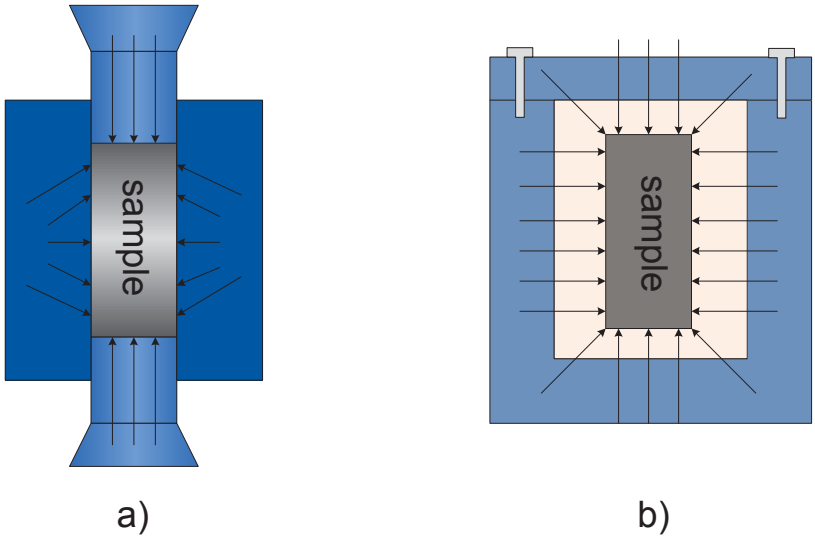

Figure 20: Schematic principles of a) uniaxial pressing and b) Cold isostatic pressing

III-1.4 Free sintering (pressureless sintering)

Sintering is the mechanism that transforms cold compacted powders into dense materials without pressure applied. A comprehensive explanation of its mechanism has been done by J.M Missiaen [BOU2002]. The macroscopic driving force operative during sintering is the reduction of the excess energy associated with surfaces. In a single phase material, the total surface energy E is a combination of the solid-gaz interfaces (particles surfaces) and the solid-solid interfaces (grain boundaries). The considered surface is called S and the specific surface energy is called γ. The total surface energy can be expressed as:

$$E = \gamma_{SG} S_{SG} + \gamma_{Ss} S_{SS} \quad (2.1)$$

As the solid-gaz interfaces are, most of the time, more energetic than the solid-solid interfaces, the reduction of E is related to the replacement of solid-gaz interfaces by solid-solid interfaces. In the same time, the reduction of grain boundaries, or grain growth, tends to reduce the solid-solid

interfaces surfaces. The sintering phenomenon is a combination of volume diffusion from the surface to the neck (densification) and diffusion from the volume to the neck (grain coarsening).

During the sintering, reaction of the particles (for examples decomposition, or reaction with the atmosphere) can lead to a weight and volume change, whereas phase transformation and solid state phase reaction can change the volume but at a given weight. These transformations usually modify the relative density of the material. It also gives a good indication on the efficiency of the sintering (having D_R = 1 or 100% means the measured density reaches the theoretical density of a fully dense material)

Three stages are observed during sintering of a single phase material, the neck formation and growth, the elimination of pore channels and then the elimination of closed porosity, as illustrated on the following figure (Figure 21)

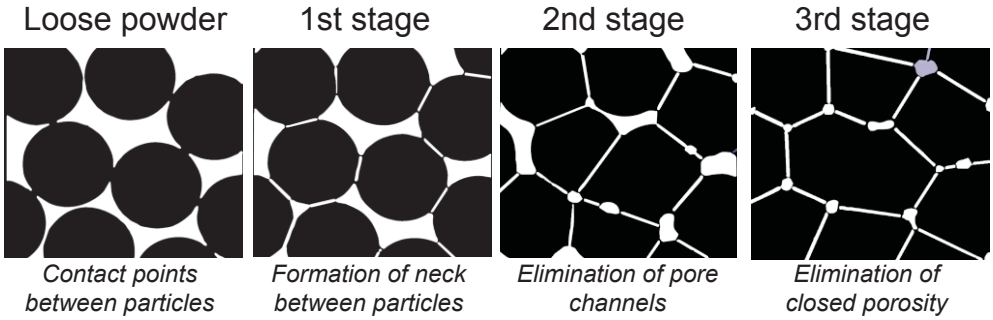

Figure 21: The three stages of sintering

The first stage is the formation of the neck between the particles in contact within the green compact, leading to a network of porous channels. The second stage is the further increasing of the contact between particles that lead to the elimination of the pore channels, leaving closed pores. The third stage is the disappearing of the closed pores, with the diffusion of mater from grain boundaries and cores.

In a presence of reinforcements, the sintering behaviour of the material will be slightly changed. Considering the densification rate of the reinforcements is independent from the one of the matrix, the densification rate of the composite will be expressed following the rule of mixture, depending on the volume fraction of the reinforcement (V_r) and the densification rate of the matrix and the reinforcement ($\dot{\varepsilon}_m$ and $\dot{\varepsilon}_r$)

$$\dot{\varepsilon} = (1 - V_r)\dot{\varepsilon}_m + V_r\dot{\varepsilon}_r \quad (2.2)$$

If there is no percolation between reinforcement, the densification rate of the reinforcement is not relevant and the equation becomes:

$$\dot{\varepsilon}_c = (1 - V_r)\dot{\varepsilon}_m \quad (2.3)$$

Therefore, the densification rate will decrease with the presence of reinforcements. The reinforcement will also act as barriers to the motion of grain boundaries and the grain growth will be slower near the reinforcement particles. If the distribution is uniform, the grain growth rate will be lower than the one without reinforcements. Considering that densification rate and grain coarsening are the basis of the free sintering, different method have been elaborated to obtain fully dense materials when free sintering is not efficient.

After free sintering, some materials, especially composites might have porosity in their structures. For example, in processing of titanium, and titanium based materials, pressureless sintering has not

be able to reach good enough density, due to the oxide layer that is formed on the surface of each particle, which decrease considerably the densification rate. To compensate it, the use of a subsequent process is commonly done industrially [LUT2003] [SAV2012].

These undesirable limitations observed during free sintering can be avoided by applying a pressure during the sintering. It is called hot forming powder metallurgy.

III-1.5 Hot forming

As for cold compaction, the processes are differentiated by the way the pressure is applied on the material. The densification mechanisms of the material during hot forming processes are related to the sum of all microscopic effects on each particle during the processing time. The effect of the applied pressure onto the sample is carried through all the contact between particles (the same as the contact point during free sintering). Considering an average contact point number per particle *Z* and an average contact surface per particle *a*, the effective pressure applied P_{eff} on each contact point can be expressed as:

$$P_{eff} = 4\pi R^2 \frac{P}{Z\ a\ D} \tag{2.4}$$

where R is the average particles radius, D the relative density and P the pressure applied. In the case of ductile powder, the particle plastic deformation depends on the yield strength σ_y of the material at the processing temperature. Therefore, in order to plastically deform the particles, the applied pressure as to reach a minimum P_{lim} value defined as:

$$P_{lim} = \frac{3\sigma_y}{4\pi R^2} Z\ a\ D \tag{2.5}$$

From there, the maximum relative density that can be reached through only plastic deformation can be expressed as:

$$D_{lim} = \left(\frac{(1 - D_0)P + D_0^3}{1.3\sigma_y} \right)^{1/3} \tag{2.6}$$

where D_0 is the relative density of the powder at the start of the process, which is regularly considered at the occupancy of the powder in a given volume. This model is verified for density lower than 0.9. However, it is unlikely that the density reach through only the effect of plastic deformation reach more than 0.9. To reach higher density, another mechanism is considered, the creep.

Creep occurs when the pressure and the temperature have relatively high values. The particles get deformed permanently under the influence of long-term exposure to high levels of stress that are still below the yield strength of the material (σ_0). Creep is more severe in materials that are subjected to high temperature for long periods. These permanent deformations are due to the diffusion of matter through necks or grain boundaries, made it easier at high temperature. As in free sintering, these diffusions will lead to the closing of pores. However, in the case of creep, the deformation rate ε is sensitive to the pressure applied, and is ruled by the motion of dislocations:

$$\varepsilon = \varepsilon_0 \left(\frac{\sigma}{\sigma_0} \right)^n \tag{2.7}$$

where ε_0, σ_0 and n are characteristics of the material and obstacles to the dislocations motion.

The densification rate dD/dt is then given by:

$$\frac{dD}{dt} = 5.3(D^2 D_0)^{\frac{1}{3}} \frac{x}{R} \varepsilon_0 \left(\frac{P_{eff}}{\sigma_0}\right)^n \quad (2.8)$$

where x is the average contact radius between particles. The applied pressure has a direct influence on the densification of the material. Moreover, an increase in temperature will have an effect of decreasing the value of the yield strength, leading to an increase of the densification during creeping. In addition of the densification by creeping, the diffusion phenomena being important at high temperature complete the densification mechanisms occurring during hot forming.

The processes in hot forming are differentiated by the way the pressure is applied on the material. The deformation can occurs either statically (hot pressing, hot isostatic pressing (HIP)) or dynamically (severe plastic deformation).

Hot pressing and HIP are similar to the cold compaction processes, except the material is pressed and heated in the same time. In HIP, the whole die will be heat using a furnace, but where in CIP the sample holder could be simple plastic sheets, during HIP the die has to handle high temperature, and soft steel are usually used, making this process costly and complicated. Hot pressing consists on a simple uniaxial compaction, and the heating process can be very various, such as classical furnace, or induction heating of a graphite mould. Hot pressing and HIP are usually done under controlled atmosphere or vacuum in order to avoid any sample contamination induce that could be induced by the heat.

Microwave sintering and spark plasma sintering (SPS) are also considered as uniaxial hot forming, but the process being peculiar and complicated, due to the fact that the sample itself is heated through radiation or resistance effect; it was not relevant to include them.

Xue *et al.*, [XUE2011] and Fruhauf *et al.* [FRU2012] have shown the possibility of obtaining fully dense Ti, Ti alloy and Ti composites by the mean of uniaxial pressure and HIP. Fruhauf has also shown the limitation of free sintering of TMC, demonstrating a good density cannot be reached by the sintering mechanism alone.

III-1.6 Densification using severe plastic deformation (SPD)

The dynamic hot forming concerns processes where a severe plastic deformation (SPD) will lead to the densification of the powder. Three main processes exist in SPD of powder, extrusion, high pressure torsion (HTP) and Equal Channel Angular Pressing (ECAP). The last one will be evocated in detail.

The principle of SPD method is to combine hot forming with shearing of the particles that will lead to a refinement of the microstructure, a fracturing of the oxide layer and having as a result the obtaining of fully dense materials. The benefits of such method are the possibility to obtain rapidly fully dense material, large samples, with a very fine and controlled grain size and with the possibility to orientate the grains. Therefore, mechanical properties such as yield strength will be better due to the fine grain size, and can be increased in one direction if the application demands it.

The extrusion of powder, illustrated on Figure 22, consist on pushing a compacted powder or loose powder (if the powder is not too fine) through a die of reduce section area, at a controlled temperature.

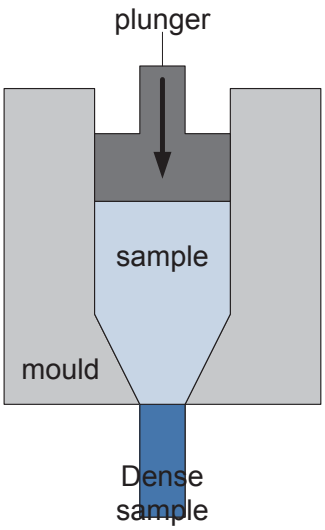

Figure 22: Schematic extrusion mould

Even if it is more common to start the extrusion processes from bulk material, Galanty *et al.* [GAL2002] have shown that high density has been reach when starting from loose powder. Fruhauf *et al.* have demonstrated the possibility of obtaining TMC starting from cold compacted powder using extrusion process. Even more, compared to the same composite obtained by HIP, the extruded one exhibits finer grain size and orientated grains.

Another SPD method is the high pressure torsion, commonly use to increase hardness of thin disk-shaped sample. The sample is placed between two anvils and is subjected to high compressive pressure (up to several GPa) and, through the rotation of one anvil, strain in torsion is applied on the sample, leading to deformation and densification of it. The principle of HPT is illustrated on Figure 23.

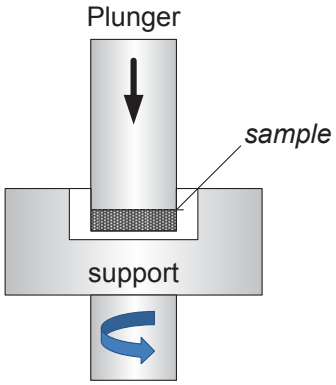

Figure 23: Schematic drawing of HTP processing

Edolati *et al.* and Alexandrov *et al.* [EDA2011] [ALE1998a] [ALE1998b] have obtained dense titanium and dense MMnCs using HTP on powder. Even though HTP is effective, its limitation stand in the shape and size of produced samples.

In regard of all the powder metallurgy process, one fundamental aspect is the starting powder. The powder will determine the efficiency of each processing. In particular in composite fabrication, the starting powders will be at the heart of the properties of the final material. That is why it is important to have the possibility to have a control of the starting powder, in term of particle size,

shape or even reinforcement distribution. To achieve that, ball milling is one of the most used processing.

III-2. Severe Plastic Deformation: Equal Channel Angular Pressing (ECAP)

Another peculiar PM method using severe plastic deformation used in this work is the Equal Channel Angular Pressing (ECAP).

The principle of this method, established by Segal *et al.* [SEG1974], was originally to introduce intense plastic strain in a metal billet by simple shear. Later, ECAP has been recognised as a promising SPD method to obtain ultrafine grains in bulk materials [VAL1991] [VAL1993] [VAL1997] and also a new way to process powder into dense material [XIA1997]. In his PhD thesis, E.Lui gives a clear and simple explanation of the ECAP mechanisms [LUI2012]. The setup for ECAP dies consists of two channels of the same cross section that intersect at an angle Φ. The outer curvature of the intersection of the channels is denoted by angle ψ. The sample has to be of the same cross section of the entrance channel. It is lubricated and placed inside the channel. A load is applied on the sample, forcing it through the intersection where it will be deformed by simple shear and emerged at the exit channel, has represented on Figure 24.

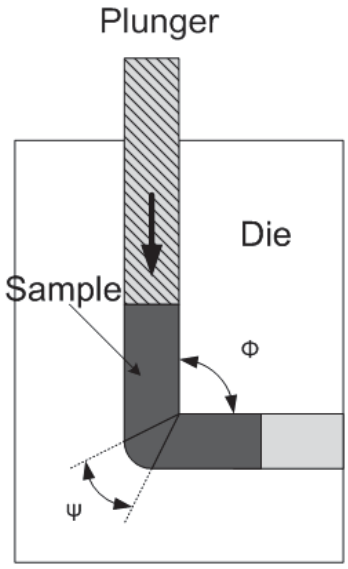

Figure 24: Schematic drawing of an ECAP setup [IWA1997]

The material is sheared when it passes through the intersection of the two channels, named the plastic deformation zone (PDZ). Several models were developed to calculate the equivalent strain [IWA1996] [IWA1997] [XIA2001]

ECAP processing offers a wide of adjustable parameter such as channel angle, processing routes, temperature, number of passes and back pressure.

The channel angle Φ is usually set at 90°, because it is the setting that is the most effective for producing ultrafine grains. Higher angle can be preferred for material that are hard to deform, due to a lower applied strain. [ALE1998a] [FIG2007]

The processing route is an important parameter in ECAP. Four different routes are commonly reported, which are defined according the rotation of the sample between each pass and are

represented on the following figure (Figure 25) [NAK2000]

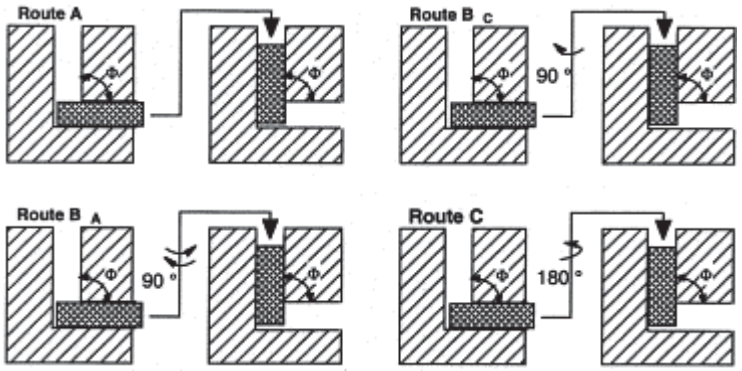

Figure 25: The four basic processing routes in ECAP [STO2001]

In the route A, the sample is not rotated after a pass. In the route B_A the sample is rotated 90° in alternate direction (if more than 2 pass) between each pass. In the route B_C the sample is rotated 90° in the same direction between each pass. And in the route C the sample is rotated 180° between each pass.

Each route has a different influence on the shear planes it imposes to the material as illustrated on the Figure 26. For both routes A and B_A, the strain in the material builds up accumulatively on the shear planes after every pass. For routes B_C and C, the strain is restored after a certain number of passes. For route C, the shear happens on the same planes during two consecutive passes but in opposite directions and the strain is restored after every two passes. For route B_C the strain in the first pass is restored by the strain in the third pass while strain in the second pass is restored in the fourth pass [SEG1995] [VAL2006] [IWA1998]

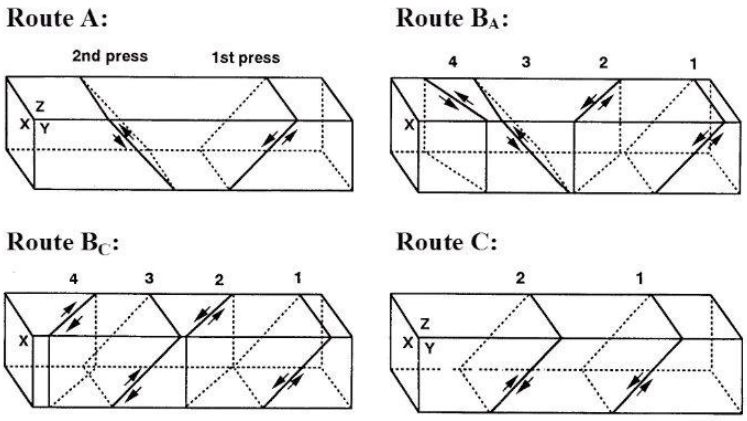

Figure 26: Shear plane for consecutive passes of the four different ECAP routes [FIG2012]

The influence on the temperature during ECAP is mainly on the grain size of the material. Generally, working at higher temperature leads to increase the final grain size and therefore decrease the yield strength. [YAM2000] [CHE2003] [HUA2004]

Some ECAP setups, as it was the case in this work, has the possibility of applying a constant back pressure (BP) using a back plunger at the exit channel. Considering bulk material, the benefit of BP is essentially observed in the uniformity of the stress-strain distribution [XU2007]. However, its benefits are much more important during consolidation of powders through ECAP. It combines high compressive pressure with the ability to apply shearing, which is ideal for metal powder consolidation a low temperature. ECAP, and more generally SPD processes, rely only on the

deformation of the particles to achieve densification.

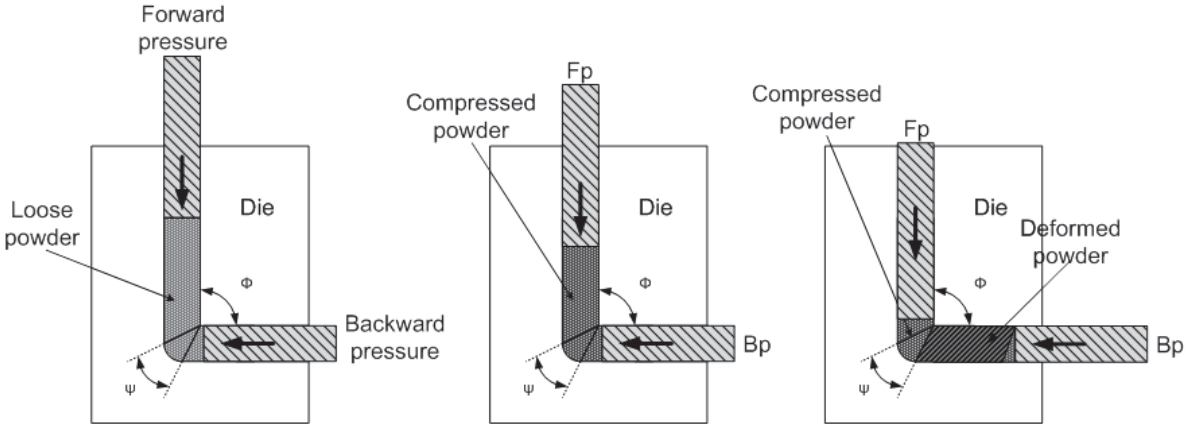

Figure 27: Schematic illustration of ECAP compaction of powder using back pressure

On bulk material, one of the main effects of ECAP is the grain refinement. The formation and subsequent concentration of dislocation during the initial stage of ECAP cause the division of coarse grain into cell blocks. These cell blocks evolve, with increasing the equivalent strain, into refined equiaxed grains. The rate of the grain refinement will gradually reduce with increasing strain and a minimum grain size is usually reached. Stolyarov *et al.* have shown in numerous of their work the effect of ECAP passes on microstructure of commercially pure titanium. Starting from a bulk with an average grain size of 10 µm, 8 passes of ECAP at 450 °C have decreased the size of the grain down to 260 nm. [STO1999] [STO2001] [STO2003]

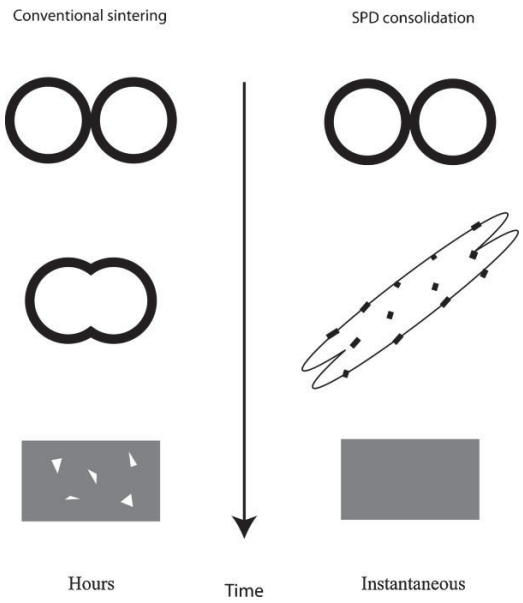

Figure 28: Schematic illustration of particle consolidation in conventional sintering (left) and ECAP consolidation (right) [XIA2010]

Metal powders are usually covered by an oxide layer at the surface. During ECAP, the compaction and shearing will plastically deform the particles, which will break the brittle oxide layer. From there, the compression applied by the BP will lead to a direct contact between freshly exposed clean and

reactive metal surfaces, and bonding happens [XIA2010]. Moreover, the material flow occurring during the deformation would close all the pores, resulting in a fully dense bulk material (Figure 28). And since the consolidation through ECAP does not rely on the diffusion process, the densification can be carried at much lower temperature and shorter processing times. For example, Xu *et al.* have obtained fully dense Ti material starting from powder, after only one pass at 600°C. [XU2008]

ECAP has also been utilised to consolidate various MMCs (such as Al alloy-TiC [SAL2009]) and MMnCs (such Al-Al_2O_3 or Al-C [XU2009] [GOU2009]). Not only have the powder mixtures of composite reached full theoretical density, but ECAP can distribute the phases to obtain more homogenized microstructure [SAB2005]. However, it is important to note that ECAP proceeding of MMCs will not be able to distribute agglomeration of reinforcements, and instead grain in each phase will be divided into smaller grain. Nevertheless, ECAP can improves the homogeneity of particle distribution as shown on Salem et al, Gutierrez *et al.* work or even Goussous *et al.* [SAL2009] [GUT2007] [GOU2009] On the following figure (Figure 29), MMC Al-7%Si is processed through ECAP, 10 passes following the route A.

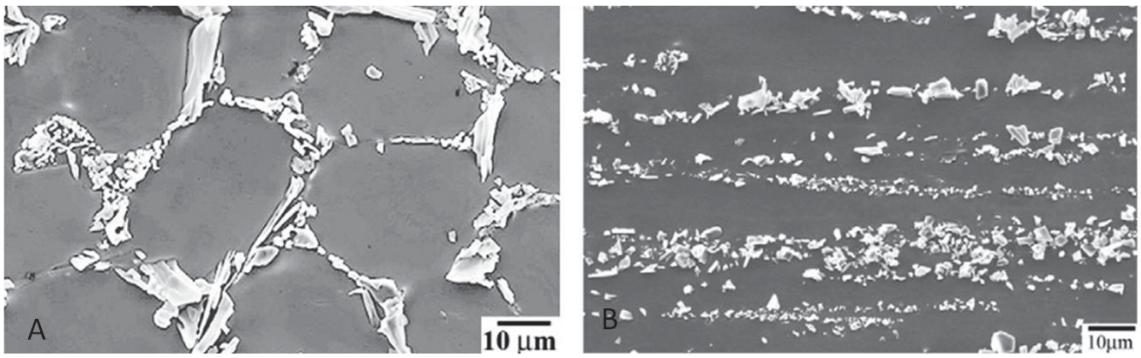

Figure 29: Microstructure in Al-7%Si a) as-cast and b) after 10 passes following route A [GUT2007]

The hard Si structure was broken up and redistributed as band structure of fine Si particles after 10 passes due to strain incompatibility between the two phases. This example illustrates the ability of ECAP to distribute hard reinforcement within softer matrix.

In this work, the aim is to use ECAP on reinforcement and matrix mixed powders in order to obtain a dense material. In addition, the possibility of the ECAP to disperse reinforcement should help to obtain uniform distribution.

III-3. Hydrogenation/dehydrogenation of titanium

One of the PM methods used in this work is the hydrogenation / dehydrogenation (HDH) process.

This process, unlike most of PM process for titanium, uses as starting powder the titanium hydride TiH_2 instead of titanium powder. TiH_2 is the hydrogenated form of titanium obtained after the reaction between Ti and H_2:

$$Ti + H_2 \rightarrow TiH_2 \qquad (2.9)$$

TiH_2 is used to refer as ε-$TiH_{1.92}$, which is stable at room temperature and has a body-centred tetragonal crystal structures. Unlike pure titanium, it has a brittle behaviour, which allows the use of milling processes to reduce its particle size. The HDH process, first report by Ivasishin in the early 00's [IVA1999a], uses the dehydrogenation of TiH_2 at relatively moderate temperatures in order to

enhance the sintering of titanium at elevated temperatures. The dehydrogenation will occurs, producing pure titanium with an activated surface (freshly exposed):

$$TiH_2 \rightarrow \alpha Ti + H_2 \qquad (2.10)$$

Since the publication of this phenomenon, numerous publications and conferences presentations have reported the use and the technical aspect of this method [IVA1999b] [IVA2005] [BHO2003a]. The theory behind this method has been studied by Borchers *et al.* [BOR2009] and Bhosle *et al.* [BHO2003b].

This dehydrogenation process has to be done under non-oxidising atmosphere, and is most often done under ultra-high vacuum (UHV) to prevent any oxidation of the freshly formed Ti particle. The dehydrogenation of titanium is a multiple step phenomena that will occur at moderate temperature, linked to the particle size of TiH_2. Indeed, it has been shown that the TiH_2 particle size has a direct influence on the dehydrogenation temperature [BHO2003b]. For relatively coarse particles (in the micrometric range or above) the dehydrogenation happens at temperature around 550°C in an apparent single step phenomenon, whereas for particles in the nanometric range size, the dehydrogenation occurs at lower temperatures (between 400°C to 500°C) in a two steps phenomenon. [BHO2003b] [WAN2010]

The differential thermal analysis (DTA) realised on the same TiH_2 powder, but with two different particle sizes, as presented on Figure 30, illustrates this influence of the particle size. It appears that the finer powder (~500 nm, in red) has its dehydrogenation peaks located between 400°C and 500°C. The coarser powder (~10 µm, in black) has its dehydrogenation single peak located around 550°C..

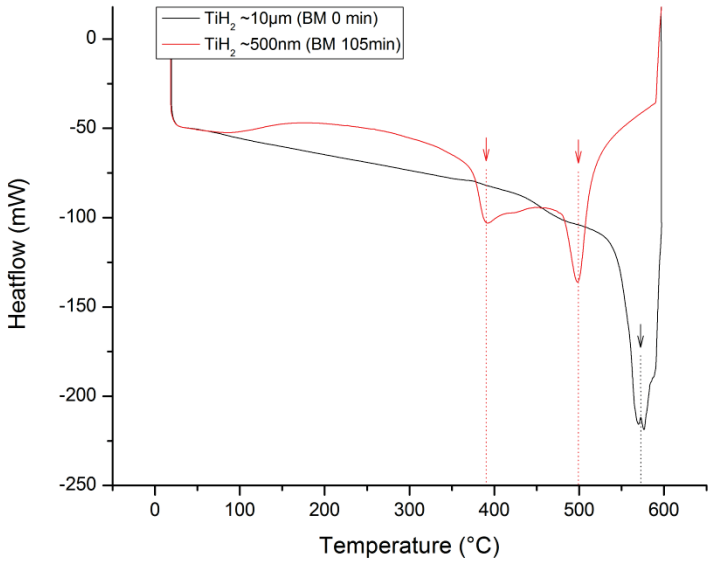

Figure 30: Evolution of the dehydrogenation temperature depending on the particle size

The apparition of two peaks for the finer powder is explained by the combination of different phenomena. The first and the more obvious is that the surface area of the fine powder will be much more important than the coarse powder. The second is that the dehydrogenation of titanium is a multiple steps phenomenon:

$$\varepsilon\text{-}TiH_{1.92} \rightarrow \delta\text{-}TiH_x + \beta\text{-}Ti(H) + H_2\uparrow \rightarrow \alpha\text{-}Ti(H) \rightarrow \alpha\text{-}Ti \qquad (\text{where } 0.7 < x < 1.92)$$

The first peak is attributed to the transformation from ε-$TiH_{1.92}$ to δ-TiH_x + β-Ti(H) and the second

one is attributed to the transformation from δ-TiH_x to α-Ti.

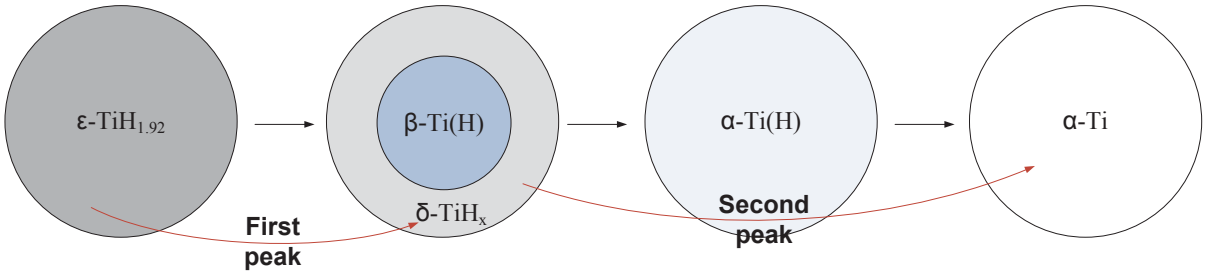

Figure 31: The titanium dehydrogenation steps

A combination between the higher surface area and the multiple steps dehydrogenation explains the presence of 2 peaks when the TiH_2 powder is finer.

The first step of the dehydrogenation process occurs at around 400°C to 500°C, which is below the β-transus temperature (882°C for pure Ti). The formation of the solid solution β-Ti(H) is explained by the fact that H is a β-stabilazing element. However, the β-transus temperature is never reached during the dehydrogenation, then, when the hydrogen content is significantly reduced (less than 5 at.%, according to the Ti-H phase diagram), the formation of the solid solution α-Ti(H) is observed [BOR2009].

Based on this knowledge, the HDH method consists on using the dehydrogenation phenomena to make dense titanium, through sintering.

In the HDH method, the particle will exhibit, after dehydrogenation, fresh titanium surface that will enhance the sintering process. The sintering therefore occurs as soon as the hydrogen is removed from the titanium.

Nonetheless, it has been shown that if the contact between TiH_2 particles is not good enough (i.e. the green density is too low), the HDH sintering will not be efficient and the final density will decrease. A threshold of 80% of relative green density for coarse TiH_2 and 70% for fine TiH_2 has been shown by Savvakin *et al.* and Wang *et al.* [SAV2012] [WAN2010].

The HDH sintering is done at 1400°C, above the β-transus. Therefore, the dehydrogenation will not follow the exact same steps. Between 25°C to 882°C, the dehydrogenation will lead to the formation of α-Ti(H) following:

$$\varepsilon\text{-}TiH_{1.92} \rightarrow \delta\text{-}TiH_x + \beta\text{-}Ti(H) + H_2\uparrow \rightarrow \alpha\text{-}Ti(H)$$

From there, the solid solution α-Ti(H) will be transformed into α-Ti or β-Ti, depends on the temperature. Then, above 882°C all the titanium will be transformed into β-Ti. And during the cooling, the β-Ti will turn into α-Ti, which is the final product.

However, the density of TiH_2 is lower than the one of Ti (3.92 $g.cm^{-3}$ to 4.5 $g.cm^{-3}$) which implies that the final volume will be lower than the starting one. This size reduction has to be compensated by the creation of contact between particles (during the cold compaction). The following figure illustrates the HDH sintering phenomena when the green density is above the threshold or not (i.e efficiency of the cold compaction).

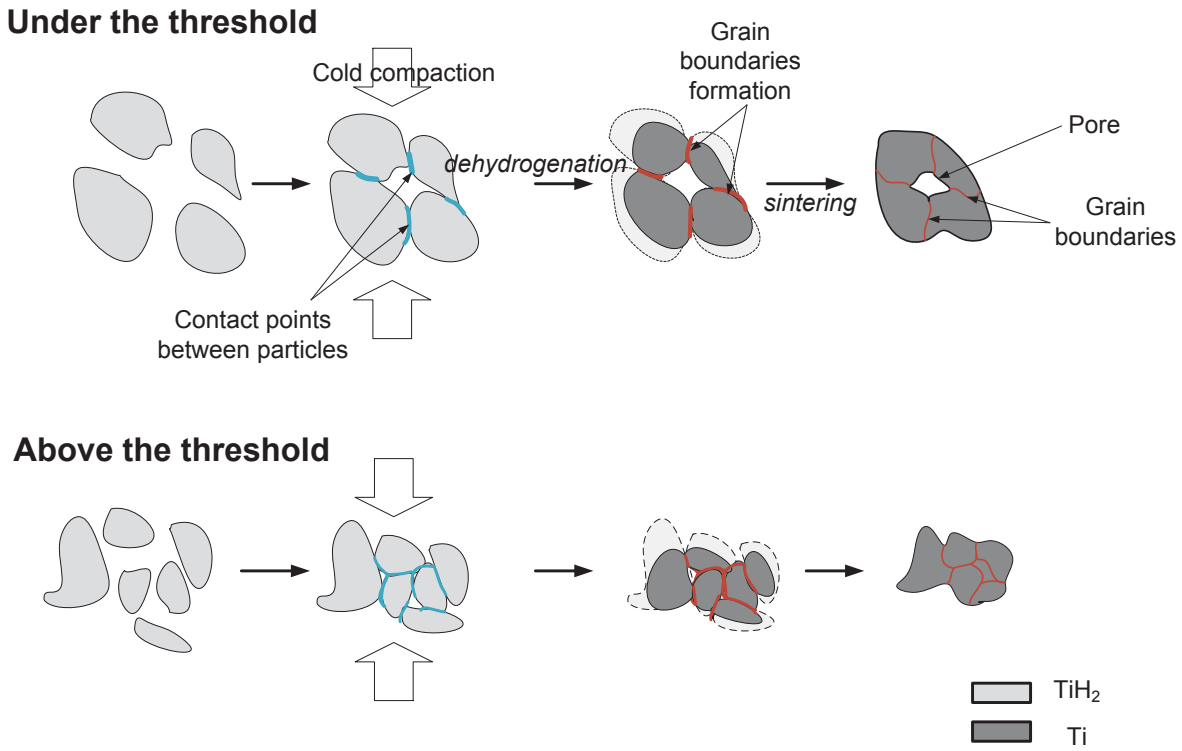

Figure 32: HDH sintering phenomena depending on the effect of the cold compaction

If the residual pore formed after the cold compaction is too important to be compensated by the sintering and the grain coarsening, then the pore will remains in the final microstructures.

Savvakin, Sun and Ivasishin, among others, have obtained dense Ti material starting with TiH_2 powder. It is important to note that the HDH process has also been done on Ti alloy powders (Ti-6Al-4V) with the same results. [IVA2005] [WAN2010]. Jang *et al.* and Jimoh *et al.* [JAN2007] [JIM2012] have done the HDH process combine with hot pressing techniques. The first work is focused on the recycling of titanium chips, which are hydrogenated, ball milled and then sintered by hot pressing. It is shown that if the temperature is not high enough, a TiH_2 phase is still present in the material. Two temperatures are tried in this work, 750°C and 1100°C, and the second leads to a pure Ti material, with a relative density of 96%. As comparison, the same process done on exclusively pure Ti powder, gives a relative density of 94.8%. The second work is focused on TMCs Ti-TiB-TiC through sintering of TiH_2 and B_4C powders. As explained before, they observe the formation of TiC and TiB reinforcements *in-situ*. It is shown in this work that adding more than 10 vol% of reinforcement necessitates the use of hot pressing to eliminate residual porosity, because free sintering does not completely lead to a fully dense material.

Other work have used non-conventional methods combine with the HDH such as SPS or microwave radiations. [PAS2013] [LUO2013]. The results show that the use of hydride powder leads to a fully dense material, which has a better residual porosity (lower), but the processes have to be done under oxygen-free atmosphere or high vacuum.

Regarding the different results, the HDH process, even though it is a fairly novel method, is promising for the production of TMCs. In this work, the HDH process will be used to obtain *in-situ* TiB_w/Ti composite and *ex-situ* TiC/Ti composite using either pressureless sintering or hot pressing.

Powder metallurgy processes offer the possibility to produce composite materials, while having the control of different parameters. These parameters, working temperature, strain or deformation

applied, time, or chemical reaction, will have a direct effect on the microstructure and the nature of the composite. This effect has an impact on the properties of the composites (particularly on the mechanical properties). Furthermore, the nature of the composite, *in-situ, ex-situ*, micrometric or nanometric will also have an impact on the mechanical properties. The next part will introduce a model for the calculation of mechanical properties of such composite, showing the influence on the different parameters controlled by the process or by the nature of the reinforcement.

IV. Mechanical Properties

As said before, mechanical properties of a single phase material are directly related to the microstructure, mainly due to its nature and the process used. When we talk about metal matrix nano-reinforced composites, the matrix properties and microstructure, the reinforcement properties, shape, size, distribution, interface with the matrix and volume fraction, and the influence of the processing on the matrix and the reinforcements will be the basis for strengthening mechanisms.

In this work, modelling of the investigated material has been done with the combination of the different mechanisms that have an influence on the strengthening of reinforced composites obtain through different PM processes. Like so, the influence of different parameters such as reinforcement size, distribution, volume fraction or even matrix microstructure has been investigated.

IV-1. The matrix

The metallic matrix is the most present component of a MMC and usually gives it its ductility. What gives a metallic material its properties is the polycrystallinity of its microstructure. Indeed, the grain boundaries strengthen the material by acting like barriers to the dislocation movement. A differentiation is made between the small-angle or low-angle grain boundary (LAGB) and the high-angle grain boundary (HAGB).

A grain boundary is a region in the polycrystalline metal where there is a mismatch between two crystalline orientations as represented on Figure 33. When the orientation mismatch between two grains is on the order of few degrees (commonly up to 15°), then it is called low angle grain boundary. At the contrary, when the angle of the misorientation is high and almost parallel to the grain boundary, it is called high angle grain boundary (Figure 33).

Usually, the LAGBs are not considered in the strengthening mechanism of metals, but some processing such as severe plastic deformation can increase the proportion of them and therefore have to be considered to estimate the mechanical properties.

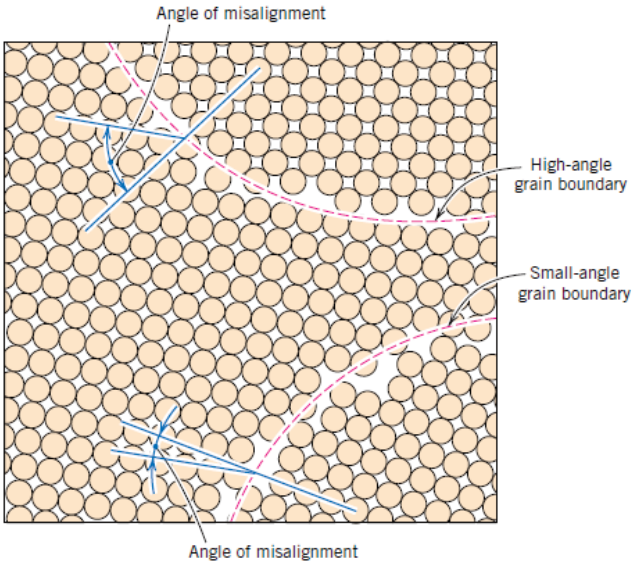

Figure 33: Schematic diagram of the LAGB and HAGB [CAL2007]

The strengthening mechanism related to the grain boundaries is described by the Hall-Petch (H-P) relationship. From it, the yield strength σ_y of a single phase material can be expressed as a function of the grain size. The relationship given by H-P between strength and grain size is:

$$\sigma_y = \sigma_0 + \frac{k}{\sqrt{D}} \tag{3.1}$$

where σ_0 is the friction stress, k is a constant and D the mean size grain. It appears from this equation that a smaller grain size will increase the strength in the material. However, it has been shown that when the grain size decrease upon a critical value D*, the H-P effect is no longer effective, and the material would tend to soften [MEY2006] [PAD2007]

When the proportion of LAGBs is substantial, the H-P model will have to take in consideration their strengthening effect $\Delta\sigma_{LAGB}$. This strengthening can be treated as dislocation strengthening, and is a contribution to the total strength [LUO2012a] [LUO2012b]. Its expression is:

$$\Delta\sigma_{LAGB} = M\alpha' G_m b\sqrt{\rho_\perp} \tag{3.2}$$

where M is the Taylor orientation factor, α' is a constant, G_m is the shear modulus, b is the Burgers vector of the dislocations, and $\rho_\perp$ is the dislocation density that will relates the fraction of LAGB in the materials. This value is hard to predict, but can be measured.

Therefore, if the strength contribution from HAGB is represented by $\Delta\sigma_{HAGB} = kD^{-1/2}$, the yield strength incorporating the contribution from LAGBs can be written as:

$$\sigma_y = \sigma_0 + \Delta\sigma_{HAGB} + \Delta\sigma_{LAGB} \tag{3.3}$$

IV-2. The composite

If most of the MMCs properties can be predicted from using simple rule of mixture (RoM), the strength need to be predicted by a different model. Indeed, there are different contributions that participate in the strengthening mechanism of discontinuous MMCs.

The shear lag model, or load bearing model, relates to the load transfer at the matrix-reinforcement interfaces. Applied to short fibre or particulate reinforcements, the load transfer is limited due to the small matrix-reinforcement interfaces. Logically, more loads can be transferred with increasing the volume fraction of the reinforcement, because for the same applied stress, the average load supported by the matrix would be lower. So, more stress is needed to plastically deform the matrix, resulting in increase in strength. Assuming the material yield when the matrix reaches its yield strength, an average strength can be expressed as:

$$\sigma_{yc} = \sigma_{ym}\left[\frac{V_r(S+2)}{2} + (1 - V_r)\right] \tag{3.4}$$

where c, m, r refer to composite, matrix and reinforcement, V is the volume fraction and S is the aspect ratio of the reinforcement defined by the ratio length over diameter (S=1 for a particulate reinforcement).

The Orowan strengthening is caused by the resistance of closely spaced hard particles to the passing of dislocations within a MMC, as presented on Figure 34. It has been described as a dislocation line movement disturbed by particles that are too strong to cut through. The dislocation line will bow between two particles and continue to move forward leaving a dislocation loop encircled the particles. This mechanism is related to the size of the particles and the distance between them (interparticle spacing λ).

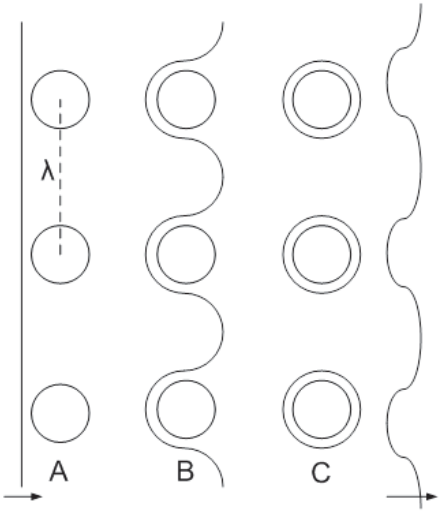

Figure 34: The Orowan process of dislocation movement A/ moving to the reinforcement particles B/ bowing between particles and C/ by passing the particles by leaving dislocation loop

It is widely acknowledged, however, that Orowan strengthening is not significant in the microsized particulate-reinforced MMCs, because the reinforcement particles are coarse and the interparticle spacing is large. The Orowan model, which describe the phenomena, exists since 1959 [ORO1959] and has been modified several times to improve the estimate of increase in flow stress in the MMnCs, reinforced with nano particles. One of the most used modifications for the MMnCs is the Orowan-Ashby Equation [ZHA2006b] [ZHA2008]:

$$\Delta\sigma_{Orowan} = \frac{0.13 G_m b}{\lambda} ln\frac{d_r}{2b} \tag{3.5}$$

where d_r is the reinforcement particles diameter. This equation considers an evenly dispersed composite, and does not consider the particles shape. The interparticle spacing, strictly dependent on the reinforcement distribution, has been estimated by two different models, the cubic model

(CM) [TAN1998] on Figure 35 and the face-centred cubic model (FCC) [KAI2011] on Figure 36.

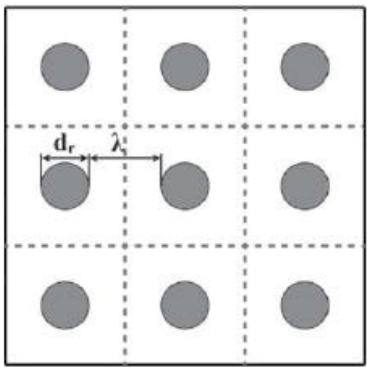

Figure 35: Cubic model for reinforcement distribution [TAN1998]

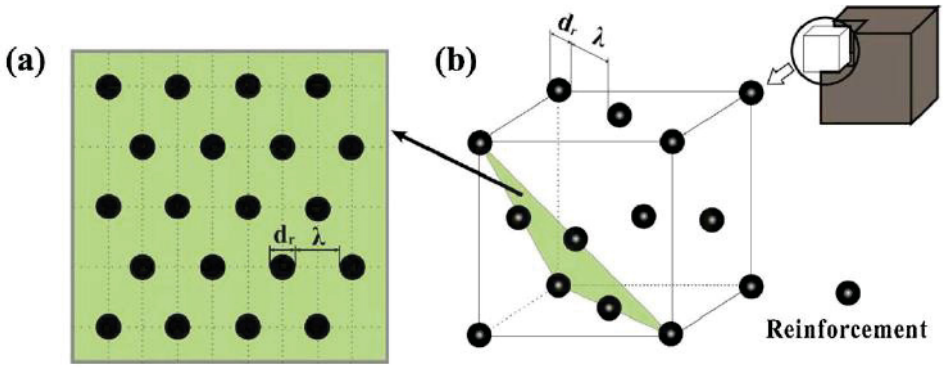

Figure 36: Face centered cubic model (a) closepacked (b) unit cell [KAI2011]

The main difference between these two models is the equations to calculate the inter-particle spacing λ between 2 reinforcement particles:

For the cubic model:

$$\lambda = d_r \left[\left(\frac{\pi}{6V_r} \right)^{\frac{1}{3}} - 1 \right] \tag{3.6}$$

For the face-centred cubic model:

$$\lambda = d_r \left[\left(\frac{\pi}{3\sqrt{2}V_r} \right)^{\frac{1}{3}} - 1 \right] \tag{3.7}$$

In the literature, the cubic model is the one used because the face-centred cubic model has been established in 2011. However, this FCC model shows promising agreement between experimental data and calculated ones.

The dislocation punching model takes in consideration the high dislocation density that exists in the matrix as a result of a thermal mismatch between the matrix and the reinforcement. The coefficient of thermal expansion (CTE) mismatch generates dislocations at the matrix-reinforcement interface. It has been expressed as:

$$\Delta\sigma_d = 1.25 G_m b \sqrt{\frac{\kappa\, \Delta T\, \Delta\alpha\, V_r}{b t_r (1 - V_r)}} \quad (3.8)$$

where κ is the geometrical factor that depends on the shape of the reinforcement (κ = 10 for short fibbers and 12 for spherical particles), and t_r the smallest value of the reinforcement dimensions (width, depth or height). Therefore, t_r is equal to d_r for spherical particles. [POL2010]

In MMnCs, all the different models cited above may be active simultaneously, depending on the size and shape of the reinforcement phase and on the processing of the material. The different strengthening mechanisms are combined using the improvement factor of each mechanism $f = \Delta\sigma/\sigma_y$. For the Load bearing, the improvement factor is f_l. For spherical particles, where R = 1, the expression is simplified to:

$$f_l = 0.5 V_r \quad (3.9)$$

When the aspect ratio becomes more important (R ≠ 1), the equation 3 is used to determine $\sigma_{ym}(1 + f_l)$. [NAR1985] The relative contribution of load-bearing effect is very small in nanocomposites due to the small volume fraction of nanoparticles

For the dislocation punching model, the improvement factor is expressed from the equation 3.8 as f_d.

$$f_d = \frac{\Delta\sigma_d}{\sigma_{ym}} \quad (3.10)$$

The Orowan model is associated with the improvement factor f_{Orowan}

$$f_{Orowan} = \frac{\Delta\sigma_{Orowan}}{\sigma_{ym}} \quad (3.11)$$

The improvement factors related to the grain-boundary strengthening as indicated by the equations 3.1 and 3.2 are f_{HAGB} and f_{LAGB} respectively for the HAGB and LAGB strengthening mechanisms

$$f_{HAGB} = \frac{k}{\sigma_{ym}\sqrt{D}} \quad (3.12)$$

$$f_{\mathrm{LAGB}} = \frac{\Delta\sigma_{LAGB}}{\sigma_{ym}} \quad (3.13)$$

Different models to predict the yield strength of a composite considering all the different improvement factors have been developed.

The multiplication model considers that f_l and f_d are dependent on each other [RAM1996].

The expression to determine the composite yield strength σ_{yc} is:

$$\sigma_{yc} = \sigma_{ym} \times (1 + f_l) \times (1 + f_d) \times (1 + f_{Orowan}) \quad (3.14)$$

This model shows good comparison with experimental data of the Mg-Al_2O_3 and Ti-Y_2O_3 MMnCs [CAS2006] [ZHA2008].

The addition model assumes that the different strengthening mechanisms are additive and are in agreement with the NiCr-based composite reinforced with nanosized Y_2O_3 and Al_2O_3. [ISL2001] [SRI2006].

$$\sigma_{yc} = \sigma_{ym}(1 + f_l + f_d + f_{Orowan}) \quad (3.15)$$

In both cases, σ_{ym} is the yield strength of the matrix after taking in consideration the grain boundary strengthening mechanisms shown in the equation 4.3.

In addition to the modelling made on the yield strength of composite, the variation of Young's Modulus E can be predicted using models. In composite with spherical reinforcements, the Halpin-Tsai is usually used to predict the Young's Modulus.

$$E_c = \frac{E_m(1 + 2SqV_r)}{1 - qV_r} \quad (3.16)$$

where E is the Young's Modulus and c, m and r represent respectively the composite, the matrix and the reinforcement, and q is a factor expressed as:

$$q = \frac{\left(\frac{E_r}{E_m}\right) - 1}{\left(\frac{E_r}{E_m}\right) + 2S} \quad (3.17)$$

However, this model assumes that all particles are perfectly aligned with the axis of measurement. When the reinforcement particles are randomly aligned, the Young's Modulus is expressed as:

$$E_c = \frac{3}{8}E_{11} + \frac{5}{8}E_{22} \quad (3.18)$$

with:

$$E_{11} = \frac{1 + 2Sq_LV_r}{1 - q_LV_r}E_m \quad (3.19)$$

$$E_{22} = \frac{1 + 2q_TV_r}{1 - q_TV_r}E_m \quad (3.20)$$

E_{11} and E_{22} represent the Young's Modulus of the unidirectional fibre composites, respectively in the longitudinal and transversal direction. The factors q_L and q_T are therefore expressed as:

$$q_L = \frac{\left(\frac{E_r}{E_m}\right) - 1}{\left(\frac{E_r}{E_m}\right) + 2S} \quad (3.21)$$

$$q_T = \frac{\left(\frac{E_r}{E_m}\right) - 1}{\left(\frac{E_r}{E_m}\right) + 2} \quad (3.22)$$

This model is in good agreement with the literature data [GOR2003] [MEN2007] [MEN2009] and gives a good idea of the theoretical Young's Modulus of a discontinuously reinforced composites.

However some critical factors are considered to validate those models: A full density, a good adhesion between the reinforcement particles and the matrix, and a uniform distribution of the reinforcement particles within the matrix. This is where the understanding and the control of the processes used to fabricate the composites are critical. To validate the strengthening mechanisms assumption, it is important to know the effects of the processing on the matrix and the reinforcements.

These models will be used in the next chapter to estimate the effect of different parameters (grain

size, volume fraction of the reinforcement...) on the investigated composites, and give the expected properties of ideal composite materials.

V. Conclusion

Titanium, as presented on this chapter, is a material with a wide range of properties for different applications, in particular where good strength is required. Also, applications that required good mechanical properties usually use titanium because it is a very versatile material. Indeed, the alloying possibility of titanium give the opportunity to have an effect on the microstructure (grain size, grains shape…) that have a direct effect on the properties. Another type of material, taking advantages of the properties of titanium, is possible, the titanium matrix composite. In addition of the properties of the Ti matrix, the reinforcements will introduce new kind of properties, which will depend on the reinforcement nature, shape, volume fraction, interaction with the matrix etc… These reinforcements can be either in-situ formed inside the matrix, or ex-situ added to the matrix. Also, the size of the reinforcement will have a different impact whether they are nanometer sized or micrometer. Indeed, nanometer sized reinforcement will have the same benefits of micrometer sized reinforcements, with the addition of combining properties that are considered exclusive when using micrometric reinforcement, such as ductility and high strength.

In this work, the processes selected to obtain the TMC are two powder metallurgy processes. After a presentation of general PM processes, a more detailed presentation on the selected processes, hydrogenation/dehydrogenation and Equal Channel Angular Pressing has been made. Both are presented promising to obtain good TMC material, with each having a different influence on the microstructure, and using different mechanism to fabricate the composite. HDH with use the dehydrogenation as leverage to the densification, in pressureless sintering or hot pressing, and ECAP uses severe plastic deformation of the powder to get fully dense material.

In this work, the objective is to fabricate composites using different PM ways, HDH (pressureless and hot pressing) and ECAP, and study the influence of the process on the final material. To do so, the processes are controlled from the obtaining of the starting powder, to the characterization of the final composite. Two types of composite are investigated, the in-situ TiB/Ti and the ex-situ TiC/Ti.

The next chapter will introduce first a modeling work on the strength of the investigated composite. To understand and comment the properties of a fabricated material, it is important to understand the impact of characteristics that can be modified with the different processes on the different composites. The influence of parameters such as grain size of titanium, volume particles of reinforcement, etc… will be investigated using the models proposed in this chapter. Then a prediction of the considered TMC will be made.

To understand the specificities of the chosen PM processes, a detailed explanation for the obtaining of the different starting powder (either for HDH or ECAP) will be done. It covers the preparation from the as received powders to the ready-to-process composite powder. Following that, a presentation of the different PM process settings used to obtain fully dense material, with the different parameters, will be done.

A presentation of each aspects of the preparation of the TMC will help to understand the different properties of the final materials. The properties of the prepared composite using the different powder metallurgy processes will be the main point of the third chapter.

List of Figures and Tables

Bibliography

[ALE1998a] - I.V. Alexandrov, Y.T. Zhu, T.C. Lowe, R.K. Islamgaliev and R.Z. Valiev, *Microstructures and Properties of Nanocomposites Obtained through SPTS Consolidation of Powders*, Metallurgical and Materials Transaction, 29A, 9, pp.2253-2260, (1998)

[ALE1998b] - I.V. Alexandrov, Y.T. Zhu, T.C. Lowe, R.K. Islamgaliev and R.Z. Valiev, *Severe plastic deformation: new technique for powder consolidation and grain size refinement,* Powder Metallurgy, 41, 1, pp.11-13 (1998)

[BEN1970] - J.S. Benjamin, *Dispersion Strengthened Superalloys by Mechanical Alloying,* Metallurgical Transactions, 1, pp.2943-2952, (1970)

[BEN1974] - J.S. Benjamin, T.E. Volin, *The Mechanism of Mechanical Alloyin,* Metallurgical Transactions, 5, pp.1929-1935, (1974)

[BET2007] - D. Bettge, B. Günther, W. Wedell, P.D. Portella, J. Hemptenmacher, P.W.M. Peters, B. Skrotzki, *Mechanical behavior and fatigue damage of a titanium matrix composite reinforced with continuous SiC fibers,* Materials Science and Engineering A, 452–453, pp.536–544, (2007)

[BHO2003a] - V. Bhosle, E.G. Baburaj, M. Miranova and K. Salama, *Dehydrogenation of Nanocrystalline TiH_2 and Consequent Consolidation to Form Dense Ti,* Metallurgical and Materials Transactions A, 34A, pp.2793-2800, (2003)

[BHO2003b] - V. Bhosle, E.G. Baburaj, M. Miranova and K. Salama, *Dehydrogenation of TiH_2,* Materials and Engineering, A356, pp.190-199, (2003)

[BOR2009] - C. Borchersa, T.I. Khomenko, A.V. Leonov and O.S. Morozova, *Interrupted thermal desorption of TiH_2,* Thermochimica Acta, 493, pp.80‑84, (2009)

[BOU2002] - D. Bouvard *et al.*, *Métallurgie des Poudres,* Ed. Lavoisier, Hermes Science, (2002)

[CAS2005] - V. de Castro, T. Leguey, A. Muñoz, M.A. Monge and R. Pareja, *Relationship between hardness and tensile tests in titanium reinforced with yttria nanoparticles,* Materials Science and Engineering A, 400–401, pp.345–348, (2005)

[CAS2006] - V. de Castro, T. Leguey, A. Muñoz, M.A. Monge and R. Pareja, *Microstructure and tensile properties of Y2O3-dispersed titanium produced by arc melting,* Materials Science and Engineering A, 422, pp.189–197, (2006)

[CAL2007] - William D. Callister, Jr., *Materials Science and Engineering: An Introduction*, Ed. John Wiley & Sons, Inc, 7th edition, (2007)

[CAL2008] - *www.calphad.com/titanium-boron.html*

[CHA2006] - N. Chawla, K.K. Chawla, *Metal Matrix composites*, Ed.Springer, (2006)

[CHE2003] - Y.C. Chen, Y.Y. Huang, C.P. Chang and P.W. Kao, *The effect of extrusion temperature on the development of deformation microstructures in 5052 aluminium alloy processed by equal channel angular extrusion*, Acta Materialia, 51, pp.2005–2015, (2003)

[CHE2007] - S. Cheng, Y.H. Zhao, Y.T. Zhu, E. Ma, *Optimizing the strength and ductility of fine structured 2024 Al alloy by nano-precipitation*, Acta Materialia, 55, pp.5822–5832, (2007)

[CHO2005] - G. Chollon, R. Naslain, C. Prentice, R. Shatwell, P. May, *High temperature properties of SiC and diamond CVD-monofilaments*, Journal of the European Ceramic Society, 25, pp. 929–1942, (2005)

[DON2000] - M. J. Donachie, *Titanium – A Technical Guide*, 2nd Edition, ASM International, (2000)

[ECK1992] - J. Eckert, J. C. Holzer, C. E. Krill, III, and W. L. Johnson, *Structural and thermodynamic properties of nanocrystalline fcc metals prepared by mechanical attrition*, Journal of Materials Research, 7, 7, pp.1751-1762, (1992)

[EDA2011] - K. Edalati, H. Iwaoka, Z. Horita, M. Konno, T. Sato, Unusual hardening in Ti/Al2O3 nanocomposites produced by high-pressure torsion followed by annealing, Materials Science and Engineering A, 529, pp. 435‑441, (2011)

[FER2001] - H. Ferkel, B.L. Mordike, Magnesium strengthened by SiC nanoparticles, Materials Science and Engineering A, 298, pp.193–199, (2001)

[FIG2007] - R.B. Figueiredo, P.R. Cetlin, T.G. Langdon, The processing of difficult-to-work alloys by ECAP with an emphasis on magnesium alloys, Acta Materialia ,55, pp. 4769–4779, (2007)

[FIG2012] - R.B. Figueiredo, T.G. Langdon, *Fabricating Ultrafine-Grained Materials through the Application of Severe Plastic Deformation: a Review of Developments in Brazil*, Journal of Materials Research and Technology, 1, pp.55–62, (2012)

[FRU2012] - J.B. Fruhauf, J. Roger, O. Dezellus, S. Gourdet, N. Karnatak, N. Peillon, S. Saunier, F. Montheillet, C. Desrayaud, *Microstructural and mechanical comparison of Ti + 15%TiCp composites prepared by free sintering, HIP and extrusion*, Materials Science and Engineering A 554, pp.22– 32, (2012)

[GAL2002] - M. Galanty, P. Kazanowski, P. Kansuwan, W.Z. Misiolek, *Consolidation of metal powders during the extrusion process,* Journal of Materials Processing Technology, 125–126, pp.491–496, (2002)

[GAR2006] - M. Garcia de Cortazar, PhD Thesis, *Development of a new reinforced titanium alloy : Basic research and technological transfert for the Ti-6Al-4V/TiB material,* Université Bordeaux 1, (2006)

[GOR1998] - S. Gorsse and Y. Le Petitcorps, A new approach in the understanding of the SiC/Ti reaction zone composition and morphology, Composites Part A, 29A, pp.1221–1227, (1998)

[GOR2003] - S. Gorsse, Y. Le Petitcorps, S. Matar, F. Rebillat, *Investigation of the Young's modulus of TiB needles in situ produced in titanium matrix composite*, Materials Science and Engineering A, 340, pp. 80-/87, (2003)

[GOU2009] - S. Goussous, W. Xu, X. Wu, K. Xia, *Al–C nanocomposites consolidated by back pressure equal channel angular pressing*, Composites Science and Technology, 69, pp.1997–2001, (2009)

[GU2010] - D. Gu, W. Meiners, Y-C. Hagedorn, K. Wissenbach and R. Poprawe, *Structural evolution and formation mechanisms of TiC/Ti nanocomposites prepared by high-energy mechanical alloying,* Journal of Physics D: Applied Physics, 43, pp.1-12, (2010)

[GUT2007] - I. Gutierrez-Urrutia, M.A. Muñoz-Morris, D.G. Morris, *Contribution of microstructural parameters to strengthening in an ultrafine-grained Al–7% Si alloy processed by severe deformation*, Acta Materialia, 55, pp.1319–1330, (2007)

[HOR2005] - Z. Horita, K. Ohashi, T. Fujita, K. Kaneko, T.G. Langdon, *Achieving High Strength and*

High Ductility in Precipitation-Hardened Alloys, Advanced Materials, 17, pp.1599-1602, (2005)

[HUA2004] - W.H. Huang, C.Y. Yu, P.W. Kao, C.P. Chang, *The effect of strain path and temperature on the microstructure developed in copper processed by ECAE,* Materials Science and Engineering A, 366, pp. 221–228, (2004)

[ISL2001] - R.K. Islamgaliev, N.F. Yunusova, I.N. Sabirov, A.V. Sergueev, R.Z. Valiev, *Deformation behavior of nanostructured aluminum alloy processed by severe plastic deformation,* Materials Science and Engineering A, 319–321, pp.877–881, (2001)

[IVA1999a] - O. M. Ivasishin, A. N. Demidik, and D. G. Savvakin, *Use of titanium Hydride for the Synthesis of Titanium Aluminides from powder materials,* Powder Metallurgy and Metal Ceramics, 38, pp.9-10, (1999)

[IVA2005] - O.M. Ivasishin, D.G. Savvakin, I.S. Bielov, V.S. Moxson, V.A. Duz, R. Davies, C. Lavender, *Microstructure and Properties of Titanium Alloys Synthesized from Hydrogenated Titanium Powders,* Materials Science and Technology, pp151-158, (2005)

[IWA1996] - Y. Iwhashi, J. Wang, Z. Horita, M. Nemoto, T.G. Langdon, *Principle of Equal-Channel Angular Pressing For The Processing of Ultra-Fine Grained Materials,* Scripta Materialia, 35, 2, pp.143-146, (1996)

[JAN2007] - J. M. Jang, W. Lee, S. H. Ko, I. H. Kim, *Titanium hydriding and Consolidation for Recycling of Titanium tuning Chip,* Advanced Materials Research, 24-25, pp.171-174, (2007)

[JIA2011] - Hai-tao Jiang, Ji-xiong Liu, Zhen-li Mi, Ai-min Zhao, and Yan-jun Bi *Texture evolution of commercial pure Ti during cold rolling and recrystallization annealing,* International Journal of Minerals, Metallurgy and Materials, 19, N°6, p.530 (2011)

[JIM2012] - A. Jimoh, I. Sigalas, M. Hermann, *In Situ Synthesis of Titanium Matrix Composite (Ti-TiB-TiC) through Sintering of TiH_2-B_4C,* Materials Sciences and Applications, 3, pp.30-35, (2012)

[KAI2011] - X.Z. Kai, Z.Q. Li, W.L. Zhang, G.L. Fan, L. Jiang, W.J. Lu, D. Zhang, *A model for volume fraction and/or particle size selection in metal matrix composite,* Materials Science and Engineering A, 530, pp.574–579, (2011)

[KAN2004] - Yung-Chang Kang, Sammy Lap-Ip Chan, *Tensile properties of nanometric Al_2O_3 particulate-reinforced aluminum matrix composites*, Materials Chemistry and Physics, 85, pp.438–443, (2004)

[KIM2008] - Jin Young Kim, Kyung-Tae Park, In Ok Shim and Soon Hyung Hong, *Globularization Behavior of ELI Grade Ti-6Al-4V Alloy during Non-Isothermal Multi-Step Forging*, Materials transactions, Vol. 49, No. 1 pp. 215 to 223, (2008)

[KNE2013] - Marko Knezevic, RicardoA.Lebensohn, OanaCazacu, Benoit Revil-Baudard, Gwenaelle Proust, Sven C.Vogel, MichaelE.Nixon, *Modelling bending of α titanium with embedded polycrystal plasticity in implicit finite elements*, Materials Science & Engineering, A 564, pp.116–126 (2013)

[KON1989] - D.G. Konitzer, M.H. Loretto, *Microstructural assessment of Ti6A14V-TiC metal-matrix composite*, Acta Metallurgica Volume 37, Issue 2, Pages 397–40, (1989)

[LEE1998] - P-Y. Lee, J-L. Yang, H-M. Lin, *Amorphization behaviour in mechanically alloyed Ni–Ta powders,* Journal of Materials Science, 33, pp.235-239, (1998)

[LEY2003] - Leyens *et al. Titanium and Titanium Alloys Fundamentals and Applications*, Edited by C. Leyens, M. Peters, (2003)

[LU2008] - W.J. Lu, L. Xiao, K. Geng, J.N. Qin, D. Zhang, *Growth mechanism of in situ synthesized TiBw in titanium matrix composites prepared by common casting technique*, Material Characterization, 59, pp.912-919, (2008)

[LUI2012] - E. Lui, PhD thesis, *Multiphase and Multiscale Al-Ti Alloys Consolidated by Severe Plastic Deformation,* Department of Mechanical Engineering, The University of Melbourne, (2012)

[LUO2012a] - P. Luo, D.T. McDonald, W. Xu, S. Palanisamy, M.S. Dargusch and K. Xia, *A modified Hall–Petch relationship in ultrafine-grained titanium recycled from chips by equal channel angular pressing,* Scripta Materialia, 66, pp.785–788, (2012)

[LUO2012b] - P. Luo, D.T. McDonald, S.M. Zhu, S. Palanisamy, M.S. Dargusch, K. Xia, *Analysis of microstructure and strengthening in pure titanium recycled from machining chips by equal channel angular pressing using electron backscatter diffraction,* Materials Science and Engineering A, 538, pp.252‐258, (2012)

[LUO2013] - S.D. Luo, Y.F. Yang, G.B. Schaffer and M. Qian, *Novel fabrication of titanium by pure microwave radiation of titanium hydride powder,* Scripta Materialia, 69, pp.69–72, (2013)

[LUT2003] - G. Lütjering, J.C. Williams, *Titanium*, Ed. Springer, (2003)

[MA2000] - Z.Y. Ma, S.C. Tjong and L. Gen, In-Situ Ti-tiB metal-matrix composite prepared by a reactive pressing process, Scripta Mater., 42, pp.367-373, (2000)

[MCC1994] - C. McCullough, H. E. Deve, T. E. Channel, *Mechanical response of continuous fiber-reinforced Al_2O_3-Al composites produced by pressure infiltration casting,* Materials Science and Engineering, A 189, pp.147-154, (1994)

[MEN2007] - Q. Meng, H. Feng, D. Jia, Y. Zhou, *Young's Modulus of in situ TiB Whiskers in Ti metal Matrix Composites,* Key Engineering Materials, 353-358, pp.365-368, (2007)

[MEN2009] - Q. Meng, H. Feng, G. Chen, R.Yu, D. Jia, Y. Zhou, *Defects formation of the in situ reaction synthesized TiB whiskers*, Journal of Crystal Growth, 311, pp.1612–1615, (2009)

[MEY2006] - M.A. Meyers, A. Mishra, D.J. Benson, *Mechanical properties of nanocrystalline materials,* Progress in Materials Science, 51, pp.427–556, (2006)

[MIR2005] - D.B. Miracle, *Metal matrix composites – From science to technological significance,* Composites Science and Technology 65, pp.2526–2540, (2005)

[MON2011] - I. Montealegre Melendez, E. Neubauer, P. Angerer, H. Danninger, J.M. Torralba, *Influence of nano-reinforcements on the mechanical properties and microstructure of titanium matrix composites*, Composites Science and Technology, 71, pp.1154–1162, (2011)

[MOR2010] - Andreas Mortensen and Javier Llorca, *Metal Matrix Composite*, Annu. Rev. Mater. Res., 40, pp.243-270 (2010)

[NAL2002] - R.K. Nalla, B.L. Boyce, J.P. Campbell, J.O. Peters and R.O. Ritchie, Influence of Microstructure on High-Cycle Fatigue of Ti-6Al-4V: bimodal vs. Lamellar Structures, Metallurgical and Materials Transaction A, 33A, pp.899-918, (2002)

[NAR1985] - V.C. Nardonne, K.M. Prewo, *On the Strength of Discontinuous Silicon Carbide Reinforced Aluminum Composites,* Scripta Metallurgica, 20, pp.43-48, (1985)

[NIX2010] - Michael E. Nixon, Oana Cazacu, Ricardo A. Lebensohn, Anisotropic response of high-purity a-titanium*: Experimental characterization and constitutive modelling*, International Journal of

Plasticity, 26, pp.516–532 (2010)

[ORO1959] - E. Orowan, *Internal Stresses and Fatigue in Metals.* Internal Stresses FA, pp.59-80, (1959)

[PAD2007] - K.A. Padmanabhan, G.P. Dinda, H. Hahn, H. Gleiter, *Inverse Hall–Petch effect and grain boundary sliding controlled flow in nanocrystalline materials,* Materials Science and Engineering A, 452–453, pp.462–468, (2007)

[PAN2003] - K.B. Panda, K.S. Ravi Chandran, *Synthesis of Ductile Titanium–Titanium Boride (Ti-TiB) Composites with a Beta-Titanium Matrix: The Nature of TiB Formation and Composite Properties*, Metallurgical and Materials Transactions A, 34A, pp.1371-1385, (2003)

[PAS2013] - C.Pascu, O. Gingu, P. Rotaru, I. Vida-Simit, A. Harabor, N. Lupu, *Bulk titanium for structural and biomedical applications obtaining by spark plasma sintering (SPS) from titanium hydride powder,* Journal of Thermal Analysis and Calorimetry, 113, pp.849-857, (2013)

[POL2010] - C. Poletti, G. Höltl, *Mechanical properties of particle reinforced titanium and titanium alloys*, Kovove Mater. 48, pp.87–95, (2010)

[QIN2003] - Ye-Xia Qin, Wei-Jie Lu, Xian-Feng Sheng, Zhi-Feng Yang, and Di Zhang, *Mechanical Properties of in situ Synthesized Titanium Matrix Composites at Elevated Temperature*, Materials Transactions, Vol. 44, No. 11, pp2282-2287, (2003)

[RAM1996] - N. Ramakrishnan, *An Analytical Study on Strengthening of Particulate Reinforced Metal Matrix Composites,* Acta Materialia, 44, 1, pp.69-77, (1996)

[SAB2005] - I. Sabirov, O. Kolednik, R.Z. Valiev, R. Pippan, *Equal channel angular pressing of metal matrix composites: Effect on particle distribution and fracture toughness,* Acta Materialia, 53, pp.4919–4930, (2005)

[SAL2009] - H.G. Salem, S. El-Eskandarany, A. Kandil, and H. Abdul Fattah, *Bulk Behavior of BallMilled AA2124 Nanostructured Powders Reinforced with TiC,* Journal of Nanomaterials, 2009, pp.1-12, (2009)

[SAV2012] - D. H. Savvakin, M.M. Humenyak, M.V. Matviichuk, and O.H. Molyar, *Role of Hydrogen in the Process of Sintering of Titanium Powders,* Materials Science, 47, 5, pp.651-661, (2012)

[SEG1974] – V.M. Segal, *Methods of Stress-Strain Analysis in Metal forming,* Physical Technical Institute Academy of Sciences of Buelorussia, (1974)

[SEG1995] – V.M. Segal, *Materials processing by simple shear,* Materials Science and Engineering A, 197, pp.157-164, (1995)

[SHE2011] - Xiangbo Shen, Zhaohui Zhang, Sai Wei, Fuchi Wang, Shukui Lee*, Microstructures and mechanical properties of the in situ TiB–Ti metal–matrix composites synthesized by spark plasma sintering process*, Journal of Alloys and Compounds, 509, pp.7692– 7696, (2011)

[SIL2012] - J.F. Silvain, C. Vincent, T. Guillemet, A. Veillere, J.M. Heintz, *Innovative process for submicronic Cu particle deposition onto various substrate,* Materials Research Bulletin 47, pp.500–503, (2012)

[SOB1994] - W.O. Soboyevo, R.J. Lederich and S.M.L. Sastry, *Mechanical behaviour of damage tolerant TiB whisker-reinforced in-situ titanium matrix composites*, Acta metallurgica materilia, 42, 8, pp.2579-2591, (1994)

[SRI2006] - Dheepa Srinivasan, Reed Corderman, P.R. Subramanian, *Strengthening mechanisms (via hardness analysis) in nanocrystalline NiCr with nanoscaled Y_2O_3 and Al_2O_3 dispersoids,* Materials Science and Engineering A 416, pp.211–218, (2006)

[STO1999] - V.V. Stolyarov, Y.T. Zhu, T.C. Lowe, R.K. Islamgaliev and R.Z. Valiev, *A Two Step SPD processing of Ultrafine-Grained Titanium,* NanoStructured Materials, 11, 7, pp.947–954, (1999)

[STO2001] - V.V. Stolyarov, Y.T. Zhu, I.V Alexandrov, T.C. Lowe, and R.Z. Valiev, *Influence of ECAP routes on the microstructure and properties of pure Ti,* Materials Science and Engineering A, 299, pp.59–67, (2001)

[STO2003] - V.V. Stolyarov, Y.T. Zhu, I.V Alexandrov, T.C. Lowe, and R.Z. Valiev, *Grain refinement and properties of pure Ti processed by warm ECAP and cold rolling,* Materials Science and Engineering A, 343, pp.43- 50, (2003)

[SUB1993] - R.B. Subramanyam, *Some recent Innovations in the Kroll process of Titanium sponge production,* Bulletin of Material Science, 16, 6, pp.433-451,(1993)

[SUR2001] - C. Suryanarayana, *Mechanical alloying and milling,* Progress in Materials Science, 46, pp.1-184, (2001)

[TAN1998] - M.J. Tan, X. Zhang*, Powder metal matrix composites: selection and processing,* Materials Science and Engineering A, 244, pp.80–85, (1998)

[THR2009a] - T. Threrujirapapong, K. Kondoh, H. Imai, J. Umeda, B. Fugetsu, *Titanium Matrix Composite Reinforced with In-situ Formed TiC Using Carbon Black Nano Particles via Wet Process*, Transaction of JWRI, 38, 1, pp.13-17, (2009)

[THR2009b] - T. Threrujirapapong, K. Kondoh, H. Imai, J. Umeda, B. Fugetsu, *Mechanical Properties of a Titanium Matrix Composite Reinforced with Low Cost Carbon Black via Powder Metallurgy Processing*, Materials Transactions, Vol. 50, No. 12, pp. 2757 to 2762, (2009)

[TJO2007] - Sie Chin Tjong**,** *Novel Nanoparticle-Reinforced Metal Matrix Composites with Enhanced Mechanical Properties*, Advanced Engineering Materials, 9, N°.8, pp.639-652, (2007)

[TJO2008] - S.C. Tjong, Yiu-Wing Mai, *Processing-structure-property aspects of particulate- and whisker-reinforced titanium matrix composites*, Composites Science and Technology, 68, pp.583–601, (2008)

[VAL1991] - R.Z. Valiev, N. A. Krasiinikov and N. K. Tsenev, *Plastic deformation of alloys with submicron-grained structure,* Materials Science and Engineering A, 137, pp.35-40, (1991)

[VAL1993] - R. Z. Valiev, A. V. Korznikov and R. R. Mulyukov, *Structure and properties of ultrafine-grained materials produced by severe plastic deformation,* Materials Science and Engineering A, 168, pp.141-148, (1993)

[VAL1997] - R. Z. Valiev, *Structure and mechanical properties of ultrafine-grained metals,* Materials Science and Engineering A, 234-236, pp.59-66, (1997)

[VAL2006] - R. Z. Valiev, T.G. Langdon, *Principles of equal-channel angular pressing as a processing tool for grain refinement,* Progress in Materials Science, 51, pp.881–981 (2006)

[VIS2007] - V. Viswanathan, T. Laha, K. Balani, A. Agarwal, S. Sea, *Challenges and advances in nanocomposite processing techniques,* Materials Science and Engineering, R 54, pp.121–285, (2006)

[WAG2003] - A.J. Wagoner Johnson, K.S. Kumar, C.L. Briant, Deformation Mechanisms in Ti-6Al-4V/TiC Composites, Metallurgical and Materials Transactions A, 34A, pp.1870-1877, (2003)

[WAN2008] - *J.F. Wang, X.Y. Liu, B. Luan, Fabrication of Ti/polymer biocomposites for load-bearing implant applications*, Journal of Materials Processing Technology, 197, pp.428-433, (2008)

[WAN2010] - H. Wang, M. Lefler, Z.Z. Fang, T. Lei, S. Fang, J. Zhang and Q. Zhao, *Titanium and Titanium Alloy via Sintering of TiH_2,* Key Engineering Materials, 436, pp.157-163, (2010)

[WEI2012] - Chongbin Wei, Xiaoyan Song, Jun Fu, Xiaosen Lv, Haibin Wang, Yang Gao, Shixian Zhao and Xuemei Liu, *Effect of Carbon Addition on Microstructure and Properties of WC–Co Cemented Carbides,* J. Mater. Sci. Technol., 28(9), pp.837–843, (2012)

[XIA1997] - S. Xiang, K. Matsuki, N. Takatsuji, M. Tokizawa, T. Yokote, J. Kusui, K. Yokoe, *Microstructure and mechanical properties of PM 2024Al±3Fe±5Ni alloy consolidated by a new process, equal channel angular pressing,* Journal of Materials Science Letters, 16, pp.1725-1727, (1997)

[XIA2001] - K. Xia, J. Wang, *Shear, Principal, and Equivalent Strains in Equal-Channel Angular Deformation,* Metallurgical and Materials Transactions A, 32A, pp.2639-2647, (2001)

[XIA2010] - K. Xia, *Consolidation of Particles by Severe Plastic Deformation: Mechanism and Applications in Processing Bulk Ultrafine and Nanostructured Alloys and Composites,* Advanced Engineering Materials, 12, 8, pp.724-729, (2010)

[XU2007] - C. Xu, K. Xia, T.G. Langdon*, The role of back pressure in the processing of pure aluminium by equal-channel angular pressing,* Acta Materialia, 55, pp.2351–2360, (2007)

[XU2008] - W. Xu, X. Wu, D. Sadedin, G. Wellwood, and K. Xia, *Ultrafine-grained titanium of high interstitial contents with a good combination of strength and ductility,* Applied Physic Letter, 92, 011924, pp.1-3, (2008)

[XU2009] - W. Xu, X. Wu, T. Honma, S.P. Ringer, K. Xia, *Nanostructured Al–Al2O3 composite formed in situ during consolidation of ultrafine Al particles by back pressure equal channel angular pressing,* Acta Materialia, 57, pp.4321–4330, (2009)

[XUE2011] - Y.Xue, L.H.Lang, G.L.Bu, L.Li, *Densification Modeling of Titanium Alloy Powder during Hot Isostatic Pressing,* Science of Sintering, 43, pp.247-260, (2011)

[YAM2000] - A. Yamashita, D. Yamaguchi, Z. Horita, T.G. Langdon, *Influence of pressing temperature on microstructural development in equal-channel angular pressing,* Materials Science and Engineering A, 287, pp.100–106 (2000)

[YAM2007] - T. Yamamoto, A. Otsuki, K. Ishihara, P.H. Shingu, *Synthesis of near net shape high density TiB:Ti composite*, Materials Science and Engineering, A239–240, pp.647–651, (1997)

[ZHA2006a] - Y-H Zhao, X-Z Liao, S. Cheng, E. Ma and Y.T. Zhu, *Simultaneously Increasing the Ductility and Strength of Nanostructured Alloys*, Adv. Mater, 18, pp.2280–2283, (2006)

[ZHA2006b] - Z. Zhang, D.L. Chen, *Consideration of Orowan strengthening effect in particulate-reinforced metal matrix nanocomposites: A model for predicting their yield strength,* Scripta Materialia, 54, pp.1321–1326, (2006)

[ZHA2007] - D. Zhang, J. Lu, W. Lu, J. Qin, *Study on In-situ Synthesized Titanium Matrix Composites*, Materials Science Forum, Vols. 561-565, pp 751-756, (2007)

[ZHA2008] - Z. Zhang, D.L. Chen, *Contribution of Orowan strengthening effect in particulate-reinforced metal matrix nanocomposites,* Materials Science and Engineering A, 483–484, pp.148–152, (2008)

[ZHA2012a] - P. Li, X. Zhang, K-M. Xue, X. Li, *Effect of equal channel angular pressing and torsion on SiC-particle distribution of SiCp–Al composites*, Transactions of Nonferrous Metals Society of China, 22, pp.402−407, (2012)

[ZHA2012b] - H. Zhang, S. Gu, J. Yi, *Fabrication and properties of Ti(C,N) based cermets reinforced by nano-CBN particles*, Ceramics International, 38, pp.4587–4591, (2012)

Chapter II - Modelling, starting powders and process

I. Introduction

This chapter will introduce the different titanium based composite materials investigated and the different powder metallurgy processes used in this work.

The selected techniques to process the investigated titanium matrix composites are the hydrogenation/dehydrogenation techniques, and the equal channel angular pressing techniques. Each of them will have a different influence on the final microstructure of the material, especially because of their difference of working temperature, and because of the deformation induced to the material. A modelling investigation will show the influence of the process use on the mechanical properties of the material. Through modelling, and investigation of each parameter (microstructure, reinforcement...) that can have an influence on the final material is done, and a general trend on what gives better properties has emerged.

The hydrogenation/dehydrogenation sintering techniques requires hydrogenated titanium as starting powder. Even if commercial TiH_2 powder is available, the one used in this work has been obtain after hydrogenation of titanium sponge. The fact that TiH_2 is slightly expensive (about 600€/kg, Sigma Aldrich) and the fact that an access to Ti hydrogenation was available made it more convenient to prepare the TiH_2 from Ti sponge (200€/kg, alfa aeser, for small quantities, down to 15€/kg for hundreds of kg). Moreover, it allows having a better control on the properties of the starting powder. For example, the particle size will be controlled using ball milling. Once the matrix powder is obtained, the reinforcement powder can be added and the HDH processes (free sintering or hot pressing) can be done.

The ECAP process does not require any modification of the starting titanium powder prior densification. However, the mixing between the reinforcement (TiC) and the matrix powders requires several hours of ball milling to be considered complete. A review of all the different steps that lead to a composite powder Ti/TiC to be process through ECAP is presented.

In this chapter, a modelling of the investigated materials properties is presented. The influence of each parameter that can be changed with the investigated powder metallurgy method is shown. Then, preparation of the powder used during the HDH process and the powder used in the ECAP process is detailed, from the initial powders (matrix and reinforcements) to the cold compacted and ready-to-process composite powder. The influence that each step can have on the powder and the way they can be controlled is explained. Finally, the selected parameters of each process used to obtain the dense composites are detailed.

II. Modelling of Ti-TiB and Ti-TiC composites

II-1. Modelling generalities and ideal material

The modelling of composite material requires the establishment of different assumptions that validate the use of different models. The first made is in all of the following calculation, the density of the materials reaches always the theoretical density, or said differently, the total absence of porosity. In the case of composite material, it is assumed that there is no pollution at the interface between reinforcement and matrix. The distribution of the reinforcement particles within the matrix is considered uniform through the entire composite.

In this modelling work, the influence of several parameters has been investigated. The TiB is present as whisker inside the Ti matrix; therefore its aspect ratio (ratio length/width) has an influence on the Young's modulus, as presented on the equation 3.16, and the yield strength, as presented on the equation 3.4. Also, it has been shown that the process use, ECAP or HDH sintering will have a different effect on the final microstructure, especially on the grain size. This grain size is closely related to the theoretical yield strength of one's material, as presented on the equation 3.1. The size of the reinforcement in a composite, when it is in a sub-micron range, will be at the origin of a strengthening mechanism (Orowan-Ashby) that will have an influence on the yield strength, as presented on the equation 3.5.

Therefore, the influence on the following parameters will by studied, in Ti/TiC and Ti/TiB ideal materials:

- Grain size of the matrix
- Aspect ratio of reinforcement
- Volume fraction of the reinforcement
- Particle size of the reinforcement

For the following computations, the matrix material is commercially pure titanium grade 2, with properties resumed on Table 3.

Ti	Impurities wt% max		Yield Strength (MPa)	Elongation (%)	Young's modulus (GPa)	Shear Modulus (GPa)	Coefficient of thermal expansion ($°C^{-1}$)
Grade 2	C O H N Fe	0.1 0.25 0.015 0.03 0.3	275-410	20	105	45.6	$8.6\ 10^{-6}$

Table 3: Properties of Ti grade 2

II-2. Influence of the grain size of the matrix

The grain size of a material can easily be modified using different processes. In this work, it has been shown in the chapter one, that ECAPed materials have small matrix grain size, in the range of few hundred nanometres. Using the Hall-Petch equation ($\sigma_m = \sigma_0 + k\frac{1}{\sqrt{D}}$), the influence of the grain size *D* on the yield strength σ_m is evident. According to literature, the variation of grain size in ECAP of pure titanium is located between about 500 nm to few microns, when the one for HDH sintering is around the powder particle size [KOO2012] [CHE2010] [CHE2011]. On a pure titanium material grade 2, and considering the improvement of the low angle grain can be neglected, the influence of the gain size D between 4 µm to 100 nm on the yield strength has been calculated. Figure shows the evolution of the yield strength depending on $\frac{1}{\sqrt{D}}$. Values for σ_0 and k have been taken from

literature. For commercially pure titanium, theoretical values commonly accepted for well annealed titanium are σ_0 = 78.45 MPa and k = 0.40 MPa $m^{1/2}$ [MEY2009]. With these values, good agreement with the experimental data when plotting the Hall-Petch Equation is obtained. However, it has been noted that when the grain size are considered lower than a micron, these experimental data deviate from the Hall Petch Equation. New set of data are therefore used, and are generally extracted from experimental data. The observation made by Kang *et al.* and Luo *et al.* [KAN2010] [LUO2012a] is that there is a discontinuity in the Hall Petch equation between the coarse grain and the small grain. In the case of coarse grains, the parameter k will be more important than in the case of submicronic grains.

In the following modelling (Figure), the Hall-Petch equation has been plotted using different set of data for σ_0 and k (from literature). Experimental results extracted from literature are displayed on the Figure , in order to compare the results obtained with the different plotting of the HP equation.

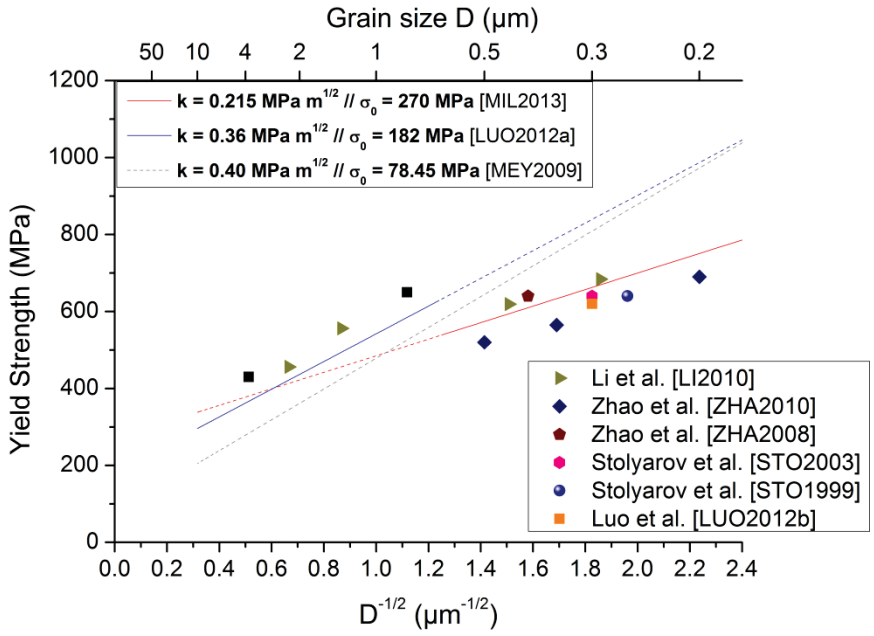

Figure 37: Yield Strength versus $D^{-1/2}$ (D is the grain size) for grade 2 titanium obeying the Hall Petch relationship, with different values for k and σ_0

The discontinuity in the Hall Petch equation is clearly observed in this graph. The relatively coarse grained titanium's data (more than 1 µm) fit the HP curves better where k is high and σ_0 is low, whereas the submicronic grained titanium's data fit the HP curves where k is lower and σ_0 is higher. Therefore, it seems that there is no single equation that can fit completely the different data of different grain size for titanium, meaning the parameter k and σ_0 has to be adjusted to fit the experimental values for each process.

This being said, reducing the grain size from 4 µm to 200 nm can multiply the yield strength of titanium by almost a factor 2, regardless the parameters data.

However, this calculation does not reflect the reality of a material because other factors have to be taken in consideration, such as a bimodal distribution of the grain size (coarse and fine) or the strengthening contribution from the low angle grain boundaries. Bimodal grain size distribution can be considered using an average grain size value $\overline{D}$ in the Hall Petch equation, with $\overline{D} = f_c D_c + (1 - f_c) D_f$. ($f_c$ is the area fraction of the coarse grains, D_c and D_f are the coarse and fine grains,

respectively). The LAGB, not included in the previous calculation, can also have an influence on the material yield strength as shown on Luo *et al.* works [LUO2012a]. The LAGB concerns the misorientation angle between two grains that is less than or equalled to 15°. Because it depends on the dislocation density, it contribution will be more important in material subject to severe plastic deformation that induces more dislocations. The strengthening contribution from LAGBs can be significant in the early stages of SPD processing when equiaxed HAGBs have not fully developed, and they can represent half the contribution from HAGB. However, modelling the LAGB strengthening contribution is complicated due to the fact that is clearly linked to the process used, and the parameter of the process (for example, the temperature and/or the number of pass during ECAP process will have a different impact on the strengthening contribution from LAGB). It is why it has not been taken into consideration in these modelling calculations. Therefore, this modelling work can slightly underestimate the Yield strength of the matrix.

II-3. Influence of the aspect ratio of the reinforcement

One aspect that can have a major influence on the properties of a composite is the aspect ratio of the reinforcement. The aspect ratio, in the models presented in this work, is the ratio of the length of the reinforcement over its diameter. In this work, even if the ex-situ TiC particles used are spherical and therefore, have their aspect ratio equals to 1, the in-situ TiB whiskers are, by definition, elongated. It then becomes interesting to know the influence of the aspect ratio of reinforcement such as TiB on the mechanical properties of the Ti/TiB_w composite. The literature [CAL2007] shows that the aspect ratio of reinforcement in a composite will have an effect on its mechanical strength and also on its Young's modulus.

On an ideal scenario, where the reinforcement is spherical, the Young's modulus of the composite will be estimated using the rule of mixture, and the only parameters that can be adjusted will be the volume fraction of the reinforcements. In the case of reinforcement with a large aspect ratio, two different possibilities are conceivable. In the first one, when all the reinforcements are perfectly aligned, the Young's modulus will be different in the transverse or the longitudinal direction. The modelling of the Young's modulus will have to be calculated in each direction. In the second possibility, which is mostly the case in this work, the reinforcement are randomly oriented, and therefore, the value of the Young's modulus of the composite will be equivalent regardless the direction investigated.

The Equation 3.18 (from chapter I) has then been used in order to evaluate the influence of the TiB aspect ratio on the Young's modulus of the composite Ti/TiB. Figure 38 displays this evolution of the Young's modulus for different aspect ratio S (S = 1, 10, 20, 40 and 60) and for different volume fractions of the reinforcement (TiB). Experimental data [MEN2007] [MIR2003] are also shown on Figure 38 for two S value (22 and 40). In order to compare the calculated data with experimental values from the literature, the value of the Young's modulus for Ti used in this modelling has to be the one of the titanium used for the experiments (*i.e.* 115 GPa).

Figure 38 shows that increasing the volume fraction of the reinforcement, regardless the aspect ratio of the reinforcement will increase significantly the Young's modulus of the composite. For S = 1 (reinforcement considered spherical) to S = 60, the Young's modulus is increased, being improved of 8.5 % (S = 1) to 11.5 % (S = 10) at a volume fraction of 0.05 and 17.4 % (S = 1) to 23.5 % (S = 10) at a volume fraction of 0.10 (increase of a factor 1.55).

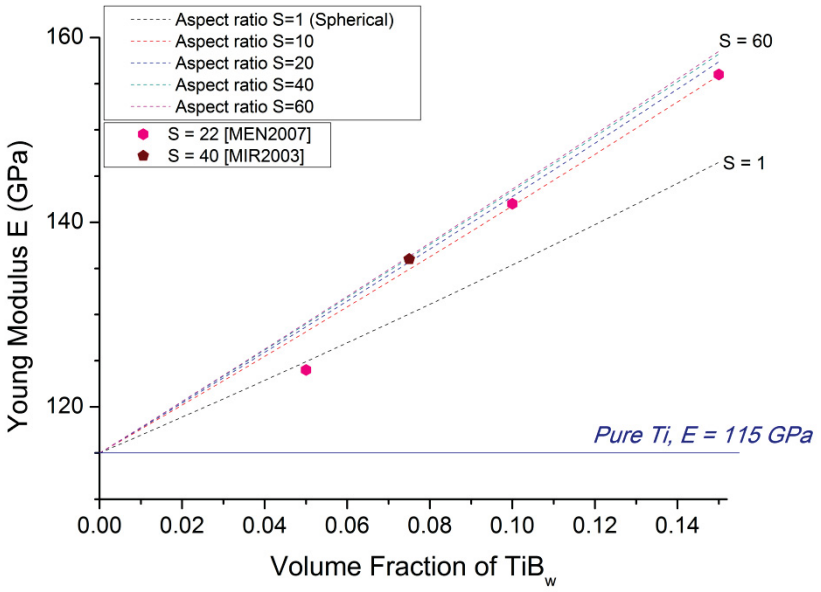

Figure 38: Young's modulus versus volume fraction of TiB_w randomly oriented, for Ti/TiB_w composite at different aspect ratio

It also appears that the aspect ratio has an effect of the improvement of the Young's modulus. However, even if this effect is obvious when comparing reinforcement without and with aspect ratio, the improvement is less significant when comparing reinforcement with different aspect ratio. For example, at a volume fraction of 0.1, the improvement of the Young's modulus goes from 11.5 % at and aspect ratio of 10 to only 13 % at an aspect ratio 6 times higher (S = 60). This means that when randomly oriented, reinforcement with an aspect ratio will have a higher impact on the Young's modulus than spherical reinforcement, but the value of the aspect ratio will be less significant on the modulus once above 10. When compared with experimental data, the theoretical values seem to be in relatively good agreement for volume fractions higher than 0.05. The experimental point, at a volume fraction of 0.05 is clearly below the expectation for reinforcement with an aspect ratio of 22 as it is for this example. This can be due to the fact that the reinforcements are not exactly randomly oriented. At low volume fraction, there are fewer reinforcements within the matrix and if only some of them are oriented, their impact can be significant on the composite's Young's modulus. In addition to this work, Gorsse *et al.* have shown an excellent agreement between the same type of model and the experimental data, for a Ti/TiB_w composite. Their results have not been plotted here due to a difference in the titanium they have used, and consequently, the difference of the Young's modulus value.

The aspect ratio does not only have an influence on the Young's modulus of the composite, but it also has an effect on the composite strength. To evaluate this influence, the modelling work will be done using improvement factors. The improvement factors f_l, f_d, and f_{Orowan}, are respectively the ones related to the load-bearing effect, the dislocation punching strengthening, and the Orowan strengthening. First, the influence of the aspect ratio and the volume fraction will be evaluated on the three improvement factors. Then, the contribution of the improvement factors of the three strengthening mechanisms will be used to model the yield strength of the composite as a function of the volume fraction at different aspect ratio. These improvement factors are combined using two models, the multiplication model (equation (3.14)) and the addition model (equation (3.15)).

$$\sigma_{yc} = \sigma_{ym} \times (1 + f_l) \times (1 + f_d) \times (1 + f_{Orowan}) \qquad (3.14)$$

$$\sigma_{yc} = \sigma_{ym}(1 + f_l + f_d + f_{Orowan}) \quad (3.15)$$

On Figure 39, the improvement factors f_{Orowan}, f_d, and f_l,are presented, as a function of the volume fraction and at different aspect ratio S. The factors are the ones detailed in the equations 3.9, 3.10, 3.11. However, the Orowan strengthening is depending on the interparticle spacing λ, for which two models are used to calculate the value, the cubic model (CM) and the face-centred cubic model (FCC) expressed in the equation 3.6 and 3.7. Consequently, the Orowan strengthening factor f_{Orowan} will be given for the CM and the FCC models.

These factors illustrate the influence of the aspect ratio of TiB_w on the composite yield strength. To estimate the dislocation punching effect, the value of t_r, which represents the smallest value of the reinforcement, so in our case, the whiskers diameter, has been considered constant regardless the aspect ratio, at 500 nm. Therefore, for an aspect ratio S = 1, a spherical particle with a diameter of 500 nm is considered.

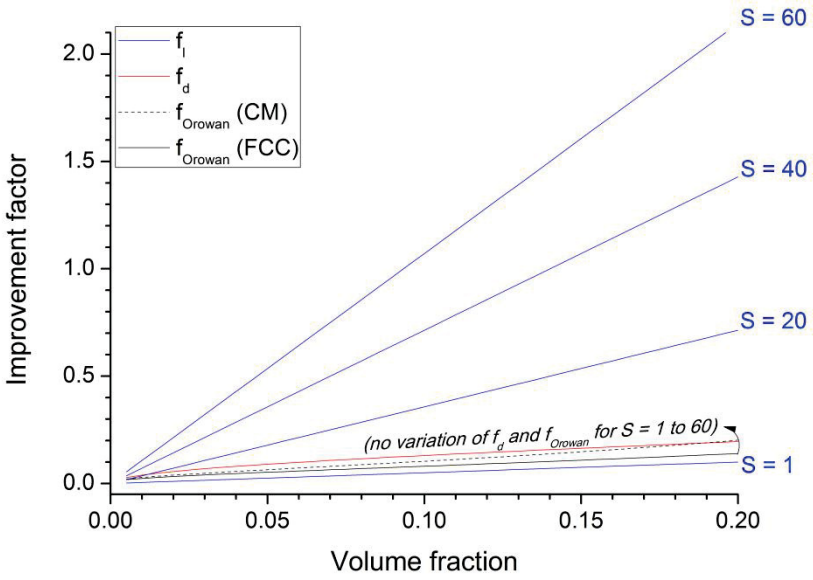

Figure 39: Improvement factor versus volume fraction for Ti/TiB_w composite at different aspect ratio

The Orowan strengthening and the dislocation punching factors f_{Orowan} and f_d , which do not depend on the aspect ratio, will remain constant regardless the value of S. Their impact can be clearly neglected when modelling the yield strength for reinforcement with high aspect ratio. However, they appear significant when a spherical particle (S = 1) is considered. The load bearing factor, which depends on the aspect ratio, becomes more significant when the aspect ratio becomes higher. These factors will then be used to model the yield strength of the Ti/TiB composite using the addition and multiplication models, using equation 4.16 and results from Figure 39. Figure 40 shows the evolution of the yield strength of the Ti/TiB_w composite as a function of the volume fraction, for different aspect ratio. In order to calculate this composite yield strength, the properties of the Ti matrix taken are the one for Ti grade 2, with an average grain size considered equiaxed of 3 µm, and no LAGB. The Hall Petch parameters used to calculate the theoretical yield strength of the matrix σ_m are the ones given by Meyers (σ_0 = 78.45 MPa and k = 0.40 MPa $m^{1/2}$).

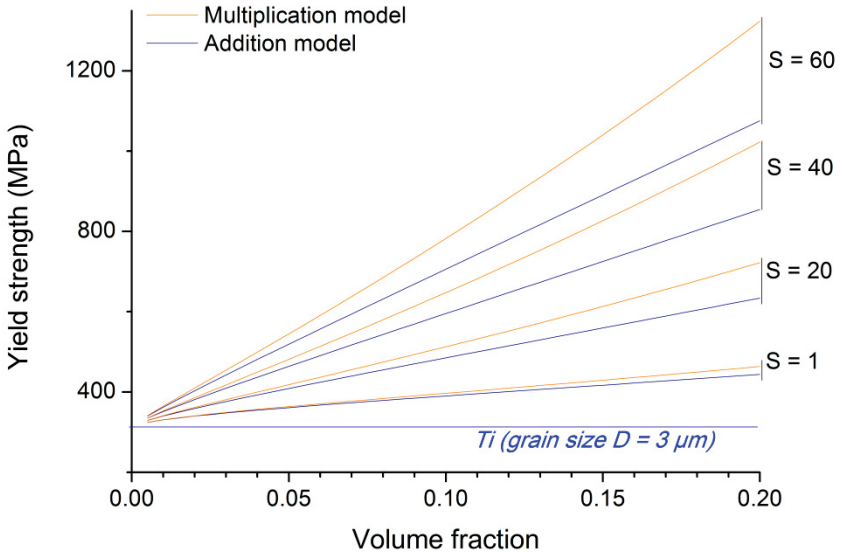

Figure 40: Yield strength versus volume fraction of TiB_w for the Ti/TiB_w composite at different aspect ratio

It appears on the graph that the aspect ratio have a clear effect on the yield strength of the composite. At high volume fraction, increasing the aspect ratio leads to a significant increase in the yield strength. Moreover, it is shown that the simple addition of particles with no aspect ratio, represented by the curve for S = 1, will still have an effect on the yield strength when the volume fraction increases. At high aspect ratio, the difference in the two models (addition and multiplication) is important, with the multiplication model being higher than the addition model. One tends to use the addition model in order to not overestimate the predicted values. Regardless the model used, it appears obvious that if one is using whisker reinforcement, the higher the aspect ratio the better. However, Figure 39 shows that when spherical particle are considered (S = 1), the Orowan strengthening factor and the dislocation punching factor are significant compares to the load bearing factor. Knowing that these factors are related to the particle size, their impact on the yield strength should be considered when the reinforcement particle are spherical (S = 1) and the size is small enough (below 500 nm).

II-4. Influence of the particle size of the reinforcement

In the considered composites, the two type of reinforcement, in-situ TIB_w or ex-situ TiC are supposed to be in the nanometric range of size. It is hard to predict the dimension of the TiB whiskers after the transformation from TiB_2. However, it is sure that the TiC used will remain nanosized because it does not go under any chemical microstructural transformation. When using nanosized reinforcements, the effect of the size on the final strength of the composite is represented in the Orowan strengthening factor and the dislocation punching factor. As showed in the chapter 1, the Orowan strengthening is based on the Orowan-Ashby equation (equation 3.5) that depends on two main parameters, the size of the reinforcement d_r, and the distance between two particles λ (also dependent on the reinforcement size). It is commonly accepted that the Orowan strengthening concerns particles in the nanometric range of size. On Figure 41, the different improvement factors are expressed as a function of the particle size, in the case of a composite Ti/TiC, for a volume fraction of 1 %. Both of the CM and FCC models are represented for f_{Orowan}. The Ti considered is Ti grade 2 and the TiC reinforcement is considered spherical.

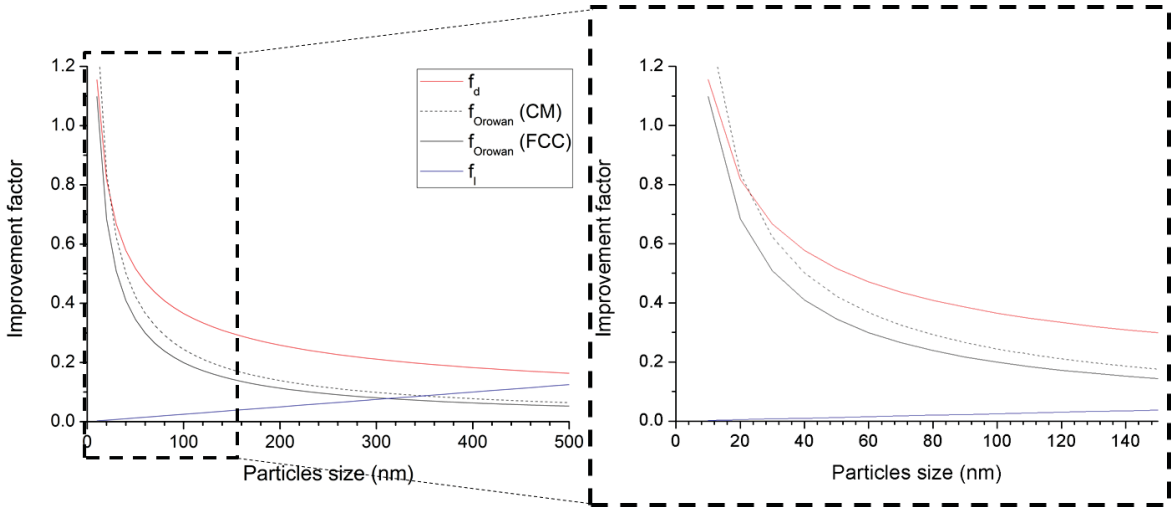

Figure 41: Improvement factors versus the particle size of TiC in a Ti/TiC composite with a volume fraction of 1%

It appears on Figure 41 that the influence of the model used for the estimation of λ (CM black dot line and FCC black plain line) is not significant when changing the particle size. It is also obvious that the Orowan strengthening effect and the dislocation punching strengthening effect increase significantly when the size of the particles decrease. For a reinforcement size under 100 nm, the improvement factors f_d and f_{Orowan} increase drastically. Meanwhile, the improvement factor f_l, which is not dependent on the particle size, but on the volume fraction (0.01 is this example), becomes negligible. At higher particle size, the three different improvement factors are all relevant for in the modelling of yield strength, with all having the same impact on the calculated yield strength value. The three improvement factors f_l, f_d and f_{Orowan} will have a moderate impact on the composite's yield strength for a reinforcement size above 100 nm compares with the impact of f_d and f_{Orowan} will have for a reinforcement size below 100 nm. Figure 42 shows the modelling of an ideal Ti/TiC (1 %vol.) using all the strengthening factors to estimate the yield strength of the composite as a function of the particle size of the reinforcement. The calculations have been done using the parameters given by Meyers to obtain the yield strength of the matrix with the Hall-Petch equation, with an average grain size of 3µm (no contribution from LAGB).

As anticipated with the Figure 41, the properties of the composite will be drastically improved for the reinforcement size below 100 nm. This value, however, will stay mostly stable when the particle size increases above 100 nm. Nonetheless, even for relatively high reinforcement size, the yield strength of the composites is higher than the one of the matrix itself. This modelling work show the relevance of using nanosized reinforcements (>100 nm) when mechanical properties are considered. A line on the figure indicates the TiC particle size use in this work (40 nm). At this size, the improvement on the composite yield strength appears clearly.

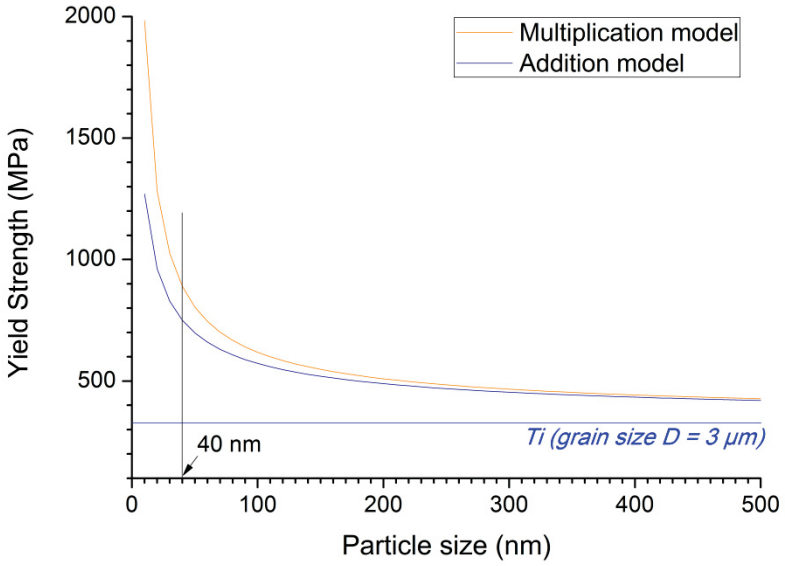

Figure 42: Yield strength of the composite Ti/TiC at a volume fraction of 1% versus the particle size of TiC

The difference between addition and multiplication model to combine the different strengthening mechanisms is not really significant at high particle size, but becomes important the reinforcement size is reduced. In order not to overestimate the composite properties, it seems more relevant to use the addition model.

If the size of the reinforcement is in general a constant, this is not the case for the volume fraction of the reinforcement that can be adjusted during the experiments. Adding more or less particles in the matrix will have a direct effect on the distance between the particles. Consequently, the relevance of the different models used (CM and FCC) will become more important.

II-5. Influence of the volume fraction of the reinforcement

Volume fraction of the reinforcement is a parameter quite easy to adjust. In the present work, 3 different volume fractions have been selected in order to see their impact on the produced material. Nonetheless, it is interesting to estimate the influence of the volume fraction of the reinforcement on the strength of the composite. By observing the influence of the reinforcement's volume fraction on the improvement factors, the effect of the different models for the interparticle distances λ is clearly shown. In the following modelling, the composite represented is again the Ti/TiC, with the matrix being calculated using the parameters given by Meyers, an average grain size of 3 µm and no LAGB. The reinforcements are TiC particles with a diameter of 40 nm.

Figure 43 presents the improvement factors, f_l, f_d and f_{Orowan} for the two models (CM and FCC), as a function of the volume fraction. The contribution of the load bearing effect, f_l, is low in this example because of the fact the particles are considered spherical that have as a consequence to have the factor equalled as half of the volume fraction (equation 3.9). Using equation 3.15 and results from Figure 43, Figure 44 shows the yield strength of the ideal composite Ti/TiC, with a particle size of 40 nm as a function of the volume fraction, and the two models to combine the different factors, addition and multiplication, are displayed.

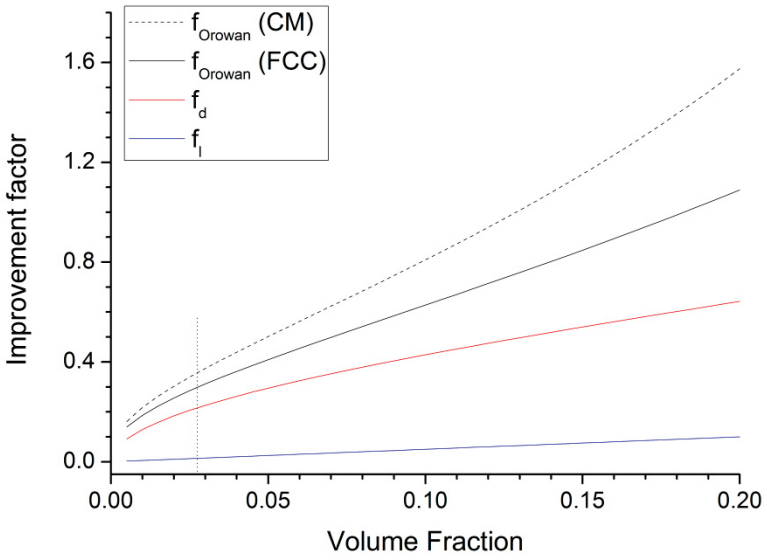

Figure 43: Improvement factors versus volume fraction of TiC in a Ti/TiC (40 nm) composite

Figure 43 shows that increasing the volume fraction of nanoparticles increases considerably both f_{Orowan} and f_d and that at high volume fraction, the Orowan strengthening effect becomes more significant than the dislocation punching effect. This observation, nevertheless, has to be taken with caution, due to the fact that nanosized particles are hardly used at high volume fraction because of agglomeration effect that can occurs. The shape of the curves, for f_d and f_{Orowan}, seems two have two domain below and above a volume fraction of 0.03 (indicated on the figure). However, this is due to the fact the expression of f_d and f_{Orowan} are, respectively as a function of $V_f^{1/2}$ and $V_f^{1/3}$. The factor improvement associated with the load bearing effect f_l is clearly not as significant as the two other, and will have almost no impact on the composite's yield strength.

With the augmentation of the volume fraction, the difference between the two models for λ (CM and FCC) becomes more important. As said before, the expression of λ in each model (CM and FCC) depends on the volume fraction V_f, that is expressed as $V_f^{1/3}$. But the factor that multiply V_f for each model, and that relates the reinforcement distribution considered (2 dimensional in CM model and 3 dimensional in FCC model, cf chapter 1), will cause the difference between the models. For the modelling of the yield strength of the composite, the improvement factor f_{Orowan} selected is the one for the FCC model. This selection has been made in order not to overestimate the composite's yield strength in regards of the expression of f_{Orowan} for both models, the one for FCC being lower than the one for CM.

The first observation is the influence of the volume fraction of TiC as reinforcement; the higher the volume fraction, the better the properties. Because the improvement factor for the load bearing strengthening is not significant, the shape of the curve is the same as the ones for f_d and f_{Orowan}.

In comparison with the yield strength of pure titanium generated with Hall-Petch for a grain size of 3 µm (blue line), adding a volume fraction of 0.01 of TiC has already an important effect on the yield strength of the composite. And using a volume fraction of 1% will not reduce the issue in regards of the reinforcement distribution within the matrix.

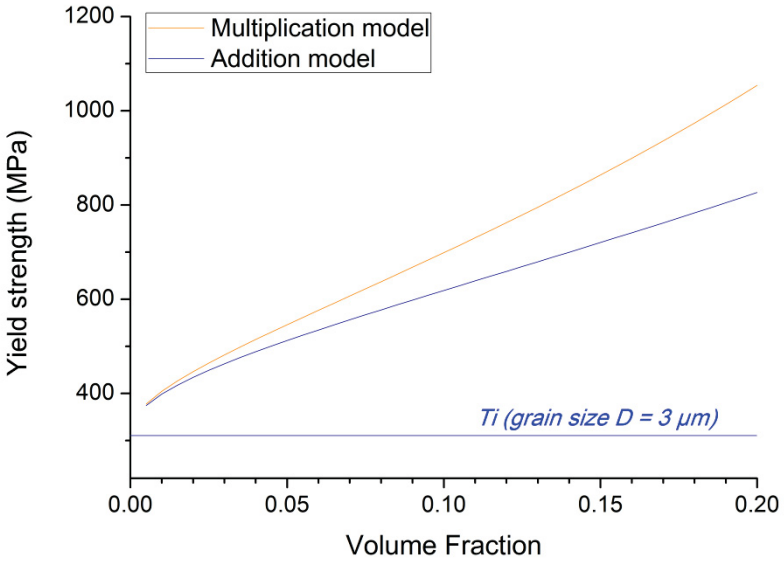

Figure 44: Yield strength of the Ti/TiC (40 nm) composite versus the volume fraction (FCC model used for λ)

The difference between the addition model and the multiplication model for the combination of all the strengthening effects is important at high volume fraction. In the same idea than with the variation of the particle size, it seems more relevant to use the addition model in order not to overestimate the theoretical value of the composite. In his thesis, on the multiphase composite Ti-Al, Lui has noted that the multiplication model was not suited for the modelling of his composite properties [LUI2012].

II-6. Modelling of the investigated composites

By combining all the different aspects that have an influence on the mechanical properties of the composite, it becomes possible to estimate ideal properties of the investigated composites. To achieve that, anticipated parameters used in the calculation of the improvement factor (and consequently on the theoretical composites yield strength) are selected according to the literature to be as closed as the ones potentially dealt with in this work, for each method. The grain size of Ti, for example, will not be the same for the composite produced by ECAP or by HDH. Two average grain sizes, according to the literature for a typical ECAP of pure Ti, and for a material obtained by HDH, will be selected, respectively 0.4 µm [STO2008] [VAL2003] and 1 µm [WAN2010]. The second parameter is the aspect ratio of the reinforcement. For TiC reinforcement, this aspect ratio will be fixed to 1, because spherical particles are considered, and for TiB_w, the aspect ratio will be fixed to 30 because the average size of a whisker is hard to predict. Table 4 resumes the parameters needed for the modelling of the composite. In bleu are shown the parameters taken from literature, with the references, and in green the one that has been inspired by the literature, to be as closed as possible as the ones anticipated in this work. The models used for the calculation are FCC for the value of λ, and addition for the combination of all the different strengthening factors. The parameters for the two processes used in this work, HDH and ECAP, are also resumed. The parameters such as the TiC particle size, the TiC aspect ratio and initial and final temperatures used in this work are known and therefore, the same one are used in the modelling.

Matrix		Grain size D (µm)	Young Modulus E (GPa)	Coefficient of thermal expansion α ($°C^{-1}$)	Initial temperature T_i (°C)	Final temperature T_f (°C)
Ti	*HDH*	1	105 [LUT2003]	$8.6\ 10^{-6}$ [LUT2003]	*25*	*1400*
	ECAP	0.400			*25*	*600*

Reinforcements	Particle size (µm)	Young Modulus (GPa)	Coefficient of thermal expansion α ($°C^{-1}$)	Aspect ratio S
TiC	*0.04*	450 [GAR2006]	$8.2\ 10^{-6}$ [DAR2004]	*1*
TiB_w	d = 0.5, l = 15	550 [GAR2006]	$8.5\ 10^{-6}$ [DAR2004]	30

Table 4: Properties of the materials used in this work

In order to generate the value of the yield strength for the pure titanium, used in the calculation of the composites yield strength as matrix, the parameters k and σ_0 used in the Hall Petch relationship were different depending on the process used. As shown previously, the Hall Petch relationship is not continuous between coarse grain and the sub-micronic grain materials. The ECAP and HDH processes are assumed to produce respectively sub-micronic and coarse grain. To model the matrix properties, for the HDH process, parameters given by Luo were selected, (D = 1 µm), σ_0 = 182 MPa and k = 0.36 MPa $m^{1/2}$, and for the ECAP process (D = 400 nm), parameters given by Miller were selected σ_0 = 270 MPa and k = 0.215 MPa $m^{1/2}$. The properties for the composite Ti/TiB produced by ECAP have not been computed because the results would be irrelevant. ECAP process is not suited for the production of Ti/TiB, owing to its low working temperature (under the TiB_2 → TiB transformation temperature) and the severe plastic deformation that could not favour the growing of whiskers. The production of Ti/TiB composite has not been investigated using the ECAP process in this work.

		Yield Strength (MPa)		Young's Modulus (GPa)
		HDH	*ECAP*	
Ti		545	610	105
Ti/TiC	*1%vol.*	632	701	106.7
	3%vol.	699	768	110
	10%vol.	864	936	122.4
Ti/TiB	*1%vol.*	590	N.A	107.7
	3%vol.	662		113.1
	10%vol.	887		132.5

Table 5: Computed properties of the investigated composites combining the different strengthening models

Table 5 presents the calculated yield strength and the Young's modulus of pure Ti, Ti/TiC and Ti/TiB_w composites for different volume fractions. The yield strength is presented for the two processes, due to the fact that the processes have an influence on the grain size. As shown, the effect of the grain size on the matrix yield strength is important. For the Ti without reinforcement, the yield strength

varies from 545 MPa for the HDH process to 610 MPa for the ECAP, only due to the considered grain size after the process. This value is the one used as σ_m. The values for the young's modulus are not represented for each process because it is considered that the process does not have any influence on them. As expected after the observation of the different strengthening mechanisms, the increase in yield strength and Young's modulus are significant when increasing the volume fraction of the reinforcement. However, these properties are expected if the material is ideal: the grains are equiaxed, in the same range of size (either coarse or fine), the material is fully dense (no porosity), the reinforcement particles are uniformly dispersed, and the impurities are in the range of Ti grade 2.

At same volume fraction, and for the same process, TiC reinforcement seems to have a more important effect on the mechanical properties than TiB, in this ideal material. For example, at a volume fraction of 0.01, Ti/TiC composite will exhibit a better Yield strength and about the same Young's Modulus than the Ti/TiB composite (632 MPa and 590 MPa for the Yield strength and 106.7 GPa and 107.7 GPa for the Young's Modulus, respectively). This is principally due to the particle size considered. However, at higher volume fraction, reinforcement with high aspect ratio such as TiB whiskers will provide a higher Young's Modulus than spherical reinforcements such as TiC. In this case, at a volume fraction of 0.1, the Young's Modulus of Ti/TiB is higher than the one of Ti/TiC. (132.5 GPa and 122.4 GPa, respectively). Both of reinforcements will have their own advantages due to their size, aspect ratio and also, as said in the chapter 1, the in-situ or ex-situ nature.

The results modelled here will be then compared with the experimental results of the materials obtained in this work, for both processes.

The different processes used in this work can encounter difficulties in the production of fully dense, uniformly dispersed materials and each process has its own effect on the final properties of the composite (grain size, dispersion). An essential step in order to have good properties is the powder preparation prior the densification. In HDH, the starting powder TiH_2 and the mixed composite powders has to be optimised prior cold compaction and sintering. In ECAP the distribution of the TiC within the Ti particles prior the densification is also very important. Therefore the preparation of powder has to be perfectly controlled, from the obtaining of the powders (reinforcement and matrix) to the mixed powder that is ready to be densified (composite mix).

III. Powder Preparation

Control of the properties of the starting powder is critical in powder metallurgy. Indeed, the nature of the powder, its particles size, its shape and others aspects can have a major influence on the densification process used [TJO2008] [CHA2006].

In the present work, the starting powder nature varies with the process to be used. In this part are presented all the steps that lead to obtain ready-to-process powders, for each process used. For the HDH process, the preparation of the TiH_2 powder is explained. Then, after an introduction of the two different reinforcement powders used, TiC and TiB_2, an explanation of the different steps to obtain composite powders, for each process ECAP and HDH, is made.

III-1. From Ti sponge to TiH_2 fine powder

The hydrogenation/dehydrogenation process presented earlier presents many steps where a good control is conceivable. From the hydrogenation of Ti sponge to the ready-to-sinter TiH_2 powder, the understanding of the different steps gives the possibility to have a control, with the aim to optimise

the needed characteristics.

III-1.1 Hydrogenation of Ti sponge

The as-received Ti sponge (Alfa Aeser, 99.7 % purity) has a mean particle size close to 2 mm. The hydrogenation vessel is a sealed tube with a volume V of about 6 10^{-5} m^3, and 36 g of Ti sponge fills it. According to the hydrogenation equation Ti + H_2 → TiH_2 a simple calculation using the ideal gas law can give an approximate value of the H_2 pressure needed to complete the process for a batch.

36 g of Ti represents a number of mole n of 0.75 mole. Because the hydrogenation equation gives a molar report between Ti and H_2 of 1, 0.75 mole of H_2 is required to fully hydrogenate the Ti batch.

Following the ideal gas law $P = \frac{nRT}{V}$, a pressure value of 7.51 10^6 Pa of H_2 would be sufficient.

During the experiment, the H_2 pressure used in the vessel was higher than calculated (about 9.8 10^6 Pa). It is easily explained by the fact that there is always uncontrolled leak issue with the vessel used during the hydrogenation of Ti. In order to initiate the hydrogenation of the Ti sponge, the sealed vessel is heated at 500°C. Once this temperature is reached, H_2 pressure decreases almost instantly. After the vessel has been filled with proper amount of H_2, the hydrogenation is considered complete when the pressure of H_2 in the vessel does not decrease anymore.

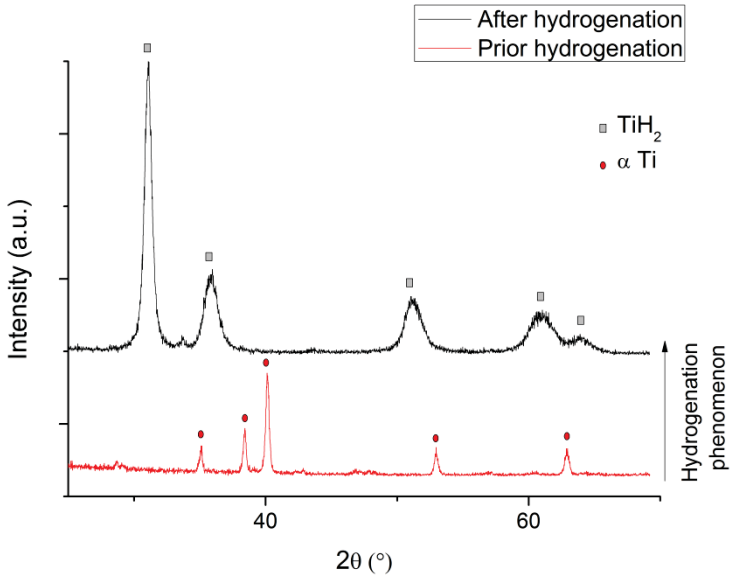

Figure 45: XRD pattern of Ti sponge prior and after hydrogenation

This XRD analysis, and all the following ones done in this work, has been done at λKα1 = 1.5405 Å, λKα2 = 1.5443 Å. The XRD analysis (Figure 45) of the resulting powder from the hydrogenation confirms the presence of only the TiH_2 phase. Moreover, Ti sponge, relatively coarse, is logically not brittle. However, TiH_2 powder obtained after hydrogenation is finer due to the fact it is a brittle material and it is easily crushed. Figure 46: Ti sponge before hydrogenation on the left (a) and after hydrogenation (TiH_2) on the right (b)Figure 46 shows the difference of the powder size before and after hydrogenation. The TiH_2 powder (b) has not been under any size reduction processes, but appears clearly finer.

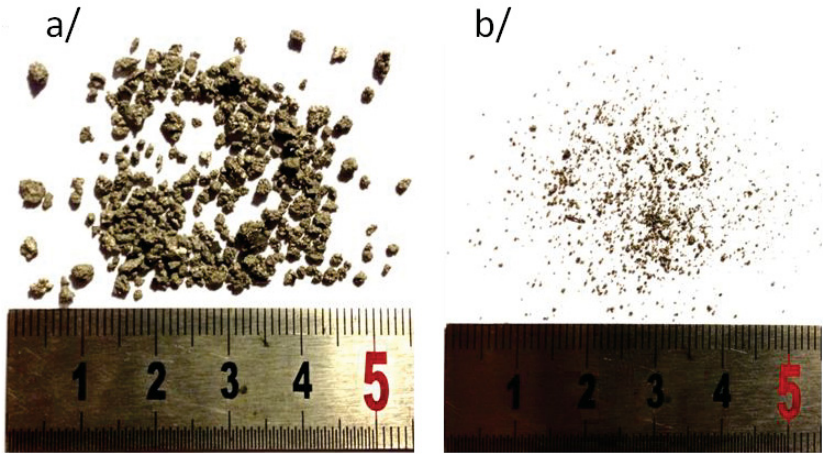

Figure 46: Ti sponge before hydrogenation on the left (a) and after hydrogenation (TiH_2) on the right (b)

III-1.2 Size reduction

The fact that the TiH_2 powder is brittle gives the possibility to have a control of the size of it, by using size reduction process. In this work, in order to reduce and control the size of the hydride powder, planetary ball milling has been used (Fritsh, Pulverisette 5) in stainless steel jars, with stainless steel balls after optimisation. The ratio ball-to-powder was set to 10 to 1. Due to the size of the jars, batches of about 8 g of TiH_2 powder were milled in each jar. The steps to avoid over heating in the ball milling were 15 minutes of milling and 2 minutes of break. The speed was 250 rotations per minutes (RPM).

Different conditions have been tried in order to obtain the finer particle size possible. It soon has been noted that after a too long time of ball milling, the TiH_2 become too fine to be handle in air atmosphere. The powder would start dehydrogenation spontaneously, in a process of self-combustion. The pyrophoric size has been observed after 2 hours of ball milling. Nevertheless, techniques exist to work with such size powder, like working in protective atmosphere (for example Argon in glove box) but make the process complicated and therefore more expensive. That is why the ball milling time tried varies from 15 minutes to 105 minutes with a step of 15 minutes. As explain in the first chapter, the ball milling of brittle material such as TiH_2 will have two main effects, reducing the particle size of the powder, and reducing the coherent domain size within a particle itself. In order to control the size, size characterisation on the powder has been done after milling time step of 15 minutes.

- *Size measurement*

In order to have an idea of the TiH_2 particle size at any given time, different methods has been used and compared. The first one is the particle size measurement using laser diffraction, also called laser granulometry. When it is about particle size measurement, by means different than image analysis, a general assumption made is that each particle is represented as a sphere and the measured value is the equivalent diameter of the sphere (Figure 47).

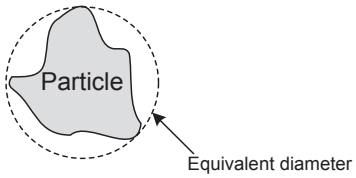

Figure 47: Equivalent diameter of a particle

This assumption gives good results when compared with image analysis, except in the case of particle with high aspect ratio such as needle or wire. A particle with high aspect ratio will give a distribution of size from its smallest and largest dimension. The result given for particle size measurement is usually the value where half of the population resides below this point, the d50 (as known as median).

In addition to the results, it is important to use the most appropriate representation of the particle size distribution. Most of the particle size analysers are based on light diffraction reports the volume distribution of the measured material. A counting-based technique such as image analysis reports the number distribution. The volume distribution is based on the appearance of larger particles that will have a bigger influence on the counting than the smaller one. On the contrary, the number distribution is based on the most numerous particles of a given size which means the biggest particles will not matter as significantly as on the volume distribution, only if they are the most numerous. However, it is possible to convert the result from volume distribution to number distribution, but errors are introduced due to the fact the conversion is only mathematical based. Nevertheless, this conversion can be considered to be indicative of the size distribution, in addition of image analysis.

The method used to obtain the average particle size of the produced material is the laser diffraction measurement. This technique is based on the Mie scattering theory that takes in consideration the diffraction and the diffusion of the particle. It works on the idea that the particle will scatter light at an angle determined by that particle's size. Larger particles will scatter at small angle and smaller particle at wide angle. A schematic representation of the laser granulometry measurement is presented on Figure 48.

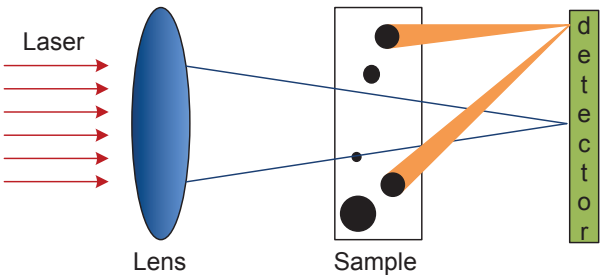

Figure 48: Schematic representation of the laser granulometry principle

- *Coherent domain measurement*

In order to understand the ball milling process to reduce the particle size, the crystallite size of the powder (coherent domain within a particle) after different time of ball milling has been calculated, using the Scherrer formula on the XRD spectra taken at different ball milling time (Figure 49). The Scherrer formula gives an estimation of the crystallite size from XRD analysis of a material. The Scherrer formula can be written as:

$$\tau = \frac{K\lambda}{\beta cos\theta} \tag{4.20}$$

where τ is the mean size of the coherent domains (crystallite), K is a dimensionless shape parameter called Scherrer factor and relates the shape of the crystallite. λ is the X-ray wavelength, β is the integral width, commonly this value is approximate to the one of the line broadening at half the maximum intensity (FMWH) and θ is the Bragg angle for the peak. Using the FWMH, different on each spectrum, this formula allows estimating the coherent domain size (crystallite size). A longer review of the possibility and the peculiarity of this formula has been done by Langford [LAN1978]. In this work, the software EVA was used to calculate the value of the crystallite size, K, λ, β and θ being calculated or in the database of the software.

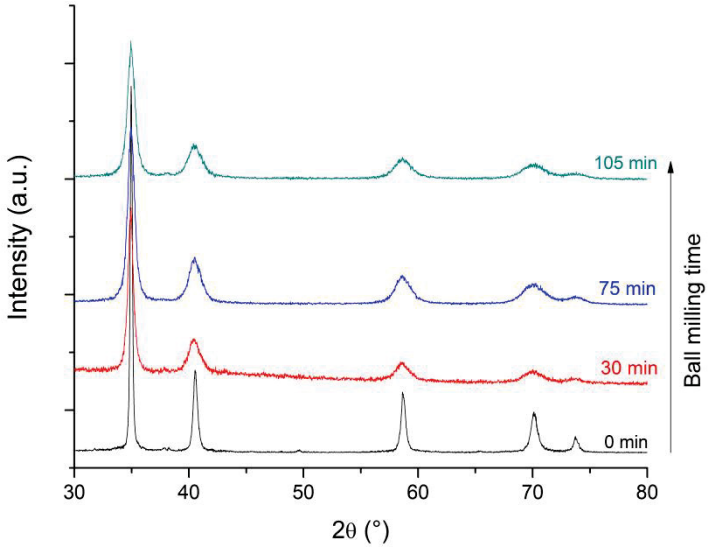

Figure 49: XRD spectra of TiH_2 powder at different ball milling times

The peak broadening observed after 30 minutes of ball milling is due to the reduction of crystallite size. The peak widths are almost similar for 30 minutes to 105 minutes ball milling time, which mean that the crystallite size remains mostly similar.

- *Results*

Both of volume and number distribution of TiH_2 particles, after different ball-milling time, are given on the Figure 50. The black dots represent the volume distribution, and so, the bigger particle size that the powder have. The red dots represent the number distribution, and so, the most numerous particle size encounter in the powder. This measurement, due to the fact that the values are different, represents a bimodal distribution of the size. One the Figure 50 is also represented the crystallite size evolution. It is important to notice the different scales on the two y-axes. Three different phases can be differentiated during the process, indicated on the figure with I, II, and III.

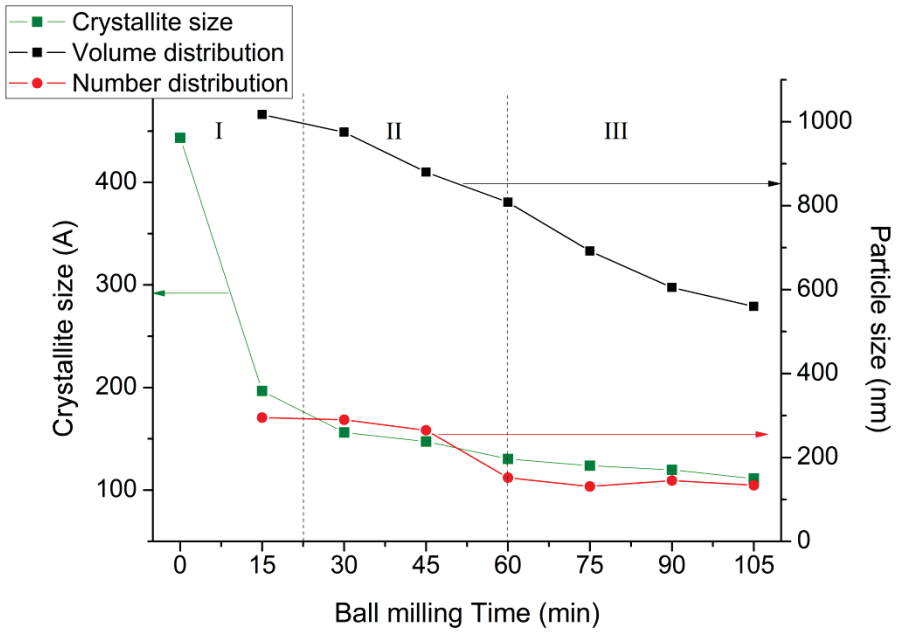

Figure 50: TiH_2 crystallite size and particle size as a function of ball milling time (green: crystallite in Å, red: particle size number distribution and black: particle size volume distribution in nm)

Phase I: 0 to 20 minutes

The first phase of ball milling concerns the start of the process. Defects are induced to the particles that will first lead to reduce the coherent domains (crystallites) to a minimum size. Once the minimum is reached (about 150 Å), fragmentation will happen over the crystallite size reduction.

Phase II: 20 to 60 minutes

More defects are induced to the particles by ball milling process. The reduction of the crystallite size is becoming not significant, which means that the fracturing of the particle will occur. Two size populations will be observed by volume and number distribution, the biggest population and the most numerous sizes of population. The bigger particles have and average diameter of 900 nm after 45 minutes of ball milling whereas most of the particles have an average diameter of 300 nm. By continuing the ball milling process, the size of the biggest particles will tend to be reduced when the size of the smallest will tend to remain mostly the same because statistically, the biggest particles are subject to the impact of the ball against the wall before the smallest. However, smallest particles will still be affected, even if it is less, by the ball milling process.

Phase III: 60 to 105 minutes

The size of the crystallite is still almost not affected by the ball milling process and the average particle size measure in number distribution tends to 180 nm. The effect on the biggest particle size (volume distribution) is still happening, reducing the size to less than 600 nm after 105 minutes of ball milling. An infinite time of ball milling would lead to a uniform single distribution in particle size. However, as said before, spontaneous combustion has been observed for powder ball milled for more than 120 minutes, because the small particles are still affected by the ball milling process.

Because the spontaneous combustion has been observe few times for powder ball milled 105 minutes, the selected ball milling time for this work is 90 minutes. The TiH_2 is then bimodal, with the two populations having an average diameter of 600 nm and 180 nm.

The ball milling can have a negative impact on the TiH_2 particles. Because of the local elevation in temperature, the high deformation induced to the particle, and the reduction in size, the nature of the powder can changed during ball milling, especially, a dehydrogenation phenomenon can occurs during ball milling. However, at any given ball milling time, only TiH_2 spectra are observed. This confirms that the TiH_2 powder is not deteriorated by the ball milling process chosen.

III-1.3 Dehydrogenation

As explained in the chapter 1, reducing the size of the TiH_2 will reduce its dehydrogenation temperature. To verify this effect on the ball milled powder, Differential Scanning Calorimetry measurement has been done for non-milled powder and the powder used (Ball milled for 90 minutes). This characterisation method allows observing the dehydrogenation temperature of the hydride (Figure 51). By reducing the particle size from few microns to 500 nm, the temperature where the dehydrogenation starts decrease from almost 570°C to about 400°C. Moreover, when the size is reduced, the 2 peaks of dehydrogenation presented as a surface dehydrogenation and a core dehydrogenation (cf. chapter I) are clearly observable. This reduction of the temperature of starting dehydrogenation is beneficial for the sintering of such powder. The sintering will start as soon as the dehydrogenation happens and leaves freshly exposed surfaces on particles. Reducing the dehydrogenation temperature will allow the sintering phenomenon to occur earlier.

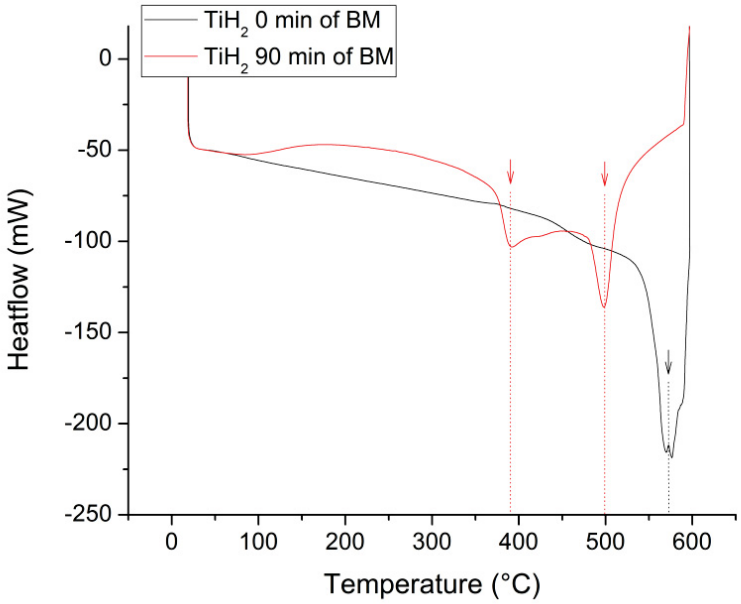

Figure 51: DSC of TiH_2 powder as received and ball milled for 105 minutes

The dehydrogenation is useful to the densification of Ti only if it is complete and the final product is pure Ti. To verify the product obtain after dehydrogenation, XRD analysis has been done on a TiH_2 powder ball milled for 90 minutes and dehydrogenate at 600°C for an hour under secondary vacuum (10^{-6} mbar) (Figure 52). The spectra of the phase obtain after dehydrogenation is the one for α-Ti only, which confirms that the process is complete after a dehydrogenation at 600°C.

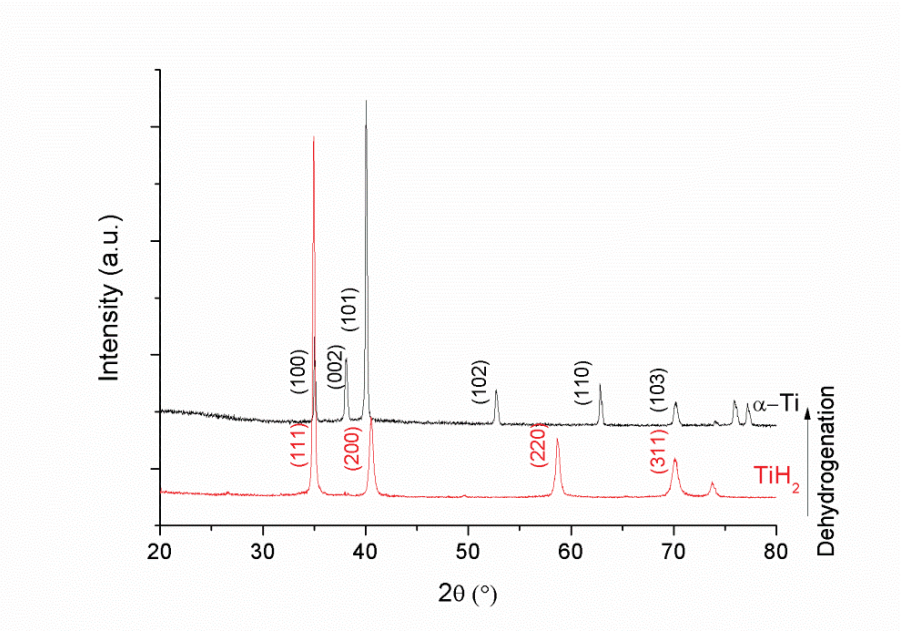

Figure 52: XRD spectra of hydrogenated and dehydrogenated powder

If the sample contamination has an effect on the properties of the final material, it is important to control that the hydrogenation and ball milling processes are not a source of impurities. To control that, Induction Coupled Plasma analysis (ICP) is done on the ball milled powder and dehydrogenated powder (Figure 53). The result shows that regardless the ball milling time, the amount of impurities in the powder does not vary. However, when the ball milling time becomes too long (more than 120 minutes) it appears that contamination from the balls occurs (increase in iron quantity detected)

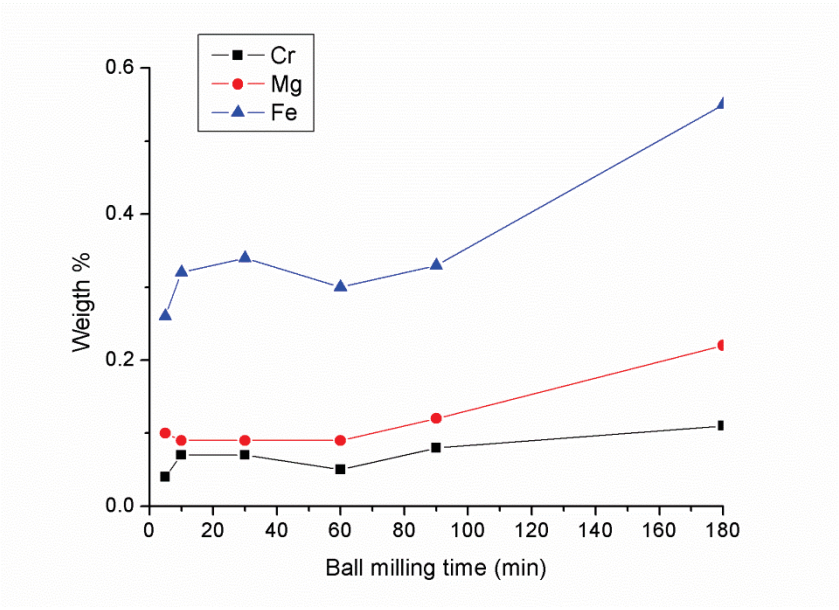

Figure 53: ICP analysis of TiH_2 powder ball milled for different times (black: Cr, red: Mg, blue: Fe)

During this work, the selected TiH_2 powder was ball milled for 90 minutes, and considered not contaminated by the ball milling process.

The size of the TiH_2 particle can be controlled, and its capability to fully dehydrogenate is shown. This powder can be therefore used as a matrix in the preparation of composite for the HDH process, pressureless sintering and hot pressing.

The matrix powder used in the ECAP process is not modified and is Ti commercial powder. TiH_2 is not used with ECAP due to the impossibility to work under controlled atmosphere or vacuum. Both of the powder will be mixed with reinforcement, by different mixing processes. It is important to know the different reinforcements used in this work.

III-2. Reinforcements

The reinforcements selected in this work are TiC and TiB_2 powders. The TiC powder, used in the ECAP process and both HDH processes (pressurless sintering and hot pressing), is used as-received. It is supposed to be 40 nm particle sizes and spherical particle. The TiB_2 powder, used in pressurless sintering HDH process, is micrometric sized. It is not used in HDH hot pressing and ECAP due to a low temperature of processing that does not allow the transformation into TiB whiskers.

In order to work with nanosized reinforcements, TiB_2 powder will be reduced using ball milling processes. TiB_2 is a hard material, and therefore, brittle when ball milled. A ball milling of 5 hours has been done with a ball-to-powder ration of 7:1, inspired by a previous work on the exact same powder (T.TAYEH) that has shown the particle size does not decrease significantly after 5 hours of ball milling. The size measured by granulometry (d50) is 550 nm for volume distribution and 250 nm for number distribution. However, it has been observed that the TiB_2 powder have the tendency to form clusters. This aspect has to be taken into consideration during the mixing with matrix powder.

The other reinforcement, TiC particles, used in both HDH processes and ECAP process, is not modified before being used to prepare composite powder.

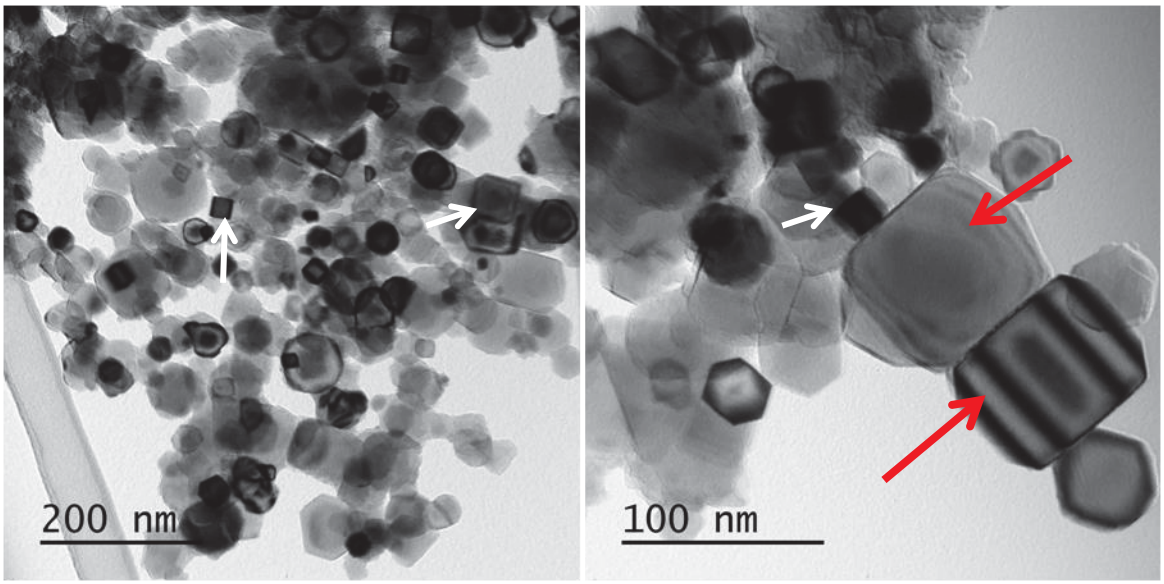

Figure 54: TEM observation of TiC particle

The TiC powder (Nanoamor, 99% purity) is described by the company as spherical particle with an average diameter of 40 nm. Nonetheless, TEM observation (Figure 54) shows 2 main sizes of particle with some particle having a cubic shape (red and white arrows respectively for the bigger and the cubic ones). By measuring several TEM micrographs, only few examples of the big particle have been found and the average size of the smaller population is 40 nm. Consequently, the TiC particle are considered spherical and with an average diameter of 40 nm.

Koo *et al.* [KOO2012] have shown in their work that after the growth of TiB whiskers in the matrix from TiB_2 particles, the average diameter of the whiskers is about half of the TiB_2 particle size. Therefore, after transformation into whiskers, their average diameter should be in a range between 300 nm to 80 nm approximately.

Another important step in the composites fabrication is the mixing between the reinforcement powder and the matrix powder. The different steps of the mixing have to be controlled in order to have an intimate mixing that will lead to a uniform distribution of the reinforcement within the matrix.

III-3. Mixing of reinforcement and matrix powders

The mixing of reinforcement and matrix powder will be different depending on the process considered. For the composite Ti/TiC prepared by ECAP, the starting powders are soft Ti (micrometric) for the matrix and hard TiC (nanometric) for the reinforcement. The mixing behaviour will be different than for the HDH mixing of starting powders. For both composites Ti/TiC and Ti/TiB prepared by HDH (pressureless sintering and hot pressing), the mixing process will consist on having an intimate mixing of the two powders without reducing the size of TiH_2 (to avoid reaching the pyrophoric size).

III-3.1 Composite powder preparation for ECAP process

Due to the difference in size between TiC powder and Ti powder (40 nm and 200 µm), and the difference of mechanical behaviour (hard and soft), the mixing of composite will be a critical point. Indeed, the reinforcement particle has to be uniformly distributed within the matrix particle, as presented in Gu *et al.* mechanism (chapter 1) [GU2010].

The ECAP process has the possibility to disperse the reinforcement more uniformly, but not the possibility to break clusters. That is why the distribution of the reinforcement inside matrix particles has to be cluster-less before the ECAP process. To achieve it, ball milling is used. The settings have been optimised using Gu's work: ball-to-powder ratio 10:1, iron balls, milling under argon protective atmosphere, and a milling time/ break time of 18 minutes/12 minutes, to avoid overheating at 250 RPM. The different steps expected were fracturing after 5 hours of ball milling, cold welding after 15 hours of ball milling and re-fracturing after 20 hours or more of ball milling. On the Figure 55, the different steps are observed after a) 1 hours, b) 5 hours, c) 15 hours, d) 20 hours and e) 30 hours. Welding against the jar's walls has been observed for a ball milling longer than 30 hours, making the powder impossible to get back.

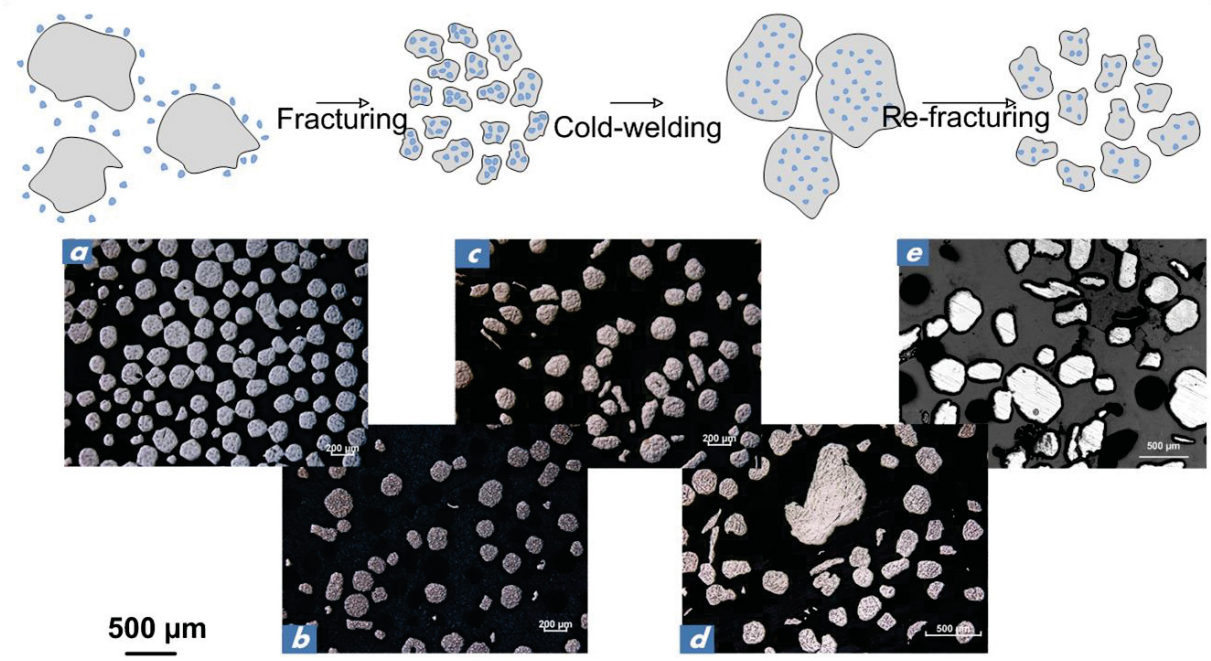

Figure 55: Theoretical drawing and optical micrographs of ball milling of Ti and tiC powders for a) 1hour, b) 5 hours, c) 15 hours d) 20 hours and e) 30 hours

After an hour of ball milling (optical micrograph a)), there is not much deformation of the Ti particles, and the shape of the particle is still spherical. After 5 hours of ball milling (optical micrograph b)) evidences that the fracturing phenomenon has started to occur are visible. Small fragment of Ti particles are visible. On the optical micrograph c) (15 hours) the fracturing phenomenon is clearly seen but cold welding phenomenon does not seem to be important at this stage. All this phenomena are not exclusive and can occur at the same time, which is why on the optical micrograph d) (20 hours) evidences of cold welding, along with evidences of fracturing are observed. It is impossible to tell if the fractured particles are from fracturing or re-fracturing, once cold welding has been observed. After 30 hours, (optical micrograph e)) the fracturing and cold welding phenomena seem to be balanced, all the particles observed having relatively similar diameter. However, due to the small size of the reinforcement, it is hard to know if the process has been fully efficient prior densification of the powder.

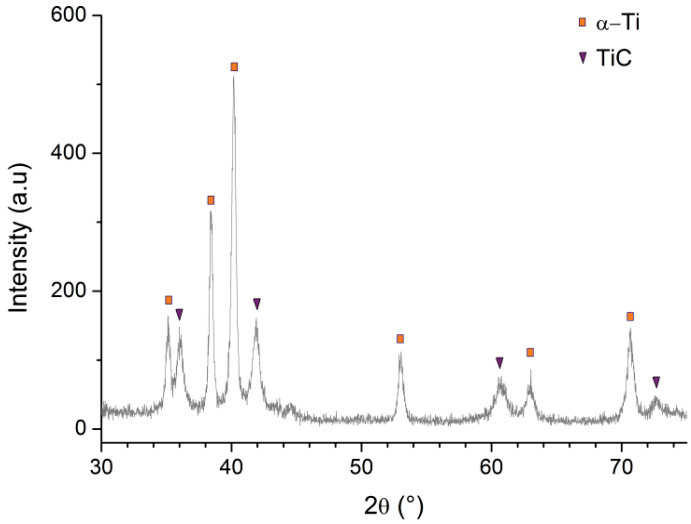

Figure 56: XRD spectrum of Ti - 10vol% TiC after 30 hours of ball milling

An XRD analysis (Figure 56) on the composite powder ball milled for 30 hours confirms that the two components are still in presence in the mixed powder after long time of ball milling. The composite powder, after ball milling, is slightly compacted inside a stainless steel foil, in a cylindrical shape (diameter of 11 mm and length of about 70 mm) in order to be process through ECAP. The purpose of the compaction is to ease the possibility to transport and insert the powder sample inside the ECAP machine.

III-3.2 Composite powder preparation for HDH processes

- *Mixing*

The TiH_2 powder and the reinforcement powder (TiC and TiB_2) are all hard material. Therefore, the previous milling process is not considered. Because the composite powder, in both of the HDH processes (pressureless sintering and hot pressing) does not go under severe plastic deformation, the distribution of the reinforcement has to be uniform before densification. Intense ball milling is not possible when using TiH_2 powder due to the fact its particle size could be reduced and the powder would not be inert in air. Therefore, in order to mix reinforcement and matrix powder, ball milling is still used, but at a lower speed of 80 RPM. At this speed, no fracturing of the matrix powder is expected, but the movement of the balls should break the clusters of both reinforcement and matrix powders. Also, because the density of Ti is not much different than the ones of TiB_2 and TiC (Ti: 4.5 $g.cm^{-3}$, TiB_2: 4.52 $g.cm^{-3}$ and TiC: 4.92 $g.cm^{-3}$), a statistical uniform distribution is expected after a long enough time of mixing. With a ball-to-powder ratio similar to the one for ball milling, 10:1, a mixing of 5 hours has been performed. But again, due to the small size of the particles, only dense materials can be used to analyse the reinforcement particle within the matrix. To verify that the ball mixing does not affect the nature of the powder, an XRD analysis has been performed on the powders afterward for the one with a volume fraction of 10% (Figure 57 and Figure 58).

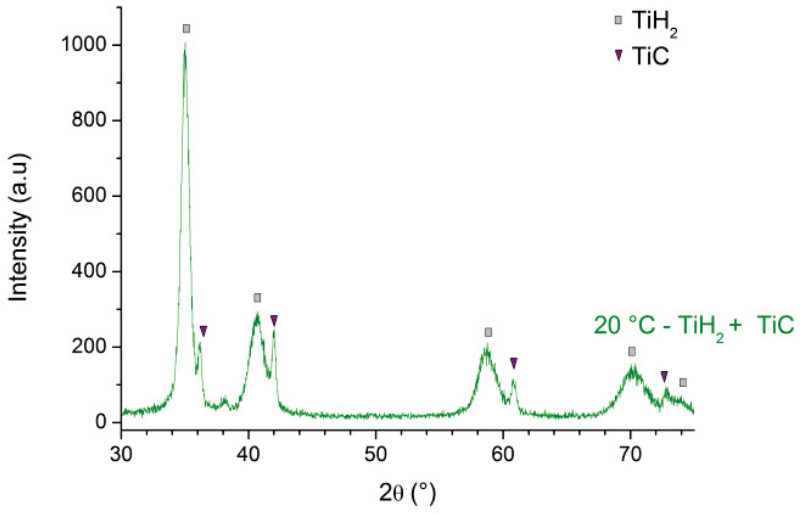

Figure 57: XRD spectrum of TiH_2 - 10vol% TiC after ball mixing

Both of the spectra (Figure 57 and Figure 58) show that the TiH_2 has not been affected by the ball mixing process, and the expected phases are observed for each composite powder. On the spectrum of Ti/TiB_2 composite powder, a signal from the sample holder is observed, but does not have influence on the powder.

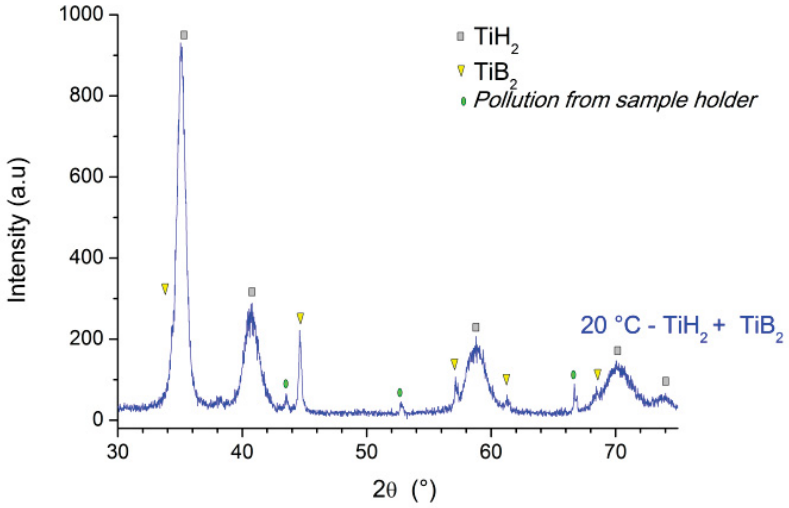

Figure 58: XRD spectrum of TiH_2 - 10vol% TiB_2 after ball mixing

As said before, the ball milling can be a source of impurities contamination for the powder, so it is important to make sure that the ball mixing has not polluted the powders. The ICP observation of the powder ball mixed had shown that the amount of impurities in the mixed powder did not changed from the amount of the powder prior ball mixing.

- *Cold compaction*

To be processed using HDH pressureless sintering, another step is necessary, the cold compaction. As said, the green density reached will be a key factor in the final density of the composite. To obtain fully dense materials using this process, a threshold of relative green density ρ_m has to be reached, otherwise the final relative density D_r cannot be 100%. For fine powders, ρ_m has to be equal or higher to 70 % [SAV2012] [WAN2010].

In this work, cold compaction is done using uniaxial pressing followed by HIP. The uniaxial pressing will shape the sample in order to be process by HIP, and in the same time reach a high enough cold compaction. The following HIP will make the pressure applied on the sample uniform, and help to reach the desired green density. The samples are pressed into pellets of 8 mm diameter, and 3 mm high. The uniaxial pressure applied on the sample is 440 MPa. Then, the pressure applied using HIP on the sample is 600 MPa. Savvakin *et al.* in their work have shown the minimum pressure to apply on a fine TiH_2 powder, in order to reach D_R = 70 %, is 600 MPa. The geometrical measured density for the TiH_2, TiH_2-TiB_2 and TiH_2-TiC (the volume fraction of the reinforcement is 10%) after cold compaction process is given on Table 6.

Sample	TiH_2	TiH_2-10vol% TiB_2	TiH_2-10vol% TiC
Apparent green density ρ ($g.cm^{-3}$)	2.780	2.819	2.849
Relative green density ρ_m (%)	70	71	71

Table 6: Relative green density of cold compacted composite powders

The densities measured reach the theoretical threshold to obtain full density after free sintering. The composites powders are therefore ready to be sinter.

For the HDH hot pressing, only TiH_2-TiC composite have been investigated. However, because the pressure is applied during the dehydrogenation step, the threshold is not an issue. The composite powder after mixing is ready to be processed using hot pressing without more compaction.

Once the matrix and reinforcement powders are mixed together, and possibly cold compacted, they are ready to be process in order to get dense composite materials. The different processes used will have different parameters that can be adjusted and that will have influence on the properties of the produced composites.

IV. Processing of the composite powders

The processing of the powder is the main step to obtain fully dense material. In the case of ECAP, it might as well have an effect on the reinforcement distribution. The different processes used in this work to obtain the composites, with their particularities and their limitations will be presented.

IV-1. Equal Channel Angular Pressing

The equipment for the ECAP used in this work is shown on the Figure 59. It is composed of 2 cylindrical channels identical in cross section, with a diameter of 11 mm. The channels intersect at an angle of 90° (1). Two plungers are used to push forward the sample through the shear zone and to apply a back pressure in the same time (2). After the first pass, the forward and back plungers swap roles. Once the sample is inserted in the dies along with the plungers, the dies are maintained close together by a pressure applied on the top. This pressure is principally here to avoid any flashing of the sample between the two inserts (3). To reduce as much as possible the friction between the sample and the dies, the sample is wrapped with graphite paper and lubricant is sprayed on the channel wall and the plungers. The pistons were set to move at a speed of 5 mm/min. Each plunger has a capacity of 25 tonnes. To reach the desired working temperature, heating blankets are used and the heating starts right before processing the sample. The control of the temperature is made by a thermocouple placed near the channel intersection and it allows keeping the selected temperature to ± 1 °C.

In this configuration, pressing the sample forward and backward is equivalent to follow the ECAP route C. Following other ECAP routes is possible with this equipment but has not been investigated due to numerous steps added to the process. Indeed, following another route requires taking the sample out between each pass, and inserting it again. To do that, the whole equipment has to be unset, and the sample has to be slightly machined in order fit into the channel. This process is more convenient when using the squared channel and bulk samples, but squared channel are not suited for powder material.

Based on the work done before on this equipment on CP Titanium, the temperature has been optimised at 600°C and the back pressure applied is fixed at 50 MPa. The number of pass tried on all the sample (no ball-milled Ti, ball-milled Ti, Ti/1%vol.TiC, Ti/3%vol.TiC and Ti/10%vol.TiC) is 2 and 8. In addition, 17 passes and 20 passes have been tried on no ball milled Ti and ball milled Ti/1%vol.TiC, respectively (the fact that it is 17 passes and not 20 is the result of reaching the machine limit in pressure applied on the sample, making it impossible to continue the process). In the regular ECAP process done in this work, about 600 MPa is applied on the sample at each pass. When the limit of

the machine is reach, the pressure applied suddenly jump to more than 1000 MPa without moving the sample, leading the plungers to retract to prevent any damages on the equipment. After the last pass, the sample is quickly extracted from the dies and quenched into cold water to retain the as-processed microstructure.

The ECAP process encounters some limitation in its possibilities. For example, the number of pass is limited by the increase of stiffness in the material and/or the flashing, and the consummation of the lubricant. The process is usually done under air, because using a protective atmosphere requires a complicated and specific setup. Working at relatively high temperature can induce pollution from the wall to the sample, therefore, only the core of the sample is used for the characterisations.

The ECAP process has, nonetheless, some unique advantages. For example, the densification of a powder sample is completed after only 2 passes. The shearing deformation induced to a sample is significant and can lead to a very fine microstructure (grain under 1 micron). In the case of powder, it can help to break oxide layer and disperse it. It also can help to disperse reinforcement more uniformly in the case of composite powder sample.

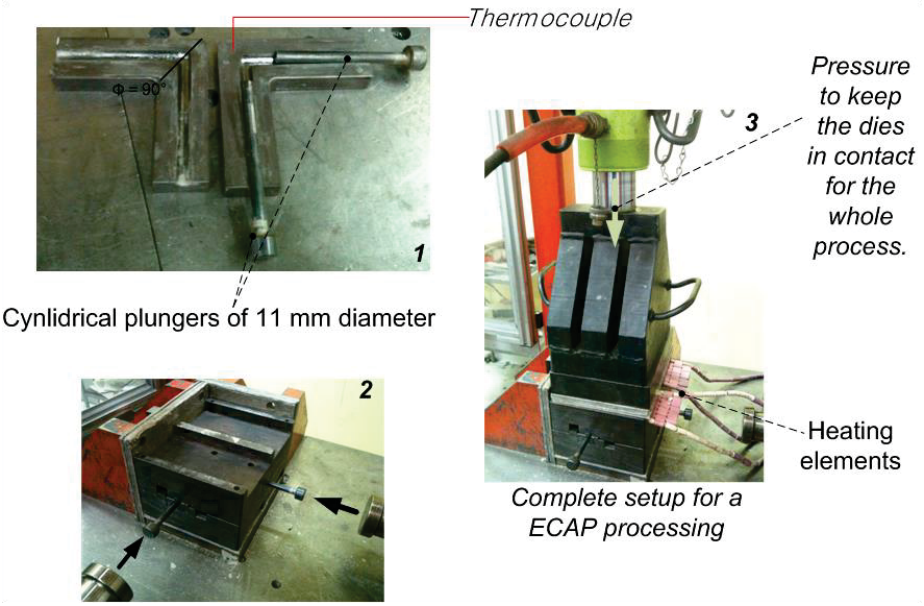

Figure 59: ECAP setup 1/ Inserts with the plungers, 2/Closed dies with the inserts and 3/Complete setup

IV-2. HDH pressureless sintering

The hydrogenation/dehydrogenation process using pressureless sintering used in this work has been done in a *Termolab* vacuum furnace. The compacted sample is inserted in the chamber of the furnace that is put under secondary vacuum (10^{-6} mbar). The sample is then sintered at 1400 °C for 4 hours, with a heating rate of 10 °C/min (Figure 60). The cooling rate is set at 20 °C/min, but its control is not as efficient as it is for the heating rate. This process has been done on the different composite TiH_2, TiH_2/1%vol.TiC, TiH_2/3%vol.TiC, TiH_2/10%vol.TiC and TiH_2/1%vol.TiB_2, TiH_2/3%vol.TiB_2, TiH_2/10%vol.TiB_2.

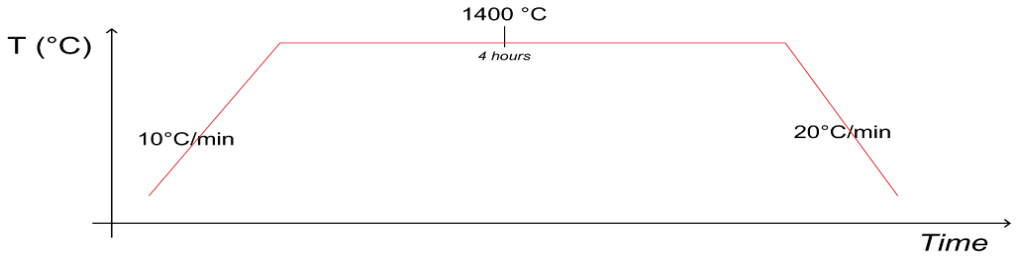

Figure 60: Heating cycle of pressureless sintering

The limitations observed for this furnace are the size of the chamber, and the impossibility to open the furnace at a temperature higher than 150 °C, making impossible any quenching. In this furnace, the size of the room (50 mm x 50 mm x 50 mm) could limit the size of the sample to sinter.

However, pressureless sintering has the main advantage to process near net shape material. In this work, only pellets are sintered but it is conceivable to have more complex shape to sinter.

IV-3. HDH hot pressing

The hydrogenation/dehydrogenation hot pressing used in this work has been done in an induction hot pressing. This technique shows three degrees of freedom: time, pressure, and temperature. By tuning these parameters, one can adjust the microstructure of the final material. In this process, heat is produced within the mould when it is subjected to a high frequency electromagnetic field, generated by using an induction coil coupled to an electronic generator (Figure 61). The mould is made out of graphite, and pressure is applied by one punch. The mould is positioned within the induction coil. The mould has to be placed at the exact centre of the coil, or the heat distribution is uneven. Loose powder is introduced into the mould, and the mould is inserted in the pressing device. After the chamber is under primary vacuum (10^{-2} bar), the heating process starts. Once the desired temperature is reached, after few minutes, the desired pressure is applied. The system is then held at these pressure and temperature during the chosen time. At the end of the process, the pressure is released, but during the cooling time, which can take several minutes, the vacuum is maintained.

In this work, the parameter selected in terms of time pressure and temperature are based on the work of the Master student Evan Schumann, who worked on the system Ti-Al, obtain after the dehydrogenation of TiH_2 with Al.

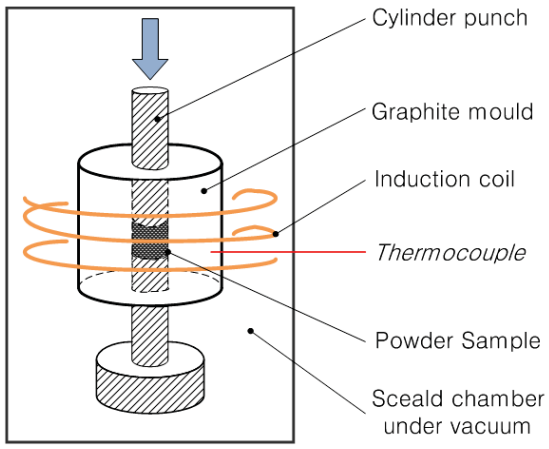

Figure 61: Hot pressing schematic drawing

The optimised parameters are a processing time of 30 minutes, at 800 °C, with a pressure applied of 80 MPa. This process has been done on the different composite TiH_2, TiH_2/1%vol.TiC, TiH_2/3%vol.TiC, TiH_2/10%vol.TiC.

The hot pressing system encounters some limitations. Indeed, the use of a graphite mould can be undesirable for samples that are highly reactive with carbon. To avoid that, steel mould can be used. However, steel shows its limits when required to hot press at elevated temperatures. Indeed, it is not possible to heat up the steel mould above 650°C without modifying its microstructure and affecting its mechanical properties. On another hand, graphite shows lower mechanical tenue but can be heated up to 1000°C under controlled temperature if needed. One should select the mould material in regards of the sample and the parameters desired.

Another disadvantage of technique such as hot pressing is the shape limitation. Indeed, complex forms will be extremely complicated (or even impossible) to obtain using moulds and therefore will require machining after the process. However, the induction heating technique is a widely spread heating method in powder metallurgy, with the advantages of being a sintering technique that is fast, with low capital cost, and low energy consumption, relative to other processes that could be employed (SPS, free sintering).

The influence of the different parameters for the different processes will have an influence on the produced composite. These influences will be the main subject of the next chapter. Moreover, the analysis of the produced composites will be an indicator of the efficiency of the powder preparation done in this work. Table 7 shows the summary of the different parameters of the investigated processes used in this work.

Process	**Temperature (°C)**	**Time**	**Vacuum**	**Pressure**
HDH pressureless	1400	4 hours	10^{-6} mbar	N.A.
HDH hot pressing	800	30 min	10^{-1} mbar	80 MPa
ECAP	600	~10 min/pass	Air	~600 MPa Back pressure: 50 MPa

Table 7: Summary of the different processes used

V. Conclusion

The modelling of the investigated composites has shown the influence of parameters on the properties, which can be adjusted by changing the nature of the composite and/or changing the process used. As expected, the Young's modulus, along with the yield strength will be affected by adding reinforcement into a matrix. But the modelling work has shown the impact of reducing the size of the reinforcement, or changing the shape (aspect ratio) of the reinforcement. In both case, the properties of the composite will be significantly improved. Applied to the investigated composite Ti/TiB_w and Ti/TiC, the modelling work has shown that by adding only a few amount of reinforcement (TiB or TiC) into the matrix (Ti), the properties, yield strength and Young's modulus, of this last one can be significantly increased, which make this work relevant and interesting. However, this modelling work is the representation of an ideal material, fully dense and with the reinforcements

uniformly distributed.

To achieve such materials, the processes used have to be perfectly controlled. The first step to control a powder metallurgy process is the powder itself. The TiH_2 powder used in this work has been obtained after hydrogenation of Ti sponge, and its size is controlled by ball milling time, in order to work with a powder size of 200 nm to 500 nm.

The reinforcement used in this work, TiC (40 nm) and TiB_2 (150 nm to 650 nm) are mixed with the TiH_2 powder and the Ti powder, respectively for HDH processes and ECAP process. The mixing processes are expecting to distribute the reinforcement in order to obtain uniform distribution of the reinforcement within the matrix after processing.

The densification of the mixed composite powder is done using 3 processes: HDH pressureless sintering, HDH hot pressing and ECAP. Different parameters are adjustable in these processes, temperature, time, heating rate for pressure less sintering, temperature, time, pressure applied for hot pressing, and number of pass, back pressure, temperature for the ECAP process.

In the next chapter are presented the composites fabricated using these processes. The observation of their microstructure along with their properties is done. The influence of each process and reinforcement can therefore be compared between the ideal situation and the different fabricated composites. The observation of their microstructure will also allow commenting the efficiency of the mixing processes.

List of Figures and Tables

Bibliography

[CAL2007] - W.D. Callister, *Material Science and Engineering: An Introduction*, John Wiley & Sons, Inc., 7th Edition, (2007)

[CHA2006] - N. Chawla, K.K Chawla, *Metal Matrix Composites*, Springer Science, (2006)

[CHE2010] - Y.J. Chen, Y.J. Li, J.C. Walmsley, S. Dumoulin, P.C. Skaret, H.J. Roven, *Microstructure evolution of commercial pure titanium during equal channel angular pressing,* Materials Science and Engineering A, 527, pp.789–796, (2010)

[CHE2011] - Y.J. Chen, Y.J. Li, J.C. Walmsley, S. Dumoulin, S.S. Gireesh, S. Armada, P.C. Skaret and H.J. Roven, *Quantitative analysis of grain refinement in titanium during equal channel angular pressing,* Scripta Materialia, 64, pp.904–907, (2011)

[DAR2004] – F. Dartigues, PhD Thesis, *La precipitation a la solidification du monoborure de titane dans l'alliage de titane (Ti-6Al-4V) peut-elle modifier sa microstructure et son comportement mecanique ?,* University of Bordeaux 1, (2004)

[GAR2006] - M. Garcia de Cortazar, PhD Thesis, *Development of a new reinforced titanium alloy: Basic research and technological transfert for the Ti-6Al-4V/TiB material,* Université Bordeaux 1, (2006)

[HOS2012] - M. Hoseini, M.H. Pourian, F. Bridier, H. Vali, J.A. Szpunar, P. Bocher, *Thermal stability and annealing behaviour of ultrafine grained commercially pure titanium,* Materials Science and Engineering A, 532 , pp. 58-63 (2012)

[KAN2010] - D-H. Kang, T-W. Kim, *Mechanical behavior and microstructural evolution of commercially pure titanium in enhanced multi-pass equal channel angular pressing and cold extrusion,* Materials and Design, 31, pp.54–60, (2010)

[KOO2012] - M.Y. Koo, J.S. Park, M.K. Park, K.T. Kim and S.H. Hong, *Effect of aspect ratios of in situ formed TiB whiskers on the mechanical properties of TiBw/Ti–6Al–4V composites,* Scripta Materialia, 66, pp.487-490, (2012)

[GU2010] - D. Gu, W. Meiners, Y-C. Hagedorn, K. Wissenbach and R. Poprawe, *Structural evolution and formation mechanisms of TiC/Ti nanocomposites prepared by high-energy mechanical alloying,* Journal of Physics D: Applied Physics, 43, pp.1-12, (2010)

[LAN1978] - J.I. Langford, A.J.C. Wilson, *Seherrer after Sixty Years: A Survey and Some New Results in the Determination of Crystallite Size*, Journal of Applied Crystallography, 11, pp.102-113, (1978)

[LI2010] - Z.Li, L. Fu, B. Fu, A. Shan, *Yield point elongation in fine-grained titanium,* Materials Letters, 96, pp.1–4, (2010)

[LUI2012] - E. Lui, PhD thesis, *Multiphase and Multiscale Al-Ti Alloys Consolidated by Severe Plastic Deformation,* Department of Mechanical Engineering, The University of Melbourne, (2012)

[LUO2012a] - P. Luo, D.T. McDonald, W. Xu, S. Palanisamy, M.S. Dargusch and K. Xia, *A modified Hall–Petch relationship in ultrafine-grained titanium recycled from chips by equal channel angular pressing,* Scripta Materialia, 66, pp.785–788, (2012)

[LUO2012b] - P. Luo, D.T. McDonald, S.M. Zhu, S. Palanisamy, M.S. Dargusch, K. Xia, *Analysis of microstructure and strengthening in pure titanium recycled from machining chips by equal channel angular pressing using electron backscatter diffraction,* Materials Science and Engineering A, 538,

pp.252‐258, (2012)

[LUT2003] - G. Lütjering, J.C. Williams, *Titanium*, Ed. Springer, (2003)

[MEY2009] – M.A. Meyers, K.K. Chawla, *Mechanical Behavior of Materials,* Cambridge Univserity Press, 2nd Edition, (2009)

[SAV2012] - D.H. Savvakin, M.M. Humenyak, M.V. Matviichuk, and O.H. Molyar, *Role of Hydrogen in the Process of Sintering of titanium Powders,* Materials Science, 47, 5, pp.641-661, (2012)

[STO1999] - V.V. Stolyarov, Y.T. Zhu, T.C. Lowe, R.K. Islamgaliev and R.Z. Valiev, *A two step SPD Processing of Ultrafine-Grained Titanium*, NanoStructured Materials, 11, 7, pp.947–954, (1999)

[STO2003] - V.V. Stolyarov, Y.T. Zhu, I.V Alexandrov, T.C. Lowe, and R.Z. Valiev, *Grain refinement and properties of pure Ti processed by warm ECAP and cold rolling,* Materials Science and Engineering A, 343, pp.43‐50, (2003)

[STO2008] - V.V. Stolyarov, L. Zeipper, B. Mingler, M. Zehetbauer, *Influence of post-deformation on CP-Ti processed by equal channel angular pressing,* Materials Science and Engineering A, 476, pp.98–105, (2008)

[TJO2008] - S.C. Tjong, Yiu-Wing Mai, *Processing-structure-property aspects of particulate- and whisker-reinforced titanium matrix composites*, Composites Science and Technology, 68, pp.583–601, (2008)

[VAL2003] - R.Z. Valiev, *Paradoxes of Severe Plastic Deformation,* Advanced Engineering Materials, 5, 5, pp.296-300, (20003)

[WAN2010] - H. Wang, M. Lefler, Z.Z. Fang, T. Lei, S. Fang, J. Zhang and Q. Zhao, *Titanium and Titanium Alloy via Sintering of TiH_2,* Key Engineering Materials, 436, pp.157-163, (2010)

[ZHA2008] - X. Zhao, W. Fu, X. Yang and T.G. Langdon, *Microstructure and properties of pure titanium processed by equal-channel angular pressing at room temperature,* Scripta Materialia, 59, pp.542–545, (2008)

[ZHA2010] - X. Zhao, X. Yang, X. Liu, X. Wang and T.G. Langdon, *The processing of pure titanium through multiple passes of ECAP at room temperature,* Materials Science and Engineering A, 527, pp.6335‐6339, (2010)

Chapter III - Characterisation of the different titanium-based composites

I. Introduction

The previous chapter has presented the relevance of the research done on Ti based composites during this work, through the modelling work. It also has presented the preparation of the different powders prior the densification of the composites and the different densification processes used to obtain the investigated materials, hydrogenation/dehydrogenation densification, and ECAP.

After using ball milling to mechanically mix the TiC powder reinforcement with the Ti powder reinforcement, ECAP process was used to obtain a dense material. The properties of the final material are linked to the different step of the process, from the ball milling to the number of ECAP pass.

The mixing between the TiH_2 powder and the reinforcement powders (whether TiC or TiB_2) has been done during what has been called ball mixing, and two different densification processes has been presented. The ball mixing step, and each densification process (pressureless sintering and hot pressing) have a different effect on the properties of the materials.

To understand the effects of the different step of the different processes on the material properties, after densification, microstructural and mechanical characterisations are done.

In this chapter are first presented the different characterisation method used, with the information they can provide. The microstructural characterisation is done using different techniques based on scanning electron microscopy, transmission electron microscopy and X-Ray analysis. These techniques provide data on the microstructure of the materials, which can be linked to the mechanical properties. This last will be measured using compression test and/or hardness.

Then, a link between the different measurements (microstructural and mechanical) will allow analysing the effect of different parameters on the fabricated materials.

II. Characterisation methods

After the fabrication of the different composites using the different powder metallurgy processes, multiple analyses have been conducted. Different microstructural characterisations and mechanical tests have been done on the composites. The idea is to understand the impact of the different processes used to fabricate the composite on its microstructures and mechanical properties. After, a comparison between the measured properties and the model material can be considered.

The microstructural characterisation techniques used are common in the field of material and their principles have been well detailed in the literature. Here, the principles of the less common method (EBSD) used will be explained. The different information that can be obtained when using these techniques on titanium based materials is also explained. The techniques used for the mechanical characterisations will be described, with their applicability for the fabricated materials and the limitations encountered.

II-1. Microstructural characterisation

It has been shown earlier that the different properties of the investigated composites are directly linked with the microstructure of the material. Indeed, the grain size, grain shape, the reinforcement distribution or even the pollution (impurities linked with the process used) have an influence on the mechanical properties of the composites. This is why it is important to fully characterise the

microstructure of the different sample in order to understand the influences of the different processes, reinforcements and treatments used. This characterisation also might provide information that can explain the mechanical results obtained.

The microstructural characterisation done on the produced material depends on three main techniques, Scanning Electron Microscopy (SEM), Transmitted Electron Microscopy (TEM) and X-Ray Diffraction (XRD). The SEM techniques will provide information on the surface of the material, usually on an area of about 100 µm² or less, and in order to have a statistical analysis, several measurements are required on the whole surface of the material. The TEM techniques are more focused, on an area of few micrometres, but will provide information on interface or interphase, at a nanoscopic scale. The XRD based techniques will provide information related to the nature of the material (phase, crystal size and orientation) at either a large sample (few millimetres) or when coupled with the SEM base technique (Energy Dispersive X-Ray Spectroscopy) on a selected area of few microns.

Therefore, combining these different characterisation methods will help to have a precise idea of the microstructure of the fabricated composite.

II-1.1 Scanning Electron Microscopy (SEM)

Scanning Electron Microscopy is a well-known technique to characterise different materials. It principle is based on the interaction between the atoms of the sample and the primary electron beam. In SEM analysis, a stream of primary electrons is focused on the sample surface resulting in a number of different particles or waves being emitted (secondary electrons (SE), back-scattered electrons (BSE), X-rays, photons or Auger electron) (Figure 62) [EGE2001].

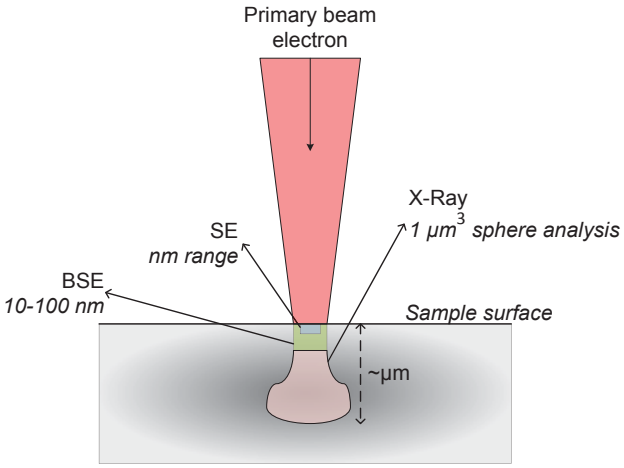

Figure 62: Electron - sample interaction pear

If both SE and BSE will characterise the surface of the material, the difference between the two comes from the depth of their interaction with the matter. Indeed, SE interacts with few nanometres of the surface when the pear of interaction of the BSE is in the range of 10 to 100 nm. Consequently, the information provided by the SE and the BSE will not be the same. In this work, SE are used to obtain a micrograph of the surface of the material, informing on 1) the particle and grain boundaries shape and thickness, 2) the distribution of the reinforcement particles if they are big enough, and 3) the analysis of the residual porosity if the process used does not provide a fully dense material. The BSE analysis is more sensible to the atomic number of the elements. Indeed, heavy elements (high atomic number) backscatter electrons differently than light elements (low atomic number). This will make the heavy elements appear brighter on the image. The different contrasts on BSE micrograph

are therefore associated with different chemical composition. However, the BSE will not provide any indication concerning the nature of the chemical composition. BSE can also be used to obtain a different contrast between grains of a crystalline material and consequently be used to observe the grain size and shape of the fabricated material.

The limitations of such analysis come from two different points in this work. First, the surface as to be free from any defect (scratches, pollution, dust). To avoid this, a fine polishing of the material has been done; mechanically first, using SiC paper under running water, then chemical-mechanically, using diamond and silica suspensions on polishing pads. The second point is that the observed material property has to be in the range of the analysis tool used. For example, if the observed grains are too small, the resolution of the SEM will not be fitted to provide any usable information. In those cases, the use of different techniques can be considered.

II-1.2 Energy Dispersive X-Ray Spectrometry (EDX)

As shown on the Figure 62, the interaction of a focused beam of electrons with the sample surface will induce X-Ray spectrum emission. Indeed, the incident electron will interact with an electron layer of a given atom, resulting in the emission of a specific X-Ray spectrum that can be analysed using a spectrometer. Each element will have specific X-Ray spectra, giving the possibility to use them as an element detector. By scanning the sample, a quantitative (determination of the concentration of the elements present) and qualitative analysis can be done, measuring area and energy of the peaks of the EDX spectra for each element in the sample.

In this work, EDX has been mainly used to analyse the possible pollution on the fabricated titanium based composite.

II-1.3 Electron Back Scattered Diffraction (EBSD)

One particular characterisation method used in this work linked to the SEM characterisation is the Electron Back Scattered Diffraction analysis. EBSD analysis gives information on the crystal orientation (i.e. texture) of a material, at a microscopic level, and also gives information of the grain shape and size [POU2004].

Two types of EBSD analysis exists, one related to the phase analysis (similar to the EDX), and the other related to the crystal orientation. In this work, only the second is considered, with the possibility to do a mapping of the sample, and to characterise the grain size, shape and the crystalline orientation. EBSD is a precise method to characterise the texture of one's material. In the case of Ti based material, the analysis of the texture is relevant due to the fact that the lattice of Ti is hexagonal, and therefore shows anisotropy in its properties.

This technique is based on the incident electrons that will be back-scattered by the crystallographic planes of the crystalline sample. The back-scattered electrons will be diffracted by the crystallographic planes into a pattern that will be observed on a phosphor screen. The bands in the pattern are called "Kikuchi lines" (Figure 63). They represent the reflecting planes in the diffracting crystal volume. Analysing these bands will provide information on the orientation of the diffracting crystal lattice, and consequently, on the texture of the sample.

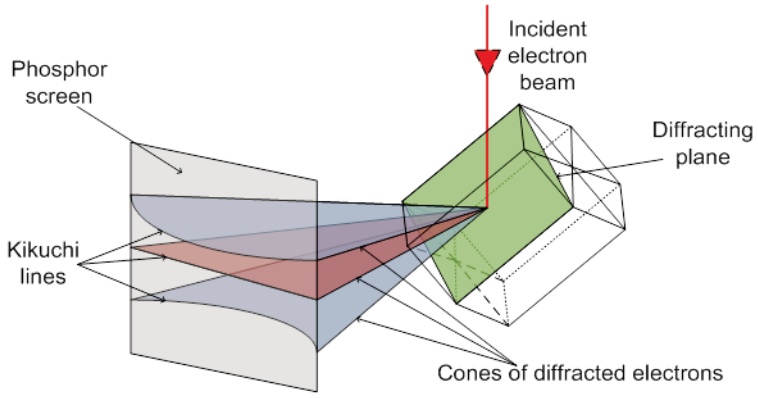

Figure 63: Kikuchi lines formation from the diffracting plan during EBSD analysis

In the common apparatus for EBSD analysis, the sample is tilted by 70°, which is the condition to obtain enough signals to analyse a sample. Conventionally, three directions are set in regards of the position of the sample, the rolling direction (RD), transverse direction (TD) and normal direction (ND) as represented on Figure 64-a. These directions will be linked to the position of the sample and will be independent from the orientation of the lattice. Figure 64-b represents the typical observation on the phosphor screen of the Kikuchi lines, on which the analysis will be conducted. These lines represent the orientation of the observed sample where the incident beam is being diffracted, which are only few nanometres wide. To have an idea of the whole sample surface orientation, a mapping of numerous observations is required.

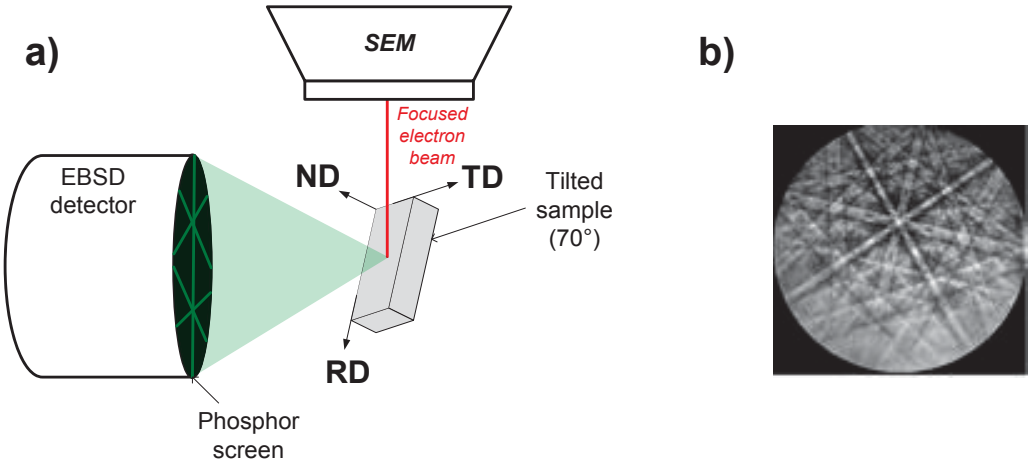

Figure 64: a) Calibration setting of an EBSD analysis and b) typical observation of the Kikuchi lines on a phosphor screen

Using the Kikuchi lines observed on the phosphor screen will lead to obtain the orientation of the lattice, and therefore the texture at this point. To do so, the software will proceed to different step in order to deduce the phase observed and its orientation (Figure 65):

- 1/ The Kikuchi lines will be detected by the software
- 2/ A Hough transform will convert these lines into dots on the Hough space (Hough Transform consists in representing a straight lines of space (x, y) into a point of space (ρ, θ))
- 3/ The points will be used to detect automatically the observed plans and indexing the bands
- 4/ Once the bands are indexed, the phase in presence and its orientation will be detected and recorded

By repeating this process on the whole surface (by moving the electron beam), a mapping can be obtained.

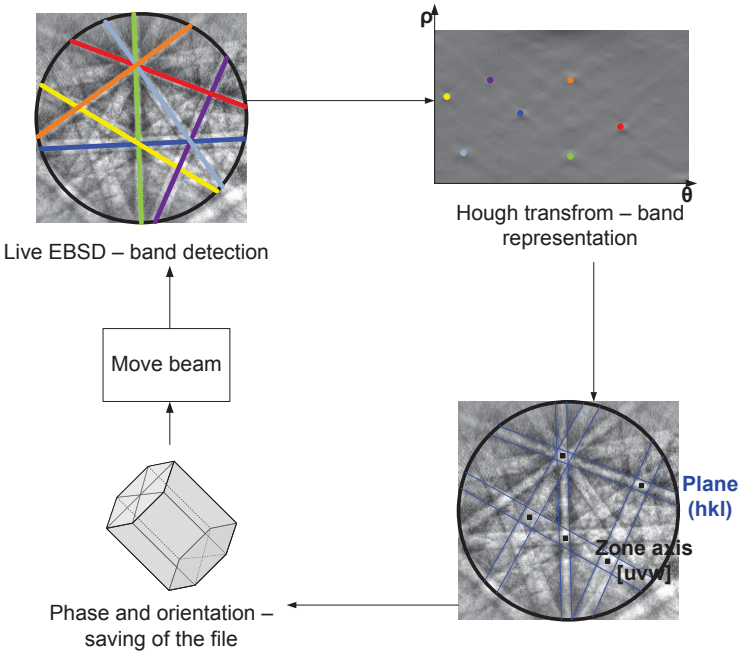

Figure 65: Different steps of the EBSD analysis on a sample

Once all the orientations are recorded for a given area, the data can be displayed in different ways: pole figure and inverse pole figure.

Pole figure gives information on the orientation of the different planes of the hexagonal lattice in regard of the rolling direction (RD), transverse direction (TD) and normal direction (ND). It consists in stereographical projection of the lattice into a circle where ND, RD and TD are fixed. The point representing the centre of a considered plan is then projected on the sphere, as shown on Figure 66.

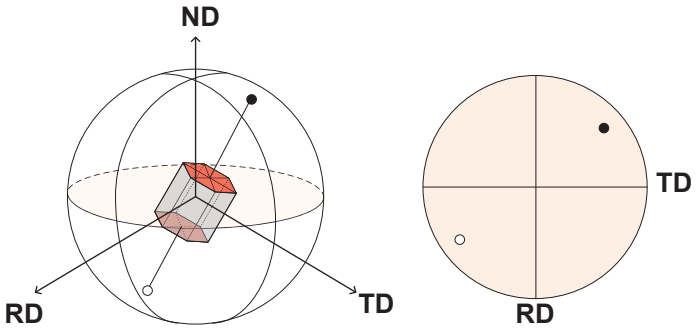

Figure 66: Construction of the stereographical projection of a hexagonal lattice

The black dot represent the plane (0001) projected on the northern hemisphere and the white dot its symmetrical plan projected on the southern hemisphere. Conventionally only the northern hemisphere is considered when constructing pole figure. Each plane direction is associated with a pole figure that will indicate the orientation of the chosen plane direction, for all the data recorded for a selected area. For example, if the sample is textured with only (0001) planes on the surface, the associated pole figure of this sample would have all the dots near the centre (being the ND, which in this case would be parallel to the C axis) To have an idea of the texturing of a material, the pole figures for the different planes are needed.

Inverse pole figure comes from a kind of global stereographical pole figure of all the main planes according to the three directions ND, RD and TD and where the axis C is considered parallel to the ND

(Figure 67).

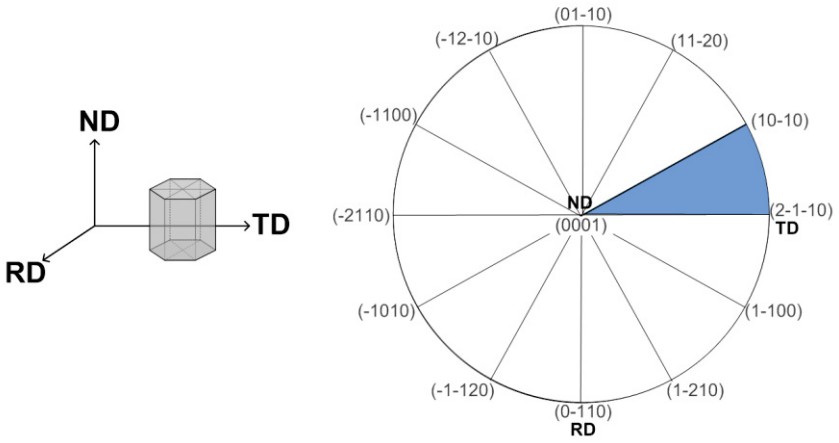

Figure 67: Inverse Pole Figure construction

While the pole figure shows only a specified plane distribution according to the three directions, the inverse pole figure will be constructed according one selected direction (usually ND also referred to as [001]), showing the main considered planes. The IPF will show which crystallographic directions in the polycrystalline material are most likely parallel to the sample normal direction. Unlike pole figure that will show all the orientation for one considered plane, the inverse pole figure will show which are the orientations seen while observing the sample surface along the ND. Figure 67 shows the construction of the inverse pole figure for hexagonal lattice. All the different planes are displayed, however, only the blue triangle is to be considered, due to the different symmetries between plans.

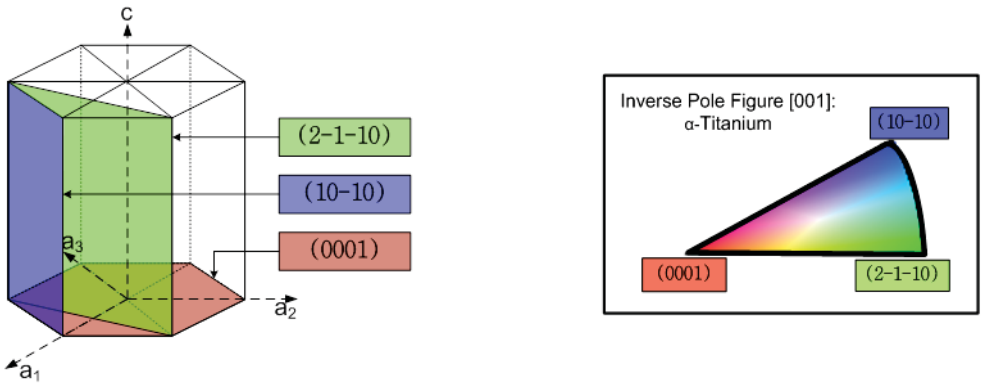

Figure 68: Plane representation for hexagonal lattice on the coloured inverse pole figure

The IPF can have two representations, the discrete plot, like on the pole figure, which will display all the points recorded on the figure according to which planes is facing the ND; and the coloured inverse pole figure in which each colour is associated to a plane, as shown on Figure 68. On this figure are displayed the different colours used for the IPF of α-Ti, with their corresponding planes on the lattice. The most common representation of a sample surface EBSD analysis is to have all the grain coloured as a function of their orientation (i.e. the plane facing the ND) as represented on the Figure 69. The same colours will be used for the EBSD analysis done in this work.

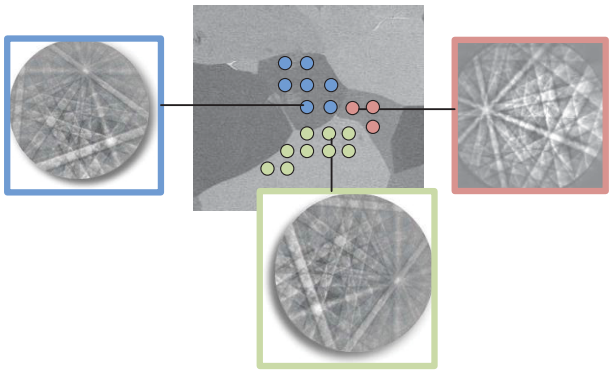

Figure 69: Example of the mapping during EBSD analysis

Conventionally, an EBSD figure is associated with discrete plot on pole figure and inverse pole figure that will provide information on the specific orientation of the analysed surface. In addition, the EBSD analysis can also automatically detect grain boundaries, and give a precise average grain size.

EBSD is a technique that is linked to an SEM apparatus and therefore will suffer from the same limitation (especially the resolution, if the grains are too small, they will not diffract for EBSD analysis).

In this work, EBSD will be useful to determine if the densification methods have an influence on the texture of the produce material. The grain size measurement associated with EBSD analysis will also be used.

II-1.4 Transmission Electron Microscopy (TEM)

Due to the limitation of the SEM analysis in term of resolution, Transmission Electron Microscopy (TEM) analysis has been used to analyse the interfacial zone (and the eventual interphase) between the Ti matrix and the reinforcement used. The high magnification also allows observing the microstructure of the sample at a lower scale, and the presence of crystal defect can be seen. Moreover, indexing the diffraction analysis, the presence or not of the phase sought (Ti, TiC or TiB) has been done.

One aspect of the TEM analysis is the range of observation that is quite narrow, unlike the magnification that is important. Consequently, only small areas of the sample can be observed meaning the TEM is not the proper technique to relate average result. However, using several zone of one ample can give an idea of a tendency and it provides relevant information about the interface, and the crystallinity of the sample observed.

II-1.5 X-Ray Diffraction (XRD)

If EBSD or TEM analysis can detect the phase in the sample, the use of X-Ray diffraction will be more relevant, the analysis being on a much bigger sample (few mm^2). In this work, XRD analysis has been done to analyse the different (crystalline) phases that are in presence on the fabricated samples. However, the grain orientation can be checked using XRD. Indeed, standard diffracting planes with the theoretical intensity for non-textured material (powder) is given by the Joint Committee on Powder Diffraction Standards (JCPDS) (Table 8). A non-textured material will therefore show the same planes and roughly same relative intensity on a XRD spectrum. By observing a difference in this intensity, and liking the concerned *hkl* plans with the corresponding EBSD planes, a confirmation of

the texturing can be done.

Standard *hkl* planes	100	002	101	102	110	103	200	112	201
Relative intensity	25	30	100	13	11	11	1	9	6
Corresponding EBSD planes	*10-10*	*0001*	*10-1-1*		*2-1-10*				

Table 8: Standard hkl plans and intensity for α-Ti with the corresponding plans in EBSD

Using the Scherrer formula, presented in the previous chapter, will provide information on the coherently scattering domains. Ungar *et al.* [UNG2005] have shown that for metallic materials, the coherently scattering domain obtained by XRD is always smaller than the size of the subgrain that can possibly be measured by TEM. However, the evolution of the size of the coherently scattering domains provides information on the influence of the densification process used on the final material. XRD analysis is used in this work to verify the phases in presence on the dense materials, and to confirm the observation made using EBSD.

Combining the different characterisation methods presented will give a precise description of the materials microstructure. Indeed all the data that can be obtain are useful to explain the mechanical properties of the investigated material.

II-2. Mechanical characterisation

Mechanical characterisation of a material can be done using multiple methods, depending on which property is measured. However, an important limitation to this measurement comes from the sample. Indeed, the size and the shape of the sample is often source of limitation to use a technique. For example, to measure the yield strength and the Young's modulus of a metal, the most precise techniques is the strengthening test. However, this technique requires having a sample cut in a specific "dog-bone" shape, with standardised dimensions. And depending on the fabrication process used, having enough material to do so is not always the case. In this work, the different mechanical characterisations have been done according to the possibility given by the fabricated samples.

II-2.1 Density

Density of the fabricated materials has been obtained using Archimedes principle. However, if this method give a satisfying idea of the porosity of the sample, it is not relevant in regards of the nano-porosity that can be observed on sample prepared by powder metallurgy.

The specimen was first weighed in air and then in distilled water. The density is calculated using the following equation:

$$\rho = \frac{m_{air}}{m_{air} - m_{wat}} \rho_0 \qquad (4.1)$$

where m_{air} is the weight of the sample in air, m_{wat} is the weight in distilled water and ρ_0 is the density of the distilled water at the testing temperature (i.e. room temperature). Six measurements were

obtained from each sample to calculate the average density. Then again, the results are given in relative density, where the measured density is given as a percentage of the theoretical density.

II-2.2 Microhardness

One simple characterisation done in this work is the Vickers microhardness measurement. The measured sample has to be fully dense, show two parallel faces and be polished. The measurement is done using micro indentation.

By measuring hardness on sample, an estimation of the yield strength can be obtained using the work of Tablor [TAB1951]. He has shown that there is a relationship between the hardness of a metal and its yield strength expressed by:

$$H_v = C\sigma_y \tag{4.2}$$

where C is a constant and H_v the Vickers hardness (expressed in MPa). The value of C is commonly equal to 3. However, De Castro *et al.* [CAS2005] have shown in their work that this relationship can also be effective with nanocomposites. To determine a proper value of C to apply on the Ti based nanocomposites, the data from several references has been plot in a graphic Yield Strength vs Hardness (Figure 70) [REF-FIG70]. The data used in this graphic concern only Ti based materials. Therefore, the estimation of the yield strength given by the formula would be more precise, even though it is only estimation.

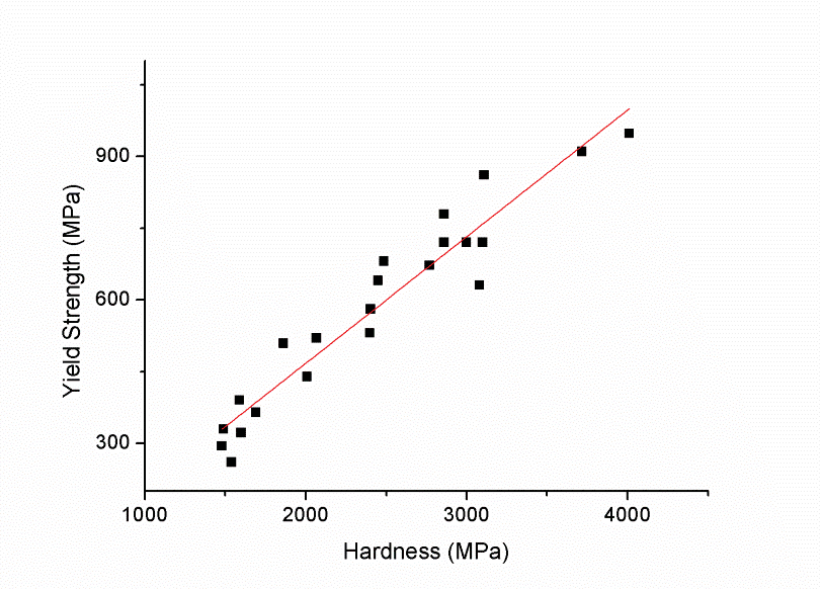

Figure 70: Yield Strength vs Hardness for several Ti based materials [REF-FIG70]

The equation of the fitted data gives:

$$\sigma_y = H_v \times 0.265 - 62.91 \tag{4.3}$$

Knowing that the properties of titanium material can be linked to the orientation, hardness measurement might be taken along different faces for a same sample if this one is textured. However, if the sample does not show any texture, the hardness measurement remains the same, regardless the direction chosen.

Nevertheless, to have a better idea of the yield strength value, and to have an idea of the ductility of the fabricated material, hardness test is not suitable.

II-2.3 Compression testing

To have a more precise value of the yield strength, and to observe a potential ductility in the samples, compressing test has been done. Due to the size and the shape of the samples obtained by the HDH methods, only ECAP sample were tested. To do so, compressive specimens of 4 × 4 × 6 mm were cut from the consolidated material with the compression axis parallel to the longitudinal direction of the ECAP sample (ECAP direction) (Figure 71). The specimens were compressed at an initial strain rate of 10^{-3} s^{-1}. A yield strength vs strain curve is obtained.

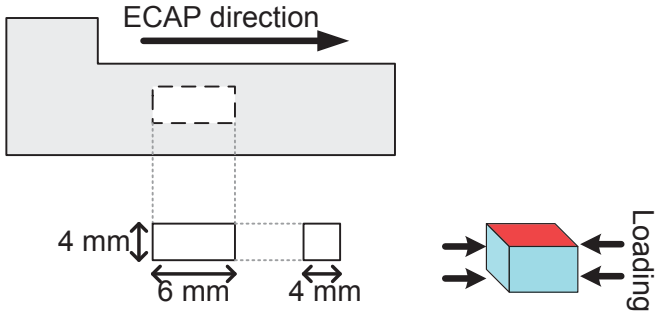

Figure 71: Compression specimen extracted from ECAP sample, with ECAP direction

The compression specimens were only cut along the ECAP direction due to the fact that the ECAP sample was not big enough.

The result obtain from compression testing will provide information on the yield strength and the ductility, and will be compared to the result obtain from hardness testing, to confirm or not the estimations made. The value of the elongation strain of the specimen, obtained by compression is not to be compared with the one in literature, commonly obtained by tension tests. It is, nevertheless, a good indication regarding the ductility of one's material.

Linking the mechanical characterisations with the microstructural characterisations will help to explain the different properties obtain on the materials, and the effect of the different process used.

Each microstructural characterisation will provide data that can be interpret in regards of the different mechanical properties measured. Not only explanation of the properties of the materials will be deducted from such characterisations, but the explanation of the effect of the process used on one's material can also be considered.

III. Ti → ECAP

One of the methods used to fabricate the material is the ECAP as presented on the previous chapter. This method based on the severe plastic deformation of the powder has a major impact on the microstructure of the produced material. Moreover, the preparation of the metal powders requires high energy ball milling, which has an impact on the starting powder. The starting powder is considered polycrystalline and a difference is made between grain boundaries and particle boundaries (Figure 72).

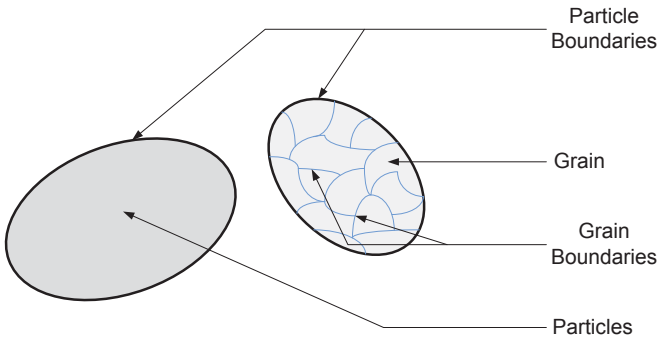

Figure 72: Particles of Ti used during the ECAP process

Different parameters can have an influence on the microstructures and the mechanical properties of the fabricated composites when using ECAP, such as the BM step, the number of pass or the volume fraction of reinforcement. To study this influence, several samples were prepared by ECAP densification, as resumed on the following table:

Sample	ECAP conditions	
Ti (without BM)	600°C Back Pressure: 80 MPa	2 Passes 8 Passes 17 Passes
Ti (BM)		2 Passes 8 Passes
Ti - 1%TiC		2 Passes 8 Passes 20 Passes
Ti - 3%TiC		8 Passes
Ti - 10%TiC		8 Passes

Table 9: Samples produced using ECAP

By characterising the different produced samples, the effect of the different parameters on the microstructure can be deducted, and the relation between the microstructure and the mechanical properties can be obtained. For the following considerations, the results obtained for the composite at 10% were found to equivalent to the composite at 3%. Consequently, the choice of characterising only the composite at 10% had been made.

III-1. Effect of ECAP process on dense material

Before any further characterisation, the density of each sample has been measured. It appears that after only 2 passes, all the samples were having a relative density of about 99%. ECAP process produces fully dense Ti based composite regardless the volume fraction of TiC considered.

Like most of the SPD densification methods, ECAP is known to texture the produce titanium [BOZ2007] [CHE2010] [GUB2003]. Even if the researches are mostly conducted on bulk titanium, the

EBSD characterisation of the produced sample seems to confirm this observation. Indeed, EBSD analysis on the sample Ti (without BM) ECAPed for 17 passes reveals that the surface is fully oriented.

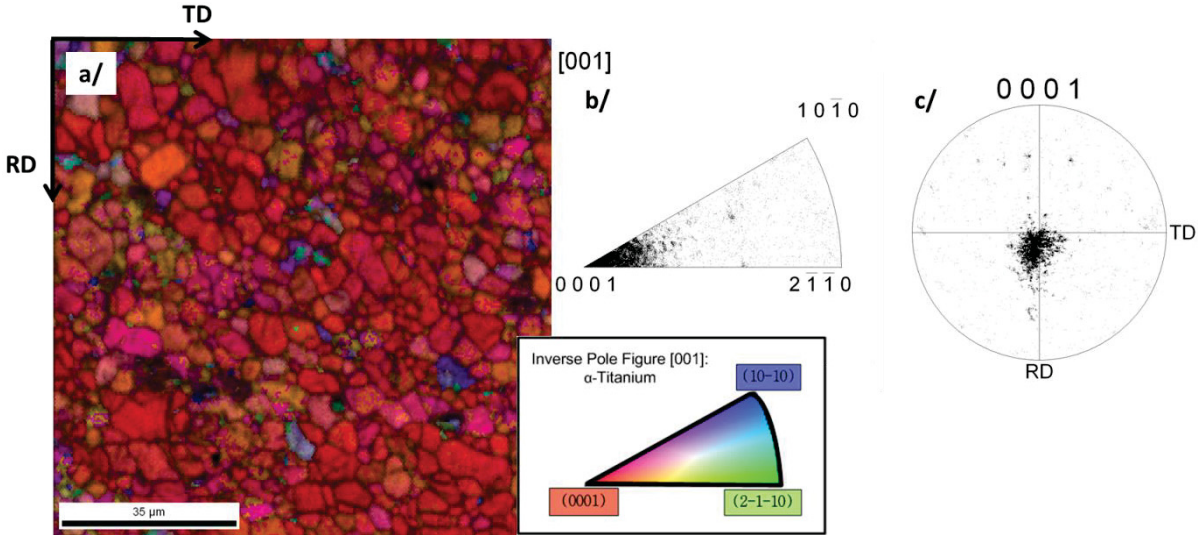

Figure 73: EBSD analysis of Ti no BM ECAPEd for 17 Passes. a) EBSD surface aera b) Inverse pole figure c) pole figure (step size: 0.50 µm, map size: 100 µm / 100 µm)

The Figure 73-a shows the EBSD analysis of the surface of sample, with the colours superposition corresponding to the facing plans (Figure 68). The fact that most of the surface is coloured in red visually indicates that the sample is textured, showing only (0001) plane. The Figure 73-b and c, that represent the inverse pole figure and the pole figure, respectively, confirm that all the grains show (0001) orientation. The observation on Figure 73 corresponds to the surface of the ECAP sample that is parallel to the ECAP direction. The Figure 74 corresponds to a surface perpendicular to the ECAP direction.

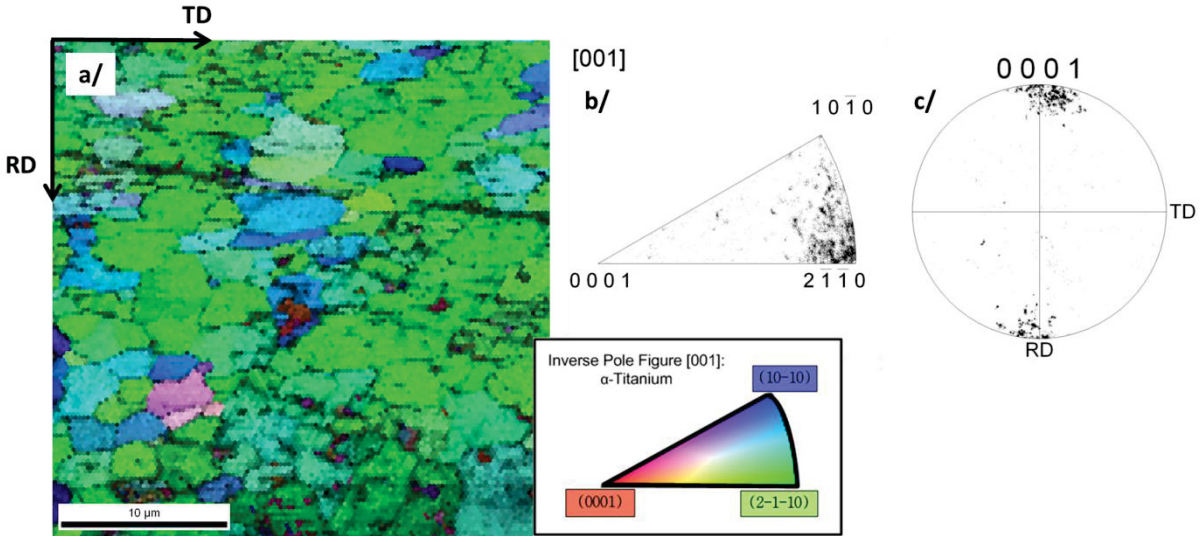

Figure 74: EBSD analysis of Ti no BM ECAPEd for 17 Passes, perpendicularly to the ECAP direction. a) EBSD surface aera b) Inverse pole figure c) pole figure (step size: 0.25 µm, map size: 30 µm / 30 µm)

This figure confirms the orientation observed on the Figure 73. Indeed, if a sample is (0001) oriented, along one ECAP direction, the perpendicular direction will show the other plans (10-10) and (2-1-10), depending on the rotation of the lattice. Figure 75 describes how the ECAP process will orient the Ti

lattice and consequently textured the produced material.

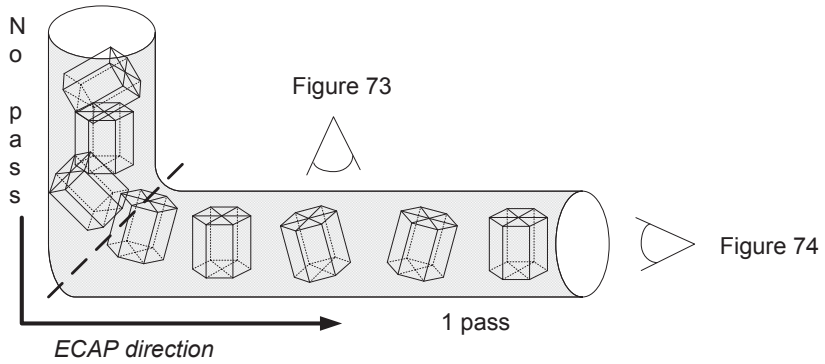

Figure 75: Effect of ECAP process on the orientation of Ti materials

To confirm this observation, XRD analysis of a sample with a surface perpendicular to the ECAP direction has been done. One the spectrum has been added the theoretical intensity expected for a non-textured Ti spectrum (red lines) and the corresponding plane observed in EBSD to the *hkl* ones (Figure 76).

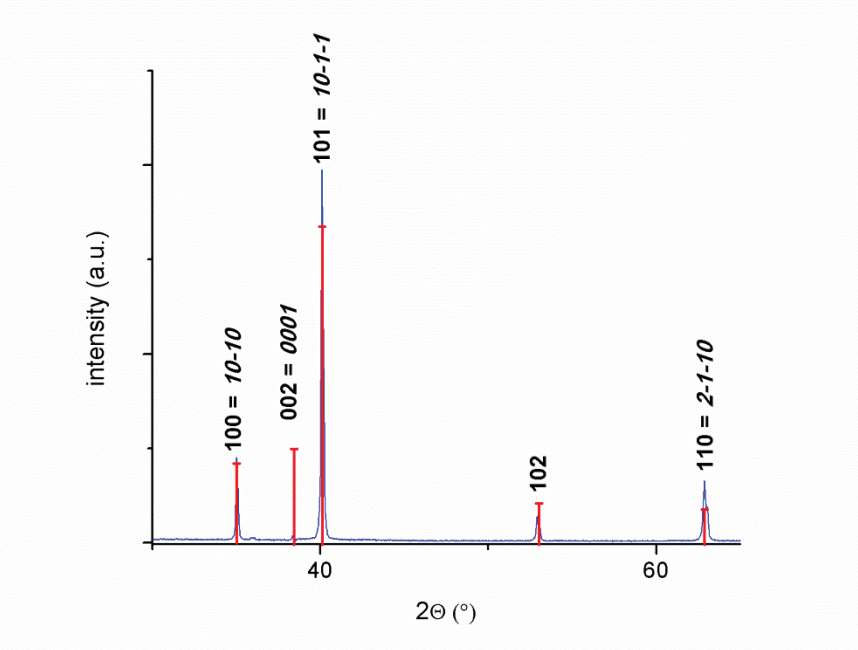

Figure 76: XRD spectrum of Ti without BM, ECAPed for 17 passes (perpendicular to the ECAP direction)

The spectrum on this figure corresponds to the surface observed on Figure 74. The orientation appears clearly, with the intensity corresponding to the (0001) plane really low, and the intensity for the (2-1-10) plane higher than the theoretical one.

The EBSD analysis and the XRD analysis indicate the orientation of the Ti crystal after ECAP processing. This important orientation has been observed by Seda *et al.* [SED2011] [SED2012] in hexagonal material after ECAP. Their work shows that the deformation mechanisms of the hexagonal lattice (slips and twinning) will rearrange the lattice to obtain the (0001) plane parallel to the shear direction. However, this orientation would not exhibit the (0001) plane parallel to the ECAP direction. This phenomenon is explained by the presence of the back pressure used in this work ECAP

densification. The sample, after passing the shear zone, will undergo a compression. Zeng *et al.* [ZEN2009a] [ZEN2009b] have shown in their work that for hot compression of Ti, the deformation activities will favour the orientation of the basal plane parallel to the compression direction. The Back pressure ECAP being a combination of shearing and compression, the orientation of the lattice having its c-axis perpendicular to the ECAP direction observed is explained, as presented on Figure 77. Moreover, the different studies have been done on bulk materials. In this work, the densification is completed on powder materials, which provide less resistance to the first deformation motions.

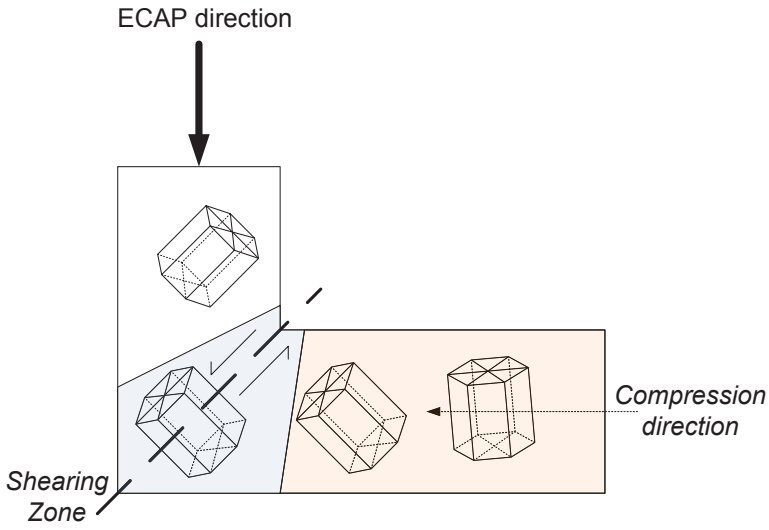

Figure 77: Schematic representation of the Ti orientation during BP-ECAP

The samples produced by ECAP are fully dense, and are textured. However, it has been shown that before going under densification, the powders are mixed using high energy ball milling. This ball milling step has an influence on the material that can be observed after densification.

III-2. Effect of the ball milling on the ECAP samples

In the previous chapter, it has been shown that the ball milling step is expected to disperse the TiC reinforcement within the Ti matrix powder. In order to understand the effect of the BM step on the final ECAP material, a comparison between ball milled and non-ball milled Ti powder (without reinforcement) has been done.

III-2.1 Titanium samples

The ball milling conducted on the Ti powder was the same of the one used to disperse TiC, 30 hours at 250 rotation per minute, with a ball-to-powder ratio of 10 to 1, under protective atmosphere.

Two effect of the ball milling are observable using SEM. Figure 78 shows that BM increases the size of the oxide layers on the Ti particles that become harder to break using ECAP. Indeed, Figure 78-a shows a sample of BM Ti ECAP for 8 passes where particle boundaries can be observed (dark lines).

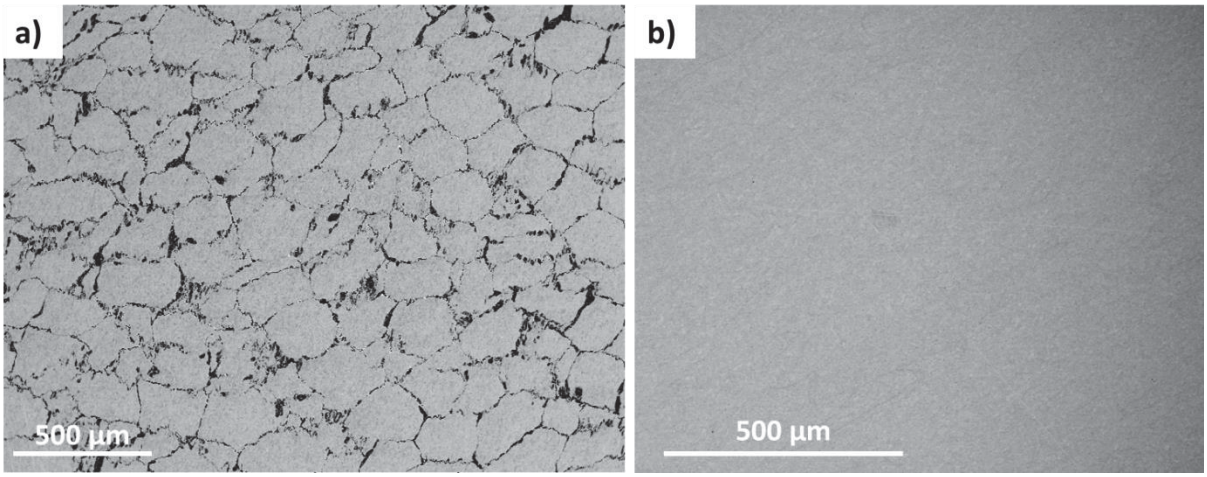

Figure 78: BSE micrographs of Ti sample ECAP for 8 passes a) With 30 hours of ball milling and b) Without ball milling

Figure 78-b shows a sample of Ti without BM ECAPed for 8 passes, where particle boundary contrast is not observed. To confirm the fact that those particle boundaries are oxide layer, microprobe analysis has been done to observe if the relative quantity of oxygen is higher at the boundary as shown on Figure 79.

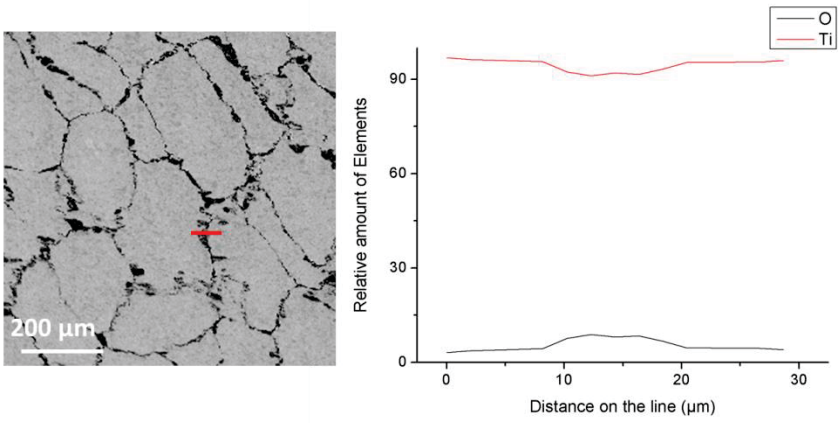

Figure 79: Microprobe on the particle boundary for Ti sample with BM

Because oxygen is a complicated element to dose out, only relative amount compares with the zone inside of a particle can be measured. Nonetheless, the result confirms the presence of oxygen at the particle boundary, confirming the fact that boundaries are the particle oxide layer not totally broken. The explanation for this increase in the size of the oxide layer during ball milling comes from the fact that even if the milling is done under protective atmosphere, residual oxygen is really difficult to eliminate. During ball milling, the Ti particle will be deformed under the impact of the balls against the jar's walls, and the thin oxide layer will be broken. The residual oxygen will form a new oxide layer where the crack has been done in the previous layer, leading to an increase of the size of the oxide layer. Repeating this phenomenon during the whole milling time leads to an increase in the oxide layer thickness.

While enhancing the magnification for the SEM observation, another effect of the ball milling on the Ti particle can be observed (Figure 80).

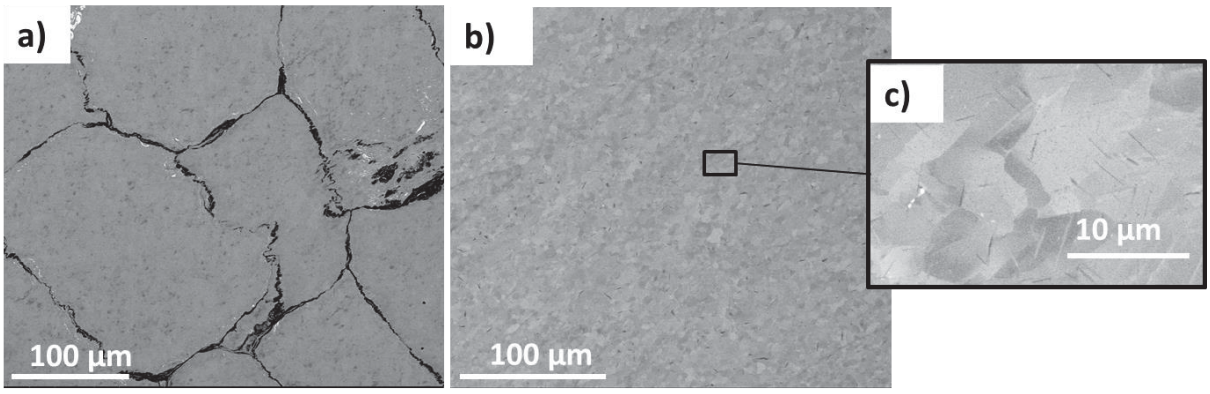

Figure 80: BSE micrographs of Ti sample ECAP for 8 passes at higher magnification a) With 30 hours of ball milling and b) Without ball milling

After polishing, no grain structure can be observed on the ball milled sample (Figure 80-a), whereas for the same conditions, grain structure is observed on the non-ball milled sample with a grain size close to 5 µm (Figure 80-b). However, particle boundaries are observed for the ball milled sample whereas they are not observed on the sample without ball milling. EBSD analysis has been performed on both sample, and different behaviours were seen. Indeed, signal for EBSD analysis was easily observed during analysis of the non-ball milled sample (as on Figure 73) with an average grain size of 5 µm. On the contrary, for the same sample preparation, EBSD's signal was never observed for the ball milled sample. TEM analysis has been performed on both materials, with and without ball milling. Examples of TEM results on the ball milled sample is shown on the Figure 81.

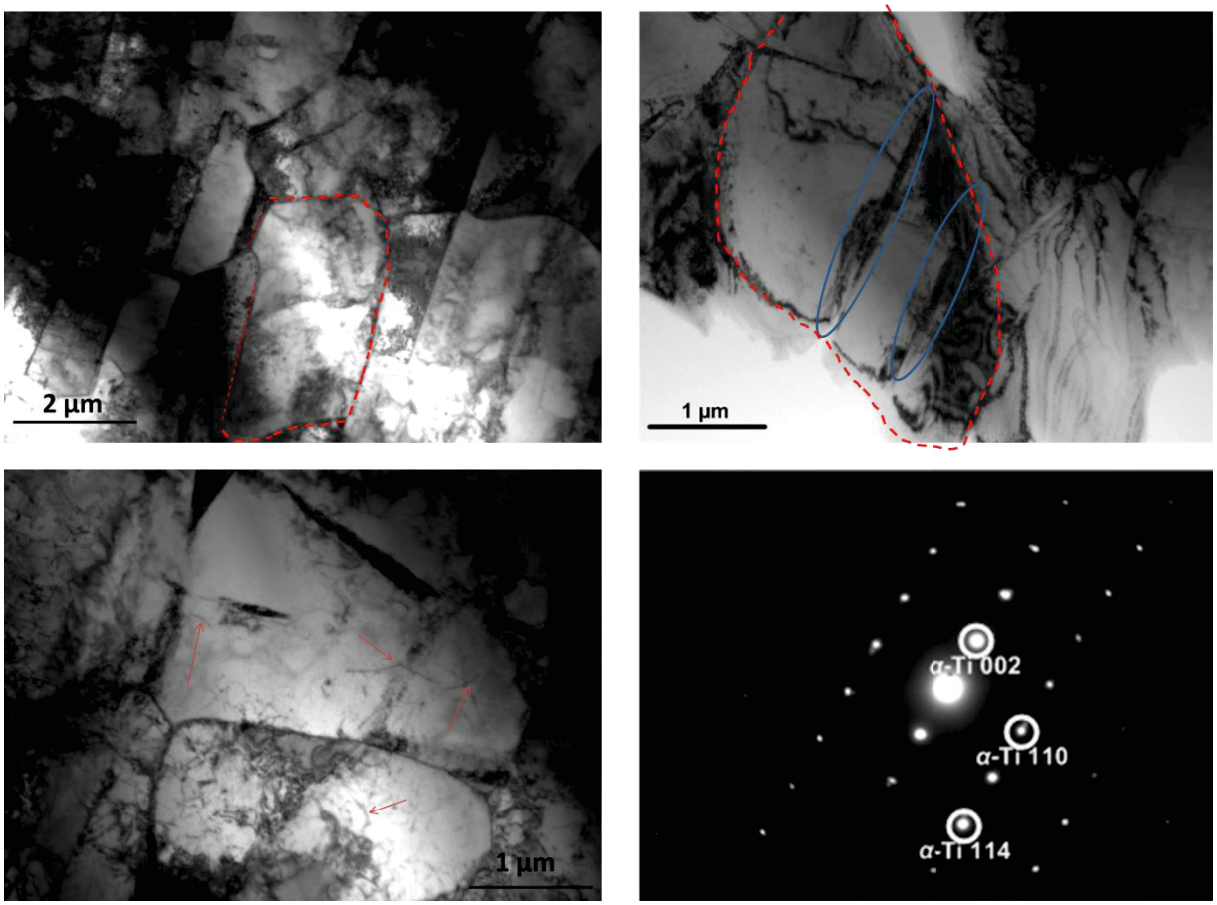

Figure 81: TEM micrographs of a ball milled Ti sample, ECAPed for 8 passes, with the indexed diffraction pattern

The micrographs show several crystallographic defects such as dislocations (red arrows), twins (blue circles) and sub-grain boundaries. Diffraction diagram of an area of several sub grains is also shown (micrograph d). Single crystal diffraction diagram pattern is clearly shown, confirming the presence of sub grain boundaries structure with small disorientation angle θ (<1 - 2°). On the non-ball milled sample, even if several defects such as dislocations and twins have also been observed, sub-grain boundary density is much smaller than for the ball milled materials. The differences observed for the sub-grain boundary structure may explain the difference observed on the EBSD's signal for the ball milled and non-ball milled samples. Indeed, if for a sub-grain boundary morphology, each sub-grain is associated with a Kikuchi lines slightly disorientated from the adjacent sub-grains, then the EBSD system was not able to detect a clear signal for a grain (constituted of multiple sub-grains), and consequently was unable to identify any orientation.

Finally, the difference of microstructure for non-ball milled and ball milled materials (dislocations and sub-grain boundary densities) and possibly local mechanical properties may explain the different BSE micrographs shown on Figure 80, and EBSD mapping obtained after mechanical polishing.

Mechanical testing of the two types of sample (ball milled and non-ball milled) provides information on the behaviour of the sample, and the impact of the BM on it. Increasing the number of defects in the structure can lead to an increase in the yield strength of the materials [HYU2010]. However, the presence of the particle boundaries in the dense material can lead to a lack of ductility, titanium oxide being brittle.

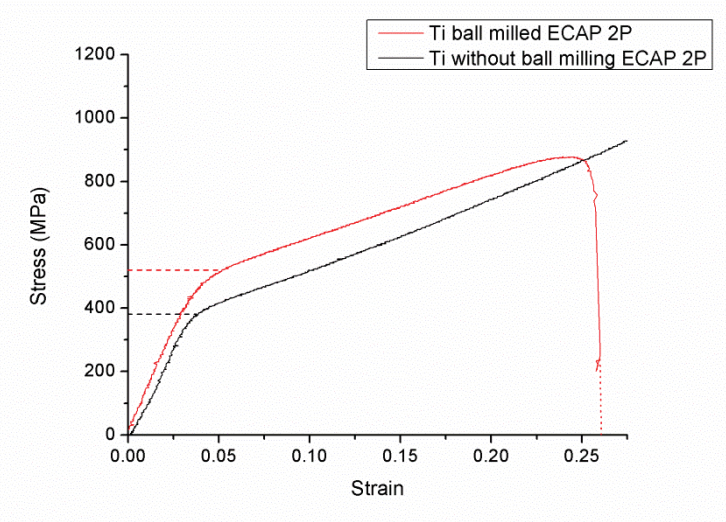

Figure 82: Compression test of Ti ECAPed for 2 passes, without ball milling (black) and with ball milling (red) – (the curves are not corrected from the equipment rigidity making the E value not accurate)

Figure 82 is the Strength-strain curves obtained from compression testing on Ti samples, with and without BM, ECAPed for 2 passes. It appears that the strain is above 20% (0.20) for both samples, which means the ductility is sufficient even after ball milling. However, the specimen with BM fails after 25% of deformation, when the specimen without BM seems to have infinite deformation (it is one of the disadvantages of the compression test, sample with good ductility do not fail). Therefore, even if the ductility is good for both samples, the oxide layer and the defects in the BM sample have negative effect on its mechanical properties: lowering its ductility, increasing its fragility. However, BM materials also show increase in yield strength. A value close to 380 MPa is measured for the non-ball milled sample against 510 MPa for the ball milled one.

Another undesirable effect of the ball milling is the fact the sample can be polluted by the mean of

the balls and the jars. EDS analysis has been done on the ball milled sample to observe if the sample has been polluted by the ball milling (Figure 83).

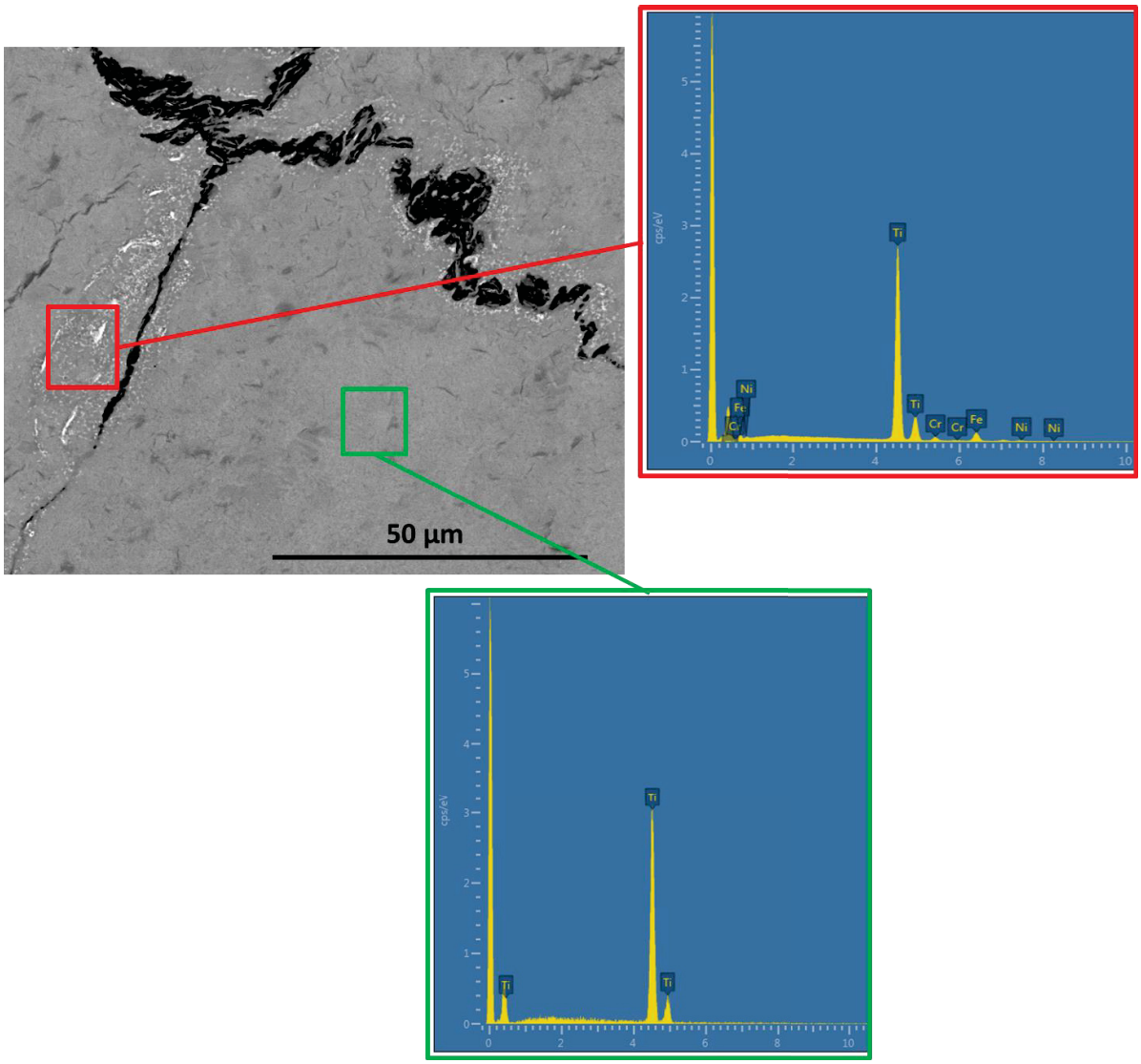

Figure 83: EDX analysis of Ti ball milled, ECAPed for 2 passes with the corresponding BSE micrographs

This figure is displaying EDS analysis of two different areas of the sample, along the particle boundary (red square) and inside the particle (green zone). It appears that inside the particle, only Ti is detected by EDS. However, near the particle boundaries, some white fragments are visible. After analysis, the white fragment has been confirmed to be iron particle from the ball or jar (stainless steel). The balls, while milling the Ti particle, are slightly grinded against each other, introducing small fragments within the particle. It is difficult to measure the impact of this pollution on the mechanical properties of the material, considering their effect will be comparable to the oxide layer.

III-2.2 Titanium matrix and TiC reinforcement

The main goal of the ball milling is to disperse the TiC reinforcement within the Ti matrix particles. Ideally, the TiC must be distributed uniformly within the matrix particles, as presented on the previous chapter. In this part, the composite samples presented are the one processed for 8 passes, in order to be sure of the effect of the ECAP densification on the sample, and to analyse fully dense sample. SEM micrographs of a Ti ball milled, Ti – 1% TiC and Ti – 10% TiC samples ECAPed for 8

passes show that the oxide layer is still present even when TiC reinforcements are used during the BM (Figure 84).

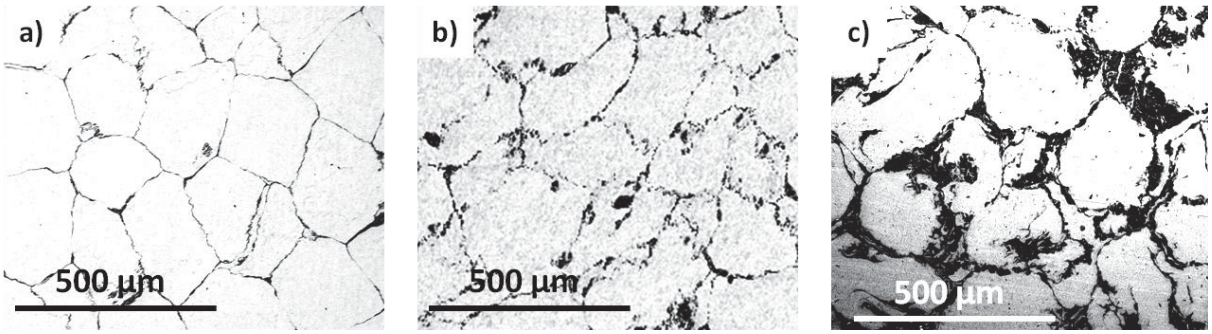

Figure 84: BSE micrographs of a) Ti, b) Ti-1% TiC and c) Ti – 10% TiC samples ECAPed for 8 passes

Increasing the volume fraction of TiC to 1% has presented the same size of the oxide layer as for the pure Ti, as shown on Figure 84 – a and b. However, it has presented some issue when increasing the volume fraction to 3 and 10 %. Indeed, clusters of TiC have been observed on the surface of the particles after densification, increasing the thickness of the particle boundaries as shown on Figure 84-c.

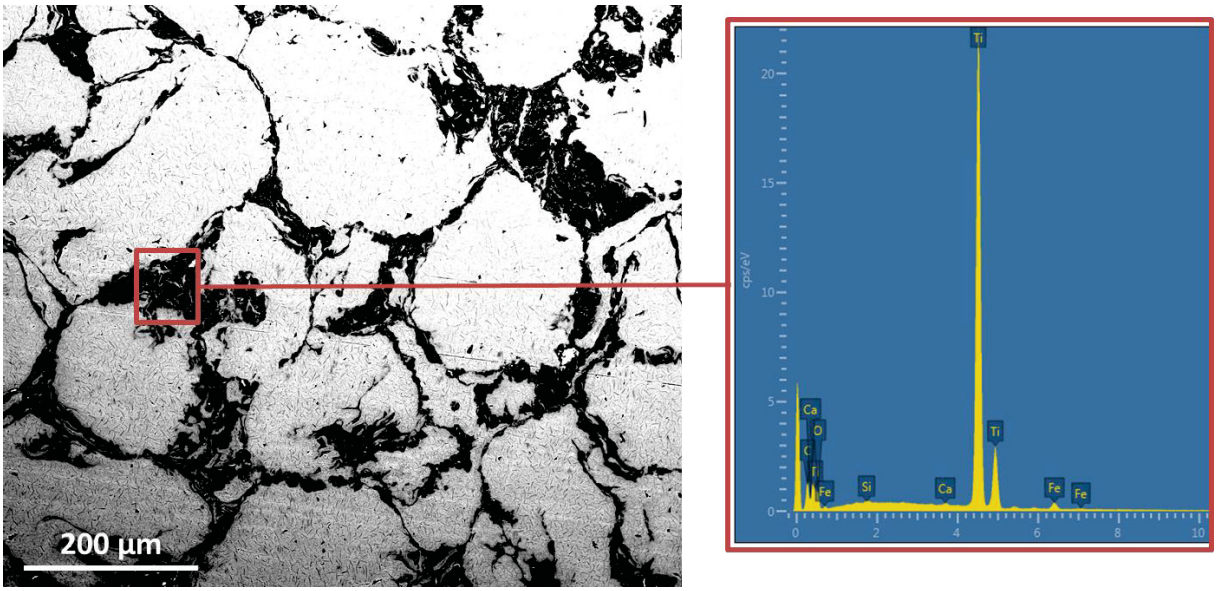

Figure 85: EDX analysis of Ti - 10% TiC ECAPed for 8 passes with corresponding BSE micrograph

Figure 85 shows EDX analysis of a Ti – 10% TiC sample ECAPed for 8 passes. TiC Clusters appear clearly at the particle boundaries, the size of this boundaries being bigger than for sample with only 1% of TiC or without TiC. Moreover, EDX analysis confirms the presence of C at the boundaries, with the presence of Iron and oxygen. It also detects Si and Ca that turn to be artefacts of measurement. The BM process used to disperse the TiC within the matrix particles is not efficient when using larger amout of TiC. This comes from the fact the TiC used is in the nanometre range increasing the volume fraction represents a considerable increase in the quantity of powder use.

When increasing the amount of TiC to a volume fraction of 10%, some will be disperse within the particles as expected by the process, but the majority of the powder will form clusters on the Ti particles surface and neither BM nor ECAP processing would be sufficient to disperse them. Nonetheless, these samples (with 10% of TiC) are helpful to observe the TiC inside Ti particle. It has been seen that grinding and polishing the sample does not offer the possibility to observe the TiC

particle using SEM. However, an opportunity to cut out the sample using Focus Ion Beam (FIB) has allowed seeing the TiC inside the matrix.

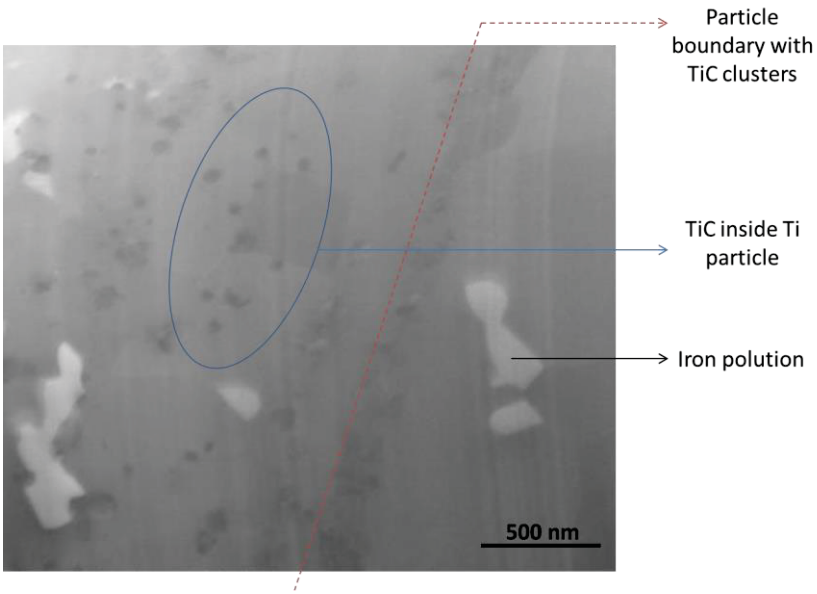

Figure 86: SEM micrograph of a surface cut using FIB, of a Ti - 10% TiC sample ECAPed for 8 passes

Figure 86 is a SEM micrograph of a Ti – 10% TiC sample ECAPed for 8 passes. The analysis has been done near a particle boundary, where the thickness of the boundary seemed the less important. Along the apparent clusters formed at the boundary, individual TiC particles are visible within the matrix, confirming the possibility of the BM process to disperse reinforcement inside Ti particles. However, the contamination of the sample by the same BM process is also visible at the particle boundary. In order to observe the interface between the reinforcement and the matrix, TEM analysis has been done. Ti – 10% TiC sample was used, in order to have the possibility to see TiC particles. Only 1% of TiC could have not been sufficient to see TiC particle, considering the fact that TiC particle are not bigger than 100 nm.

The TEM micrographs on Figure 87 show the composite sample Ti – 10% TiC. Several TiC particles can be observed at relative low magnification (black arrows on micrograph a). A Ti cluster is also observed (micrograph c) but no interfacial reaction zone can be observed by TEM showing a clean Ti/TiC interface between the matrix and the cluster. On the micrograph b, a single TiC particle is isolated. No interphase between the TiC particle and the Ti matrix is visible, meaning there is no reaction at the interface, and no pollution either. The fact that the interface does not present any contamination the fact that the TiC particles can have a benefit effect on the mechanical properties of the composite, if the distribution is uniform and no clusters are observed.

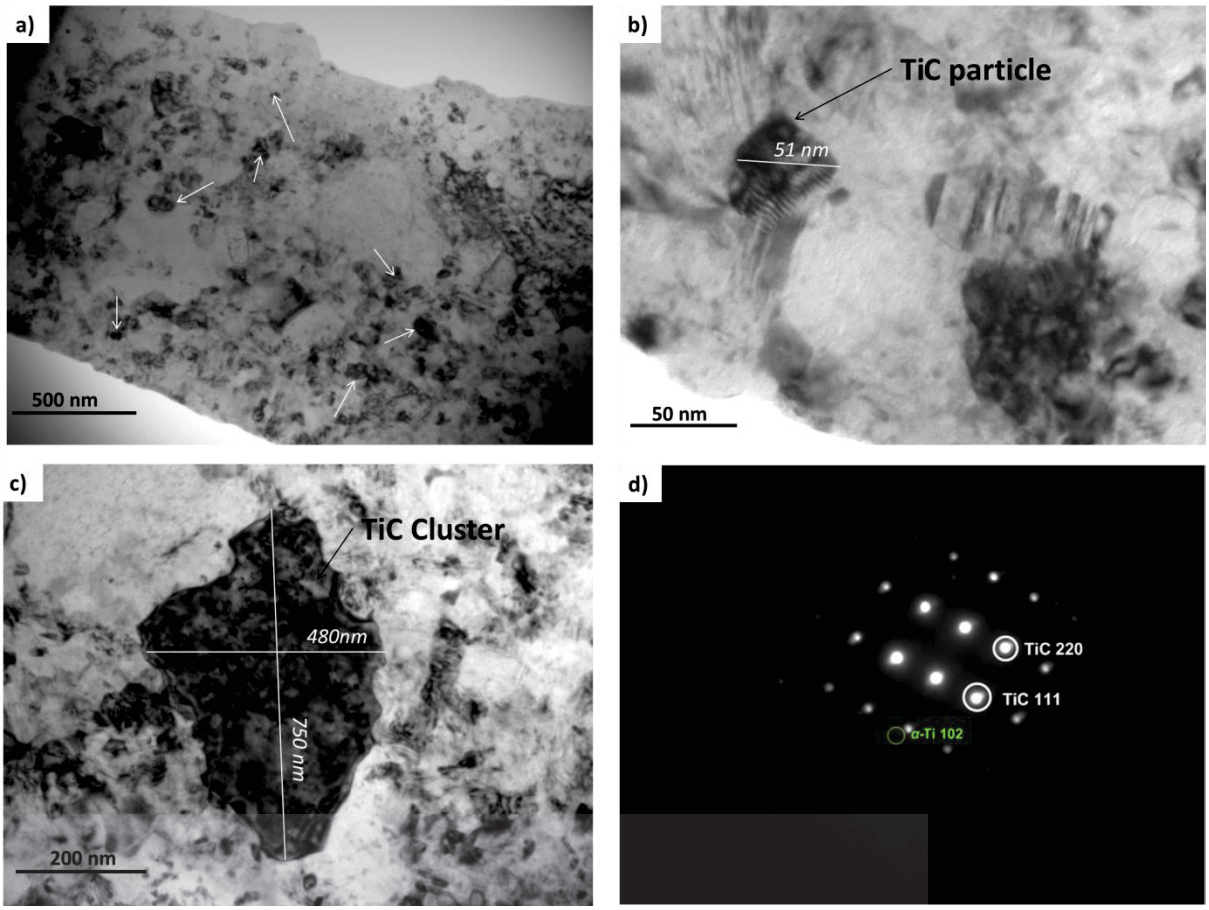

Figure 87: TEM micrographs of Ti - 10% TiC sample, ECAPed for 8 passes, with (d) the indexed diffraction pattern of the cluster on (c)

Compression test on a Ti – 1% TiC sample has been done to determine the efficiency of the BM on the distribution of the TiC particle (Figure 88). The first observation is the complete lack of ductility in the composite sample.

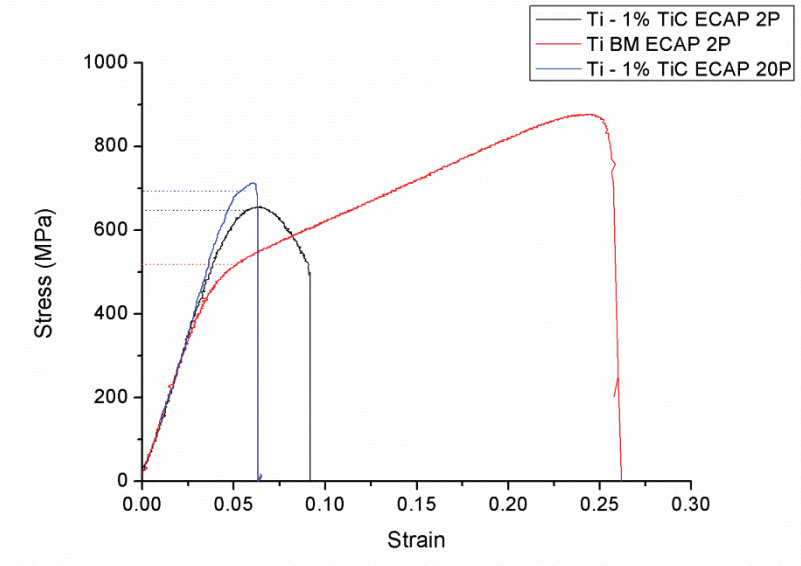

Figure 88: Compression test of Ti -1% TiC ECAPed for 2 passes (black) compared to Ti BM (red) – (the curves are not corrected from the equipment rigidity making the E value not accurate)

Compared with the pure Ti ball milled, the lack of ductility is obvious (8% for composite and 27% for pure Ti). However, the yield strength is higher for the composite (650 MPa to 510 MPa). Despite the lack of ductility, effect of the reinforcements is observed on the Yield strength of the material, increasing it for composite.

One of the reasons that could be responsible for this lack of ductility is the presence of clusters of TiC in the composite (as on the Figure 87-b), that will act as crack source during the mechanical testing. To avoid that, the solution of increasing the BM time, or the BM speed has be considered, but as explained in the previous chapter, unsuccessful, due to the fact the Ti particles weld against the wall of the jars at these conditions. Another solution consists in increasing the number of pass to increasing the shearing of the material that can help to disperse the reinforcement.

III-3. Effect of the number of pass

Increasing the number of pass from 2 to 20 for the sample Ti – 1% TiC should help to disperse the TiC particles and to break and disperse the boundary particles. By increasing the shearing of the material, the fragile boundaries, and the TiC clusters would go under a lot of deformation that could break the clusters and the boundaries, distributing them into the composite. SEM observations confirm the severe deformation of the particle for a high number of pass.

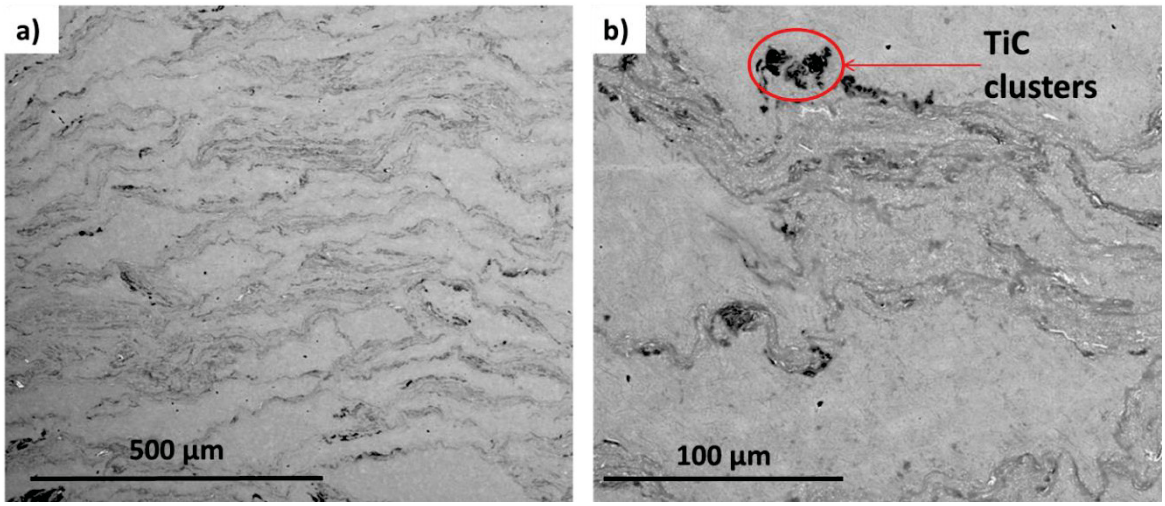

Figure 89: SEM micrographs of Ti - 1%TiC ECAPed for 20 passes

Figure 89 shows the deformation of the Ti particles, where the boundaries are less defined. However, the boundaries are still observed, along with the iron contamination. And instead of breaking the clusters and disperse them, increasing the number of ECAP passes seemed to have the opposite effect. Indeed, TiC clusters are visible by SEM (Figure 89-b), meaning that instead of breaking the clusters, a segregation phenomenon has occurred for the clusters, while the oxide boundaries were deformed and dispersed. Compression test performed on the Ti – 1% TiC ECAPed for 20 passes confirms the presence of clusters, when the fracturing of the composite occurs at lower strain than for the ECAP for 2 passes (about 5% to 8% deformation for Ti – 1%TiC ECAPed 2P) (Figure 88)

Increasing the number of pass will help to break and disperse the particle boundaries of the matrix powder, as observed by Xia *et al.* [XIA2010]. Nevertheless, the expected effect to break the cluster does not occur, with the opposite happening, seemingly segregation of the clusters. The dispersion of the reinforcement within the matrix has to be optimized before considering increasing the number of pass.

III-4. Conclusion

Despite the observation made on the effect of ECAP on composite powder materials, different composites have been fabricated using this technique and their mechanical properties measured.

Sample	ECAP conditions	Measured Hardness (Hv)	Calculated Yield Strength (from hardness) (MPa)	Measured Yield Strength (Compression) (MPa)
Ti (without BM)	2 Passes 17 Passes	159 162	351 359	380 -
Ti (BM)	2 Passes 8 Passes	205 209	470 480	510 -
Ti - 1%TiC	2 Passes 8 Passes 20 Passes	265 282 280	625 670 665	650 - 670
Ti - 10%TiC	8 Passes	244	570	-

Table 10: Measured hardness, calculated yield strength and measured yield strength for the Ti - TiC composites obtained by ECAP

The process used, to fabricate Ti – TiC composites via ECAP, has limitations that have been observed. The BM step is the critical point of the process. It is necessary in order to distribute reinforcement within the matrix particles, but has negative effect due to the contamination that can occur. The iron contamination (stainless steel, as the matter of the balls and jars used) is only detected in the ball milled sample. This pollution can be a major issue as it could act as crack source during deformation, or has a barrier for the grain coarsening during heat treatment, leading to a material with two grain size populations. Another limitation of the ball milling process observed is the impossibility to disperse TiC when the amount of it is too important. When dealing with a volume fraction of reinforcement higher than 1%, cluster of TiC has been directly observed on the Ti boundary particles, after ECAP densification. On the other hand, some benefits of the use of BM are also observed. The fact that Individual TiC particles has been spotted inside Ti particles confirm the possibility of the BM to disperse the nanosized reinforcement within the matrix particles. If individual TiC can be distributed inside a Ti particle, ECAP process will be able to get uniform distribution of them.

The ECAP process allows the fabrication of materials at low temperature (600°C) and in a short delay (few minutes). The consequences of that will be economic (easy and fast production), a limitation of the grain coarsening (therefore, increase in mechanical properties), and a reduction of the reactions at the interface between reinforcements and matrix in a case of composite materials. In addition to that, ECAP process, which is known to textured bulk material, also has effect on the orientation of powder material. Grain orientation is observed for powder material after ECAP densification. The hexagonal Ti lattice tends to have its c axis aligned with the shear direction, perpendicularly to the ECAP direction. This texturing of powder material can be useful when seeking anisotropic properties on the dense material. It has also been observed that increasing the number of pass during ECAP help to deform the particle oxide layers and distribute them inside the dense material. However, this process will increase the crystallographic defects of the materials, and so far, only relative small samples have been achieved.

In Table 10 are listed the hardness measured for the different ECAP sample, the value of the Yield strength obtained from the hardness measurement, converted using the equation presented earlier, and when it's applicable, the value of the Yield strength obtained by compression test. It appears

that the estimation for the Yield Strength value obtained from the hardness measurements is not far from the one measured using the compression test, the conversion tending to slightly underestimate the Yield Strength. However, the hardness measurements do not relate the lack of ductility that can be observed on the sample during compression.

On the composite mechanical properties, different effects have been noted. When ball milled Ti powder is used, resulting ECAPed sample shows an increase in its yield strength, and a limit in its ductility, compared to the non-ball milled sample, which has an excellent ductility and lower yield strength. Ball milling increase the defects in the material that has to effect to increase the yield strength. Adding TiC, despite the lack of ductility, will have a composite effect with an increase in yield strength, in comparison to the pure Ti ball milled.

ECAP processing of Ti based powder composites, combined with ball milling dispersion of the composite, shows a great potential in the rapid and efficient way of producing such composites. With the possibility to work at moderate temperature, disperse reinforcements, texture the material, ECAP process shows promising results, even if the different steps have to be optimised in order to fully achieve good dispersion and good ductility in the composite fabricated.

IV. TiH_2

Another process used in this work, in order to fabricate dense Ti based composite materials, is the Hydrogenation/Dehydrogenation sintering of Titanium. As explained in chapter I, the principle of the techniques is to use the dehydrogenation of the Ti as a leverage of the sintering. After hydrogenation of the titanium powder, and size reduction using ball milling, the reinforcement is mixed with the matrix powder (now TiH_2) using ball milling (ball mixing). Two different processes are used to dehydrogenate the composites, free sintering and hot pressing. The first one consists in a pre-compaction of the mixed powders and a pressureless sintering, and the second consists in combining the dehydrogenation and the pressing of the powders in a single step.

IV-1. Free Sintering

As presented on the previous chapter, the matrix powder (TiH_2) and the reinforcement powders (TiB_2 or TiC) are cold compacted after ball mixing. Three different materials are prepared, TiH_2, TiH_2 – TiC and TiH_2 – TiB_2. The volume fraction studied in this work for the reinforcement is of 10%. After densification, the relative density measured was more than 97% for the three materials. Consequently, microstructure of the three materials has been investigated. However, after grinding and polishing, porosity has appeared on the materials. Thereby, due to the presence of porosity, mechanical characterisation would not be relevant on such material. Nonetheless, investigation on the effect of the process used, on the microstructure of the composite, remains interesting to understand.

The first thing that has been verified is the efficiency of the process to achieve the dehydrogenation of the TiH_2 powder. To do so, the sintering done under secondary vacuum (10°C/min and 10^{-6} mbar), has been stop at different stage to determine the dehydrogenation temperature of the cold compacted powder.

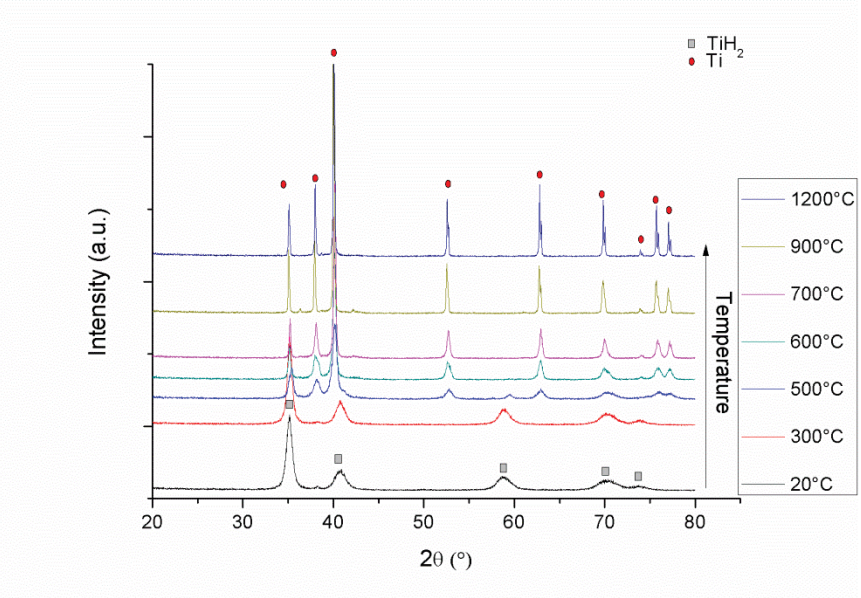

Figure 90: XRD spectra of TiH_2 dehydrogenation process under secondary vacuum, at different temperatures

Figure 90 is displaying the XRD spectra of the TiH_2 cold compacted powder, sintered pressureless under secondary vacuum at room temperature, 300°C, 500°C, 600°C, 700°C, 900°C, and 1200°C. At room temperature, only TiH_2 is detected, whereas at 1200°C, all the TiH_2 has been transformed into Ti. The first peaks of Ti appear between 300°C and 500°C, and both TiH_2 and Ti are visible at 500°C. At 600°C, only Ti is visible. The dehydrogenation is therefore completed at 600°C, as expected after the measurement made using DSC (cf chapter II). If this process is working to fully dehydrogenate the TiH_2, it is important to verify if this dehydrogenation will occur while working with composite mixed powders. Indeed, two different types of composite are studied in this work, ex-situ Ti-TiC, and in situ Ti-TiB. Concerning the Ti-TiC composite, it is important that the TiC particles do not prevent the dehydrogenation to occur. Concerning the Ti-TiB composite, in addition to the fact that the TiB_2 particles should not prevent the TiH_2 to dehydrogenate, TiB_2 particles are expected to be transformed into TiB whiskers during the sintering. XRD analysis has been performed to analyse the sintering behaviour of these composite materials.

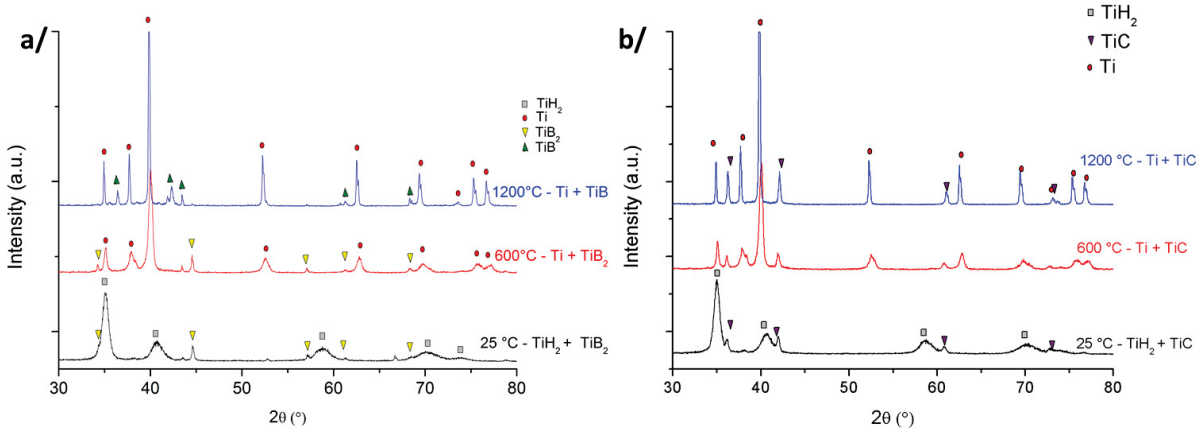

Figure 91: XRD spectra of the pressureless sintering behaviour of a) TiH_2 - 10% TiB_2 and b) TiH_2 - 10% TiC

Figure 91 are the XRD spectra of the dehydrogenation behaviour of the TiH_2 – TiB_2 and TiH_2 – TiC composite powders, at a volume fraction of 10%. For both of the composites, the dehydrogenation is

completed at 600°C. Reinforcement particles, regardless of their size (about 40 nm for TiC and 550 nm for TiB_2) are not an obstacle to the dehydrogenation of the TiH_2, during pressureless sintering. The TiC particles are not affected by the sintering process, and they are still observed at 1200°C. On the contrary, TiB_2 particles will be fully transformed into TiB whiskers at 1200°C, as expected. No TiB_2 is detected at this temperature. The pressureless dehydrogenation process allows the fabrication of both ex-situ and in-situ titanium based composites.

Another important aspect of the process is the distribution, after densification, of the reinforcement within the matrix. If TiC particles are hard to observe due to their size, it is not the case for the TiB whiskers that have grown inside the composite. Using the possibility of the EBSD to display the different phases recorded in different colours, the effect of the process used on the distribution of the reinforcement is studied. In addition to that, the effect of the pressureless sintering on the texture of the fabricated composite can also be observed using EBSD. Figure 92 is the EBSD analysis of the Ti reinforced with 10% TiB in volume fraction. On the Figure 92-a, the porosity is clearly observable, the pores being the dark hole in the micrograph.

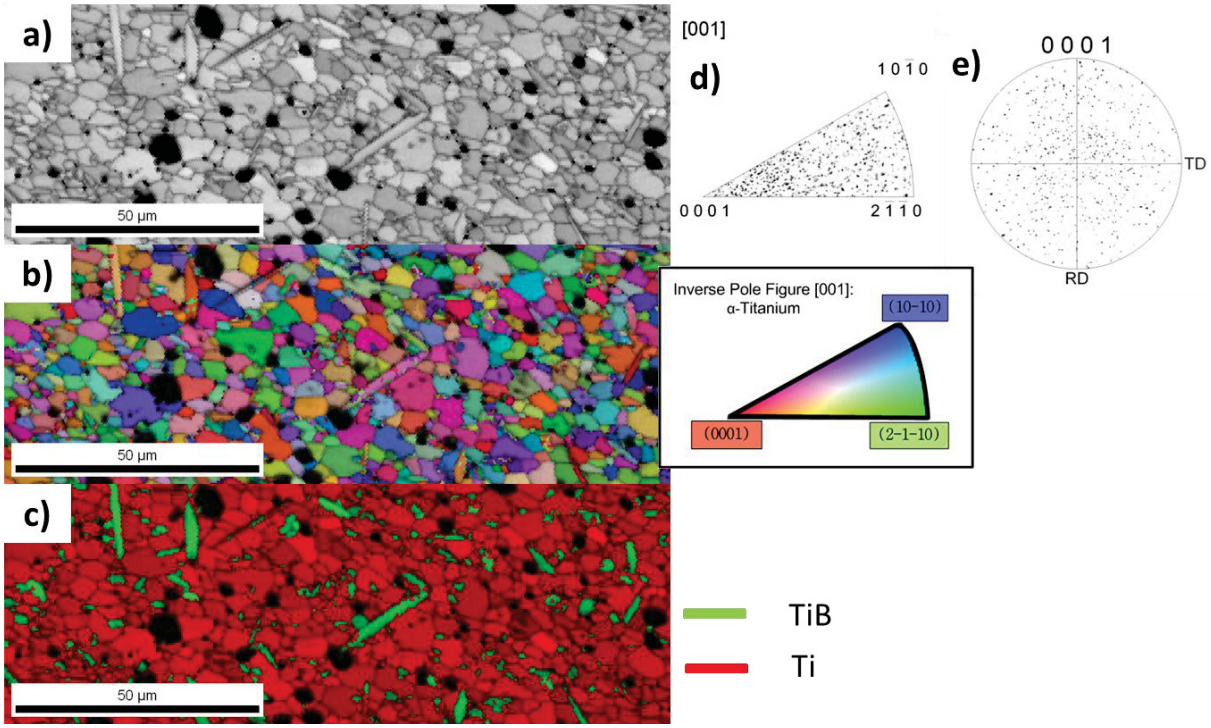

Figure 92: EBSD analysis of Ti - 10% TiB sample (pressureless sintering) with a) SEM micrograph, b) grain orientation, c) phases, d) inverse pole figure for Ti and e) pole figure for Ti (step size 0.50 µm, map size: 140 µm / 50 µm)

Figure 92-a, after analyses by the EBSD software, shows a grain size for the Ti matrix of 2 populations of 1.2 µm and 7 µm. The Figure 92-b shows that the process seems to have no influence on the grain orientation of the final material. This observation is confirmed by the Inverse pole figure and the pole figure (Figure 92-d and e) that does not show any orientation of the material. Despite the cold compaction step, that could have an influence on the orientation of the grain, a texture free material is obtained using pressureless sintering. On Figure 92-c, a uniform distribution of the TiB whiskers (in green) and their random orientation is revealed. SEM micrograph of a fracture confirms the random uniform distribution of the TiB whiskers (Figure 93, black arrows).

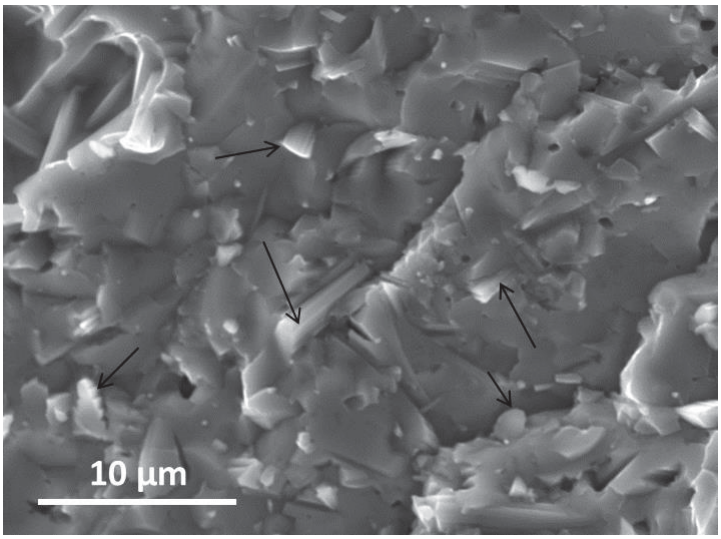

Figure 93: SEM micrograph of a fracture of Ti- 10% TiB sample

The average size measured for the TiB whiskers, using SEM and EBSD detection is a diameter of 1 µm and a length of 15 µm. When starting with TiB_2 particles of a mean diameter of 250 nm to 550 nm, smaller diameter for the whiskers was expected. However, TiB_2 powder tends to form cluster easily. The ball mixing process used is not efficient to break the TiB_2 cluster when mixing 10% of reinforcement. Nevertheless, the TiB whiskers are uniformly distributed, and randomly oriented. The interface between the whiskers and the matrix is observed using TEM analysis.

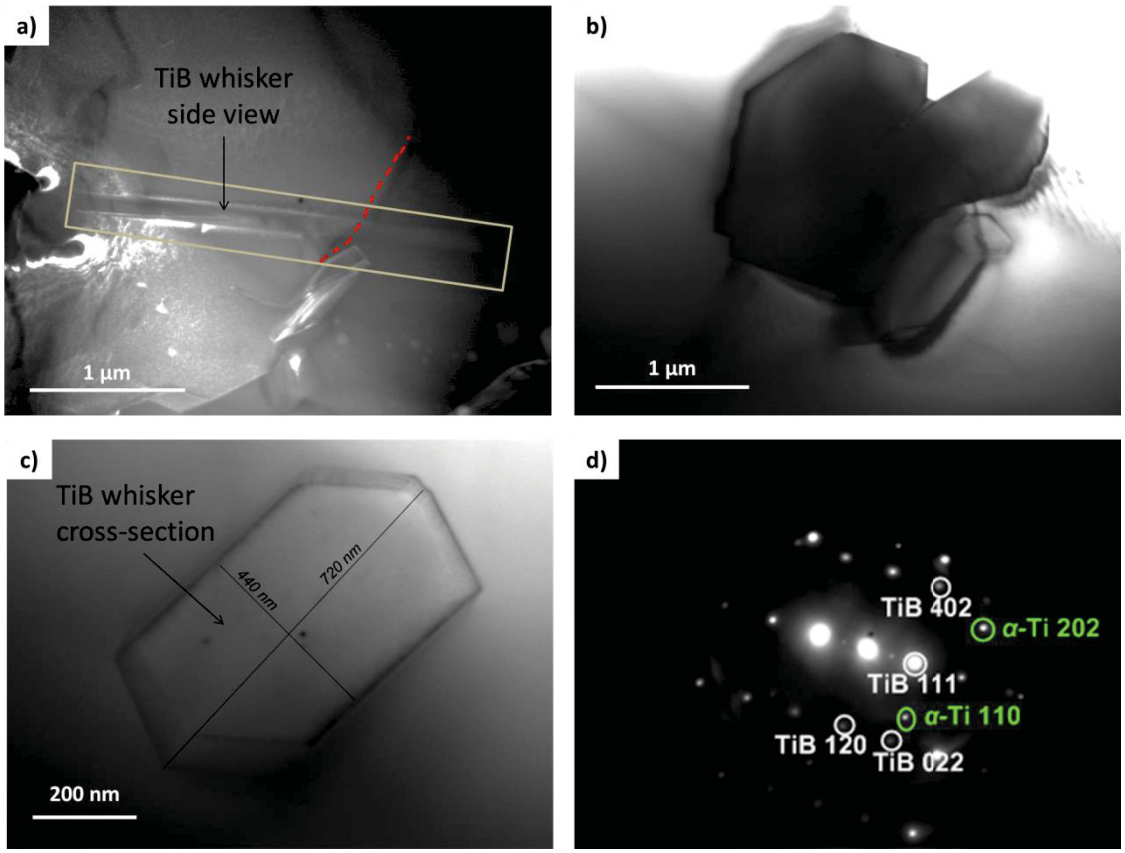

Figure 94: TEM micrographs of the TiB whiskers inside Ti matrix, for a pressureless sintered material, and indexed diffraction pattern (d)

Figure 94 shows the TEM micrographs of the Ti – 10% TiB sample. On the Figure 94-b and c, no interphase (clean interface) can be seen between the whiskers and the matrix. The shape of the whisker on Figure 94-b reveals the presence of clusters during the densification. Indeed, during in situ transformation of TiB_2 to TiB, the shape of the whisker expected is the one observed on the Figure 94-c [MIR2003]. The Figure 94-a and c show that the whisker can grow inside a grain, and can also be trans-granular (micrograph a, the whisker goes through 2 grains, the grain boundary is indicated by the red dot line). Figure 94-d show typical diffraction diagram pattern (here from Figure 94-d) with both Ti and TiB diffraction spots. During the ball mixing, the reinforcement particles and the matrix particle will be uniformly dispersed, and during the sintering, the particle boundaries does not act as a barrier to the whisker growth, of to the grain coarsening. Moreover, for the different composite obtained using pressureless sintering, no pollution from the ball milling has been observed.

To summarise, the analysis of the composite obtained by HDH pressureless sintering shows that the dehydrogenation occurs at the temperature expected for the used size of TiH_2 powder (dehydrogenation to be complete at 600°C for an average particle size of 500 nm) despite the cold compaction. Moreover, the dehydrogenation process is not blocked or delayed by the presence of reinforcements. The observation of the distribution of the reinforcements confirms the efficiency of the ball mixing to obtain a homogenous mix of the matrix and reinforcement particles. And despite the dehydrogenation, there is no contamination of undesired interface between the matrix and the in-situ reinforcement. However, porosity is observed on the composite obtained using pressureless sintering, revealing that the cold compaction used is not important enough for the TiH_2 particles size used. Consequently, the mechanical properties of the sintered sample cannot be measured.

To prevent the porosity in the fabricated material, hot pressing is used. This process allows the dehydrogenation to occur at the same time as the compaction.

IV-2. Hot pressing

The HDH hot pressing used in this work does not require cold compaction prior the densification. It also have the advantage to process the powder faster at a lower temperature, due to the combined effect of pressure (80 MPa) and heating (800°C for 30 minutes). The apparatus used as a working vacuum of 10^{-1} mbar, which is considerably lower than the one used during free sintering.

Because of the lower working temperature, the Ti – TiB composites are not investigated using this method (temperature under the TiB_2 – TiB transformation temperature). Ti and Ti – TiC materials have been fabricated using the HDH hot pressing. The relative densities measured for the fabricated composites are above 97%, after grinding and polishing. Unlike free sintering, which relies on a pre-compaction shaping of the powders that reveals to be a critical step in the densification process, hot pressing allows applying a constant pressure during the dehydrogenation, avoiding the formation of pores inside the structure. XRD analysis of the dense material shows the completion of the dehydrogenation process during hot pressing.

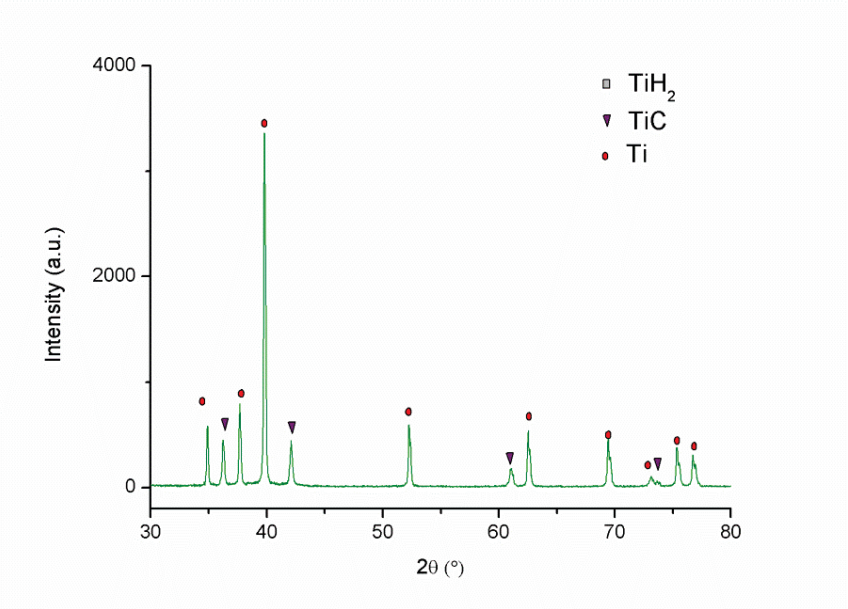

Figure 95: XRD spectrum of Ti - 10% TiC hot pressed at 800°C for 30 minutes

Figure 95 shows a XRD spectrum of a Ti – 10% TiC composite HDH hot pressed at 800°C for 30 minutes, where no evidence of TiH_2 is visible. As for the pressureless sintering, TiC reinforcement does not act as a barrier to the dehydrogenation that is fully achieved after hot pressing.

An effect of the short densification time at moderate temperature is the observation of residual nanoporosity. Indeed, TEM analysis has revealed the presence of nanopores in the materials, after densification. However, nanopores have not a major impact on the mechanical properties of the material, even though at a certain level it can affect the durability of metals [BET2011].

Figure 96 shows typical TEM micrographs of a Ti sample, after HDH hot pressing densification. The indexed diffraction pattern shows that only Ti is observed in the material. However, the micrographs a, b and c shows the presence of nanoporosity, no bigger than 200 nm (black arrow). This porosity is attributed to the dehydrogenation process occurring in constrained volume. H_2 cannot be freely released off the volume, and is trapped, forming the nanopores. Nonetheless, the micrographs show that Ti grains after dehydrogenation are all in the same size range, with a mean diameter of 1 µm. The grains are much smaller compares with the one from pressureless sintering (1.5 to 7 µm) due to the short time processing of the hot pressing compares with the pressurless sintering (30 min and 4 hours, respectively) and its lower working temperature (800°C and 1400°C, respectively). After dehydrogenation is completed during hot pressing, the temperature and the time at which the sample is treated does not permit grain coarsening as it is for pressureless sintering. This results in grains being 7 times smaller. If the mean diameter of the grains is 1 µm, grains of 500 nm have been observed, which is closed to the size of the TiH_2 starting powder. The material prepared by HDH hot pressing will have a grain size slightly higher than the TiH_2 particle size used (about 2 times bigger).

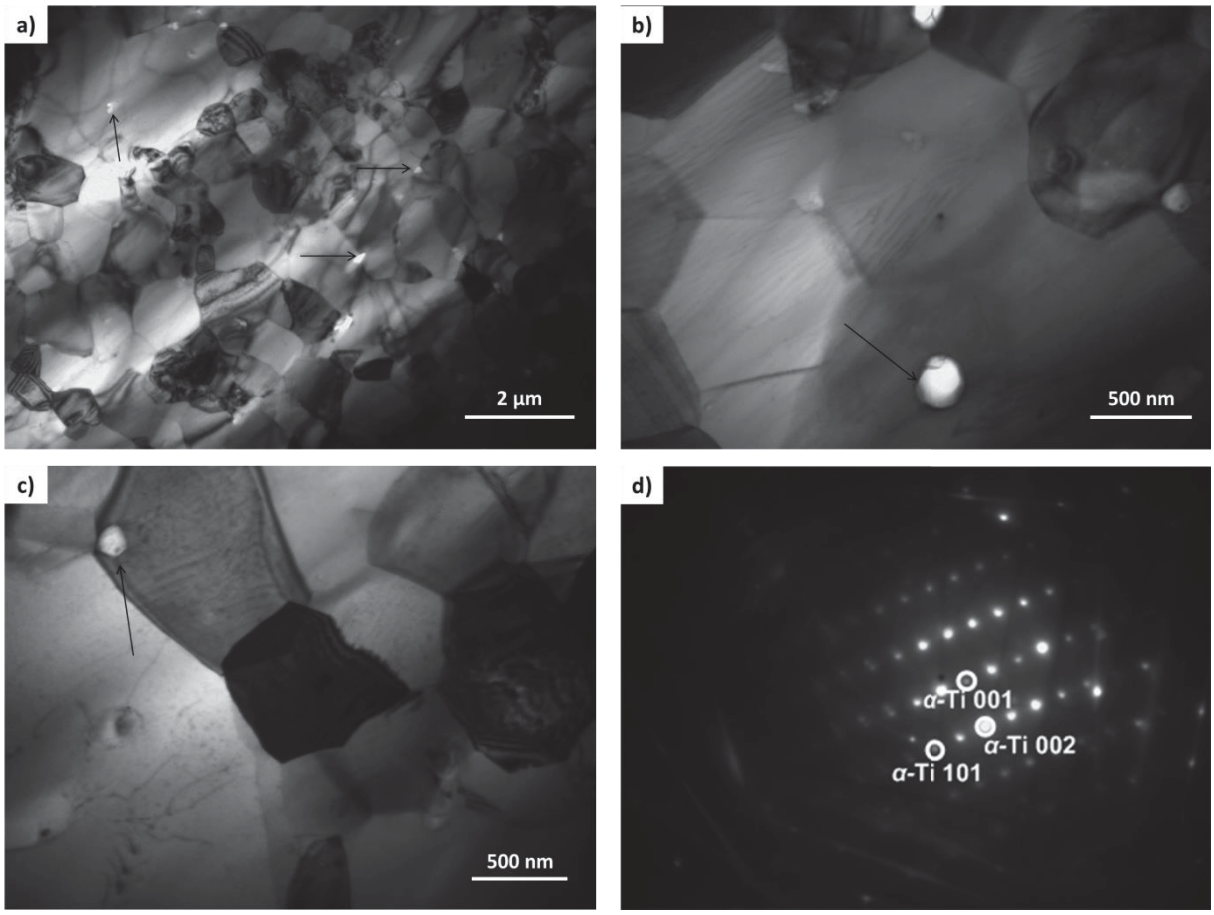

Figure 96: TEM micrographs of Ti sample HDH hot pressed, with indexed diffraction pattern (d)

Hot pressing process consists in applying a constant pressure during the dehydrogenation on the powder material. This pressure can have an influence on the orientation of the grains, aligning the hexagonal lattice perpendicularly to the pressing direction [DHA2012]. EBSD analysis has shown that in this process, no orientation is observed (Figure 98).

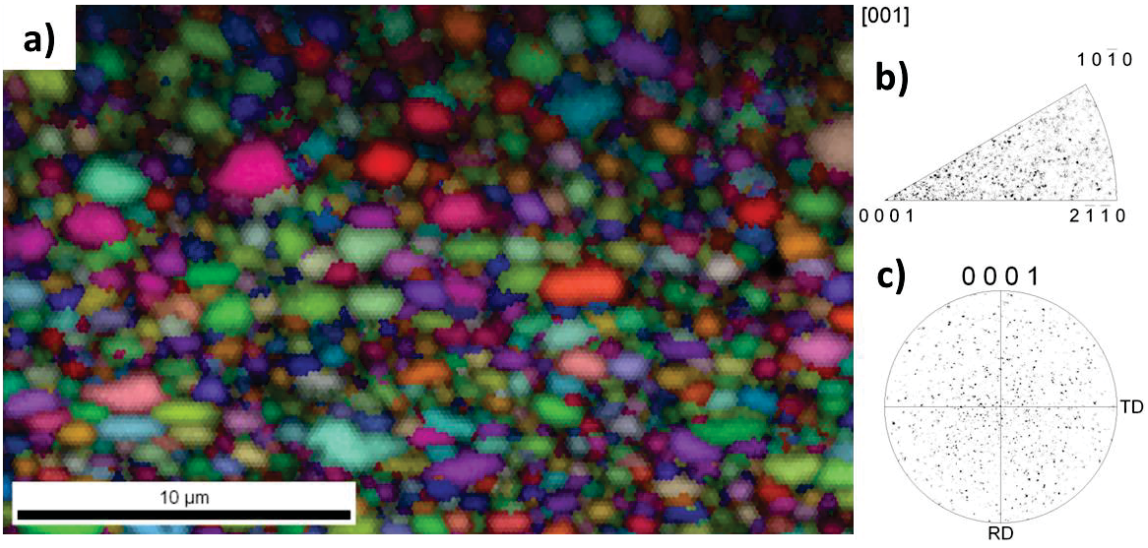

Figure 97: EBSD analysis of the Ti hot pressed sample a) EBSD surface area, b) inverse pole figure, c) pole figure (step size: 0.35 µm, map size: 35 µm / 25 µm)

The coloured surface area of the EBSD analysis (Figure 97-a) shows that no grain orientation is

favoured after densification by HDH hot pressing. This observation is confirmed by the inverse pole figure and the pole figure (Figure 97-b and c). Despite the pressure apply on the grain during the dehydrogenation, the Ti grain are not oriented by the dehydrogenation.

Ti – TiC composites obtained using HDH hot pressing has been observed using TEM analysis in order to analyse the behaviour of the reinforcement particles within the matrix.

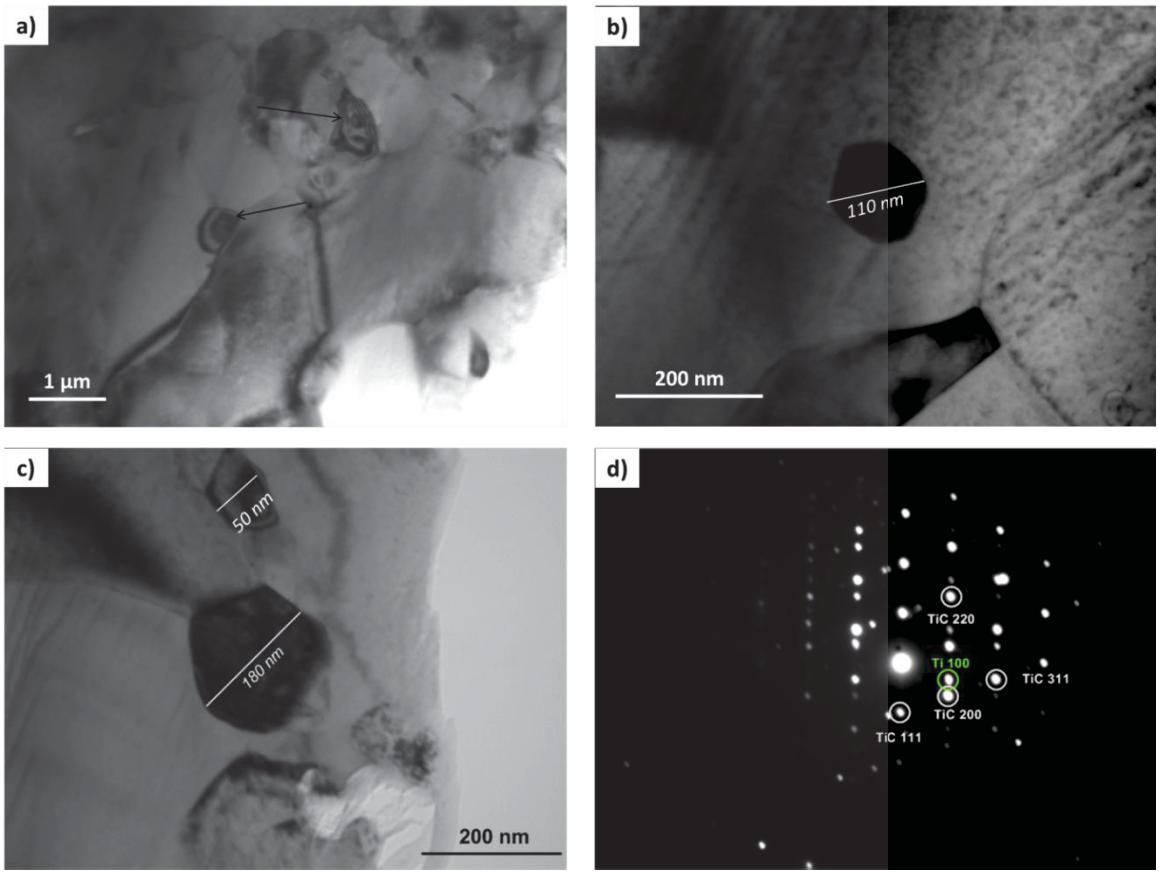

Figure 98: TEM micrographs of the Ti - 10% TiC HDH hot pressed sample, with indexed diffraction pattern (d)

As for the in-situ reinforcement composites obtained by pressureless sintering, no interphase zone between the TiC reinforcement and the matrix (clean interface) can be observed. The micrographs b and c on the Figure 98 of large TiC particles shows that they do not form clusters. Moreover, the micrograph b shows that the TiC particle can be located inside a Ti grain, even if the tendency observed for the whole sample was to have the particles at the grain boundaries (as on the micrographs a and c). The diffraction pattern indicates that only Ti and TiC has been observed in the sample.

The distribution of the TiC particles appeared uniform using the TEM analysis, but this technique is not appropriate to conclude about the process efficiency. However, the fact that the TiB whiskers are uniformly distributed, and the apparent uniformity observed during the TEM analysis, tends to confirm the efficiency of the mixing process to disperse TiC particles.

The mechanical properties of the materials have been measured using hardness measurement, because the size of the sample did not offer the possibility to use compression testing. The first values obtained were considerably higher than expected as shown on the Table 11.

Sample	Measured Hardness (H_v)	Calculated Yield Strength (From Hardness) (MPa)
Ti	650	1507
Ti – 10% TiC	870	2145

Table 11: Hardness measurements and calculated Yield strength for the Ti and Ti - TiC samples obtained by HDH hot pressing

The hardness results for the fabricated materials are considerably above the value for pure Ti obtained by ECAP (about 160 H_v). The mark made by the indentation during the hardness measurement on the material shows cracks at the angle of the square as represented on Figure 99.

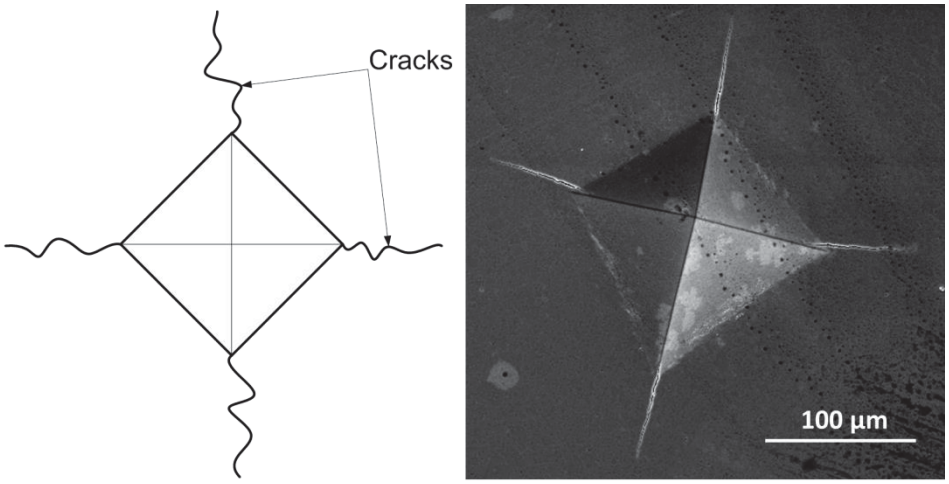

Figure 99: Squared hardness mark with the cracks along the angles

These cracks are usually observed when measuring the hardness of fragile materials, such as ceramics. Therefore, hot pressed Ti materials have a fragile mechanical behaviour. Chemical analysis of the samples revealed that the quantity of residual hydrogen in the composite is really high, without offering the possibility to dose it due to the fact it is not in the range of the apparatus capability. Even if no TiH_2 is observed by XRD analysis, the hydrogen can be in solid solution, inserted in the Ti lattice. Excess of hydrogen in a Ti structure have been shown to confer a fragile behaviour to the Ti mechanical properties. The presence of residual hydrogen can be explained by the use of primary vacuum during the hot pressing. Indeed, the vacuum being not sufficient and constrained environment of the sample does not provide sufficient conditions to allow a total dehydrogenation of the sample. Therefore, hydrogen diffuses in the Ti lattice resulting in a degradation of its properties. A way to prevent this phenomenon would be to do the hot pressing under secondary vacuum, which could allow a total dehydrogenation. However, the equipment used did not offer this possibility.

In conclusion, the different HDH densification processes used did not offer the possibility to obtain a usable sample in order to complete mechanical testing. The porosity remaining after pressureless sintering is a limiting factor in the capability of this method. With different equipment, increasing the pressure applied during the isostatic cold compaction could have prevented the formation of this porosity. The residual hydrogen remaining after hot pressing densification, which limit the mechanical properties of Ti, could be prevented using a better vacuum during the process. Nevertheless, different aspects of the techniques are encouraging. Indeed, the fact that the reinforcement can be correctly distributed within the matrix, with no interphase, and without adding

pollution to the sample is a benefit offers by the fact the mixing occurs during fragile-fragile ball milling. In addition, the grain size of the material can be controlled by controlling the size of the starting TiH_2 particles.

V. Conclusion

Microstructural and mechanical characterisations of the produced samples have shown the effect of the processes used on the properties of the composites.

Equal Channel Angular Pressing offers the possibility to obtain dense Ti material after only 2 passes at moderate temperature (600°C). EBSD analysis has shown that this process produced textured material when starting from powders. However, in order to produce Ti-TiC composite material using ECAP, a ball milling step to disperse the TiC reinforcements within the matrix is needed.

BM has been shown to be a critical step of the process. Indeed SEM and EDX analysis have shown that this step is responsible of contamination of the sample (stainless steel from the balls and jars). In addition, BM has en effect of the particle boundaries, increasing its thickness, making them harder to disperse during ECAP. Despite that, TiC has been observed with TEM analysis inside Ti material, presenting no interphase between the particle and the matrix. Nonetheless, this process has to be optimised, because it is not effective for a volume fraction of reinforcement higher than 1%.

The mechanical characterisations done on the samples produce via ECAP have shown that adding reinforcement particles has a negative effect on the ductility. Indeed, pure Ti produced using ECAP (with and without ball milling) have ductility higher than 20%, whereas composite material (Ti-1%TiC) have very few ductility (about 5%). This limitation ductility can be explained by the presence of TiC clusters and pollution that act like crack source. However, the yield strength of the composite samples is higher than the one of pure Ti (660 MPa to 380 MPa) showing the benefit of using reinforcement.

The ECAP process shows great possibilities in the fabrication of Ti based composite, at moderate temperature and in short time (few minutes).

Pressureless sintering using HDH have shown limitation in the possibility to obtain dense materials. Indeed, the cold compaction processed used in this work was not able to lead to a final sintered material that is dense. Consequently, no mechanical property was relevant to measured. However, XRD analysis has shown that the dehydrogenation is completed at 600°C, and is not blocked by the presence of reinforcement (TiC or TiB_2). It also shows that the transformation of TiB_2 powder into TiB whiskers occurs during the process at about 1000°C. EBSD and SEM analyses show that the whisker grows in random direction inside the matrix. In addition, these analyses show that the whiskers are uniformly distributed, meaning the ball mixing process is effective to disperse the reinforcement particle within the matrix powder for the HDH based processes. TEM analysis shows that there is no interphase between the TiB whiskers and the Ti matrix, or between the TiC particles and the Ti matrix. Ball mixing condition for HDH processes are optimised, distributing the reinforcement uniformly in the matrix, but pressureless sintering does not lead to a dense material.

Hot pressing using HDH has produced dense materials. XRD analysis has shown that the dehydrogenation phenomenon seemed complete after the densification. However, the mechanical analysis reveals the fragile behaviour of the produced material. This may be due to an important amount of residual hydrogen. Indeed, because of the use of primary vacuum in the hot pressing apparatus, the dehydrogenation was not effective, leaving residual hydrogen in the material, making

it fragile. However, a dense material can be obtained using hot pressing HDH at moderate temperature compares to the free sintering (800°C to 1400°C) and at a lower time (30 min to 4 hours).

Even if not successful, the HDH processes shows encouraging possibility in the fabrication of Ti based nano composites, at moderate temperature, and with a good distribution of the reinforcements within the matrix.

List of Figures and Tables

Bibliography

[BET2011] - V.I. Betekhtin, E.D. Tabachnikova, A.G. Kadomstev, M.V. Narykova, R. Lapovok, *Efect of Counterpressure during Equal-Channel Angular Pressing on Nanoporosity Formation in Ultrafine-Grained Copper,* Technical Physics Letters, 37, 8, pp.767-768, (2011)

[BOZ2007] - N. Bozzolo, N.Dewobroto, H.R. Wenk, F. Wagner, *Microstructure and microtexture of highly cold-rolled commercially pure titanium,* Journal of Materials Science, 42, pp.2405-2416, (2007)

[CAS2005] - V. de Castro, T. Leguey, A. Muñoz, M.A. Monge and R. Pareja, *Relationship between hardness and tensile tests in titanium reinforced with yttria nanoparticles,* Materials Science and Engineering A, 400–401, pp.345–348, (2005)

[CHE2010] - Y.J. Chen, Y.J. Li, J.C. Walmsley, S. Dumoulin, P.C. Skaret, H.J. Roven, *Microstructure evolution of commercially pure titanium during equal channel angular pressing,* Materials Science and Engineering A, 527, pp.789-796, (2010)

[CON2010] - R.J. Contieri, M. Zanotello, R. Caram, *Recrystallisation and grain growth in higly cold worked CP-Titanium,* Materials Science and Engineering A, 527, pp.3994-4000, (2010)

[DHA2012] - C. Dharmendra, K.P. Rao, Y.V.R.K. Prasad, N. Hort, K.U. Kainer, *Hot working mechanisms and texture development in Mg-3Sn-2Ca-0.4Al alloy,* Materials Chemistry and Physics, 136, 2–3, pp.1081–1091, (2012)

[EGE2001] - R.F. Egerton, Physical Principles of Electron Microscopy, An introduction to TEM, SEM and AEM, Ed Sringer Science, (2001)

[FOG2003] - J.B. Fogagnolo, F. Velasco, M.H. Robert, J.M. Torralba, *Effects of mechanical alloying on the morphology, microstructure, and properties of aluminium matrix composite powders,* Materials Science and Engineering A, 342, pp.131-143, (2003)

[GUB2003] - J. Gubicza, I.C. Dragomir, G. Ribarik, Y.T. Zhu, R. Valiev, T. Ungar, *Characterization of Microstructure of Severely Deformed Titanium by X-Ray Diffraction Profile Analysis,* Materials Science Forum, 414-415, pp.229-234, (2003)

[HYU2010] - C-Y. Hyun, J-H. Lee, H-K. Kim, *Microstructures and mechanical properties of ultrafine grained pure Ti produced by severe plastic deformation,* Research on Chemical Intermediates, 36, pp.629-638, (2010)

[MIR2003] - D. Miracle, S. Firstov, L. Kulak, M. Kuzmenko, O. Vasylyev, *Structure and Mechanical Properties of In-situ Discontinuously Reinforced Composites of Ti-TiB-System,* Materials Science Forum, 426-432, pp.4591-4596, (2003)

[POU2002] - J-L. Pouchou, L'analyse EBSD, Principes et applications, Ed. EDP Science, (2004)

[REF-FIG70]:

[BER1996] - E. Berg, G. Davik, T. Hegdahl, N.R. Gjerdet, *Hardness, Strenght, and Ductility of prefabricated titanium rods used in the manufacture of spark erosion crowns,* The journal of Prosthetic Dentistry, 75, 4, pp.419-425, (1996)

[CAS2005] - V. de Castro, T. Leguey, A. Muñoz, M.A. Monge and R. Pareja, *Relationship between hardness and tensile tests in titanium reinforced with yttria nanoparticles,* Materials Science and Engineering A, 400–401, pp.345–348, (2005)

[LUI2012] - E. Lui, PhD thesis, *Multiphase and Multiscale Al-Ti Alloys Consolidated by Severe Plastic Deformation,* Department of Mechanical Engineering, The University of Melbourne, (2012)

[PAV2008] – E.J. Pavlina, C.J. Van Tyne, *Correlation of Yield Strength and Tensile Strength with Hardness for Steels,* Journal of Materials Engineering anf Performances, 17, 6, pp.888-893, (2008)

[WHI2012] - D. Whittaker, *Powder processing, consolidation and metallurgy of titanium,* Powder Metallurgy, 55, 1, pp.6-10, (2012)

[XIR2009] - Y. Xirong, Z. Xicheng, F. Wenjie, *Deformed Microstructures and Mechanical Properties of CP-Ti by Multi-Pass ECAP at Room Temperature,* Rare Metal Materials and Engineering, 38, 6, pp.955-957, (2009)

[XU2012] - C. Xu, W-F. Zhu, *Comparison of microstructures and mechanical properties between forging and rolling processes for commercially pure titanium,* Transaction of nonferrous Metals Society of China, 22, pp.1939-1946, (2012)

[SED2011] - P. Seda, A.Jager, P. Lejcek, *Microstructure and Texture of Magnesium Single Crystals Processed by ECAP,* Materials Science Forum, 667-669, pp.355-360, (2001)

[SED2012] - P. Seda, A. Ostapovets, A.Jager, P. Lejcek, *Texture Evolution in Oriented Magnesium Single Crystals Processed by Equal channel Angular Pressing,* Philosophical Magazine, 92, 10, pp.1223-1237, (2012)

[UNG2005] - T. Ungar, G. Tichy, J. Gubicza, R.J. Hellmig, *Correlation between subgrains and coherently scattering domains,* Powder Diffraction, 20, 4, pp.367-375, (2005)

[XIA2010] - K. Xia, *Consolidation of Particles by Severe Plastic Deformation: Mechanism and Applications in Processing Bulk Ultrafine and Nanostructured Alloys and Composites,* Advanced Engineering Materials, 12, 8, pp.724-729, (2010)

[ZEN2009a] - Z. Zeng, Y. Zhang, S. Jonsson, *Microstructure and Texture Evolution of commercial pure Titanium deformed at elevated Temperatures,* Materials Science and Engineering A, 513-514, pp83-90, (2009)

[ZEN2009b] - Z. Zeng, S. Jonsson, H.J. Roven, *The effects of deformation conditions on microstructure and texture of commercially pure Ti,* Acta Materialia, 57, pp.5822-5833, (2009)

Conclusion and future work

Titanium (and its alloys) is a well-used material in various applications, from biomedical to aerospace. It is known to have good properties such as high strength, low density, good creep resistance at high temperature, chemically inert or good ductility. A way to improve Titanium is to increase its strength in order to make it competitive with the different steel currently used. This study shows the possibility to use powder metallurgy to fabricate titanium based composite in order to increase its mechanical properties.

The present work was focused on two types of reinforcement, *in-situ* TiB and *ex-situ* TiC, the have the potential to improve the mechanical properties of the titanium and have a good compatibility with the matrix. The reinforcement size used was in the nanometre range, in order to enhance the mechanical properties without affecting the ductility. To achieve the densification of the composites, two different powder metallurgy processes were used: Equal Channel Angular Pressing (ECAP) and hydrogenation/dehydrogenation sintering. Each process used has several parameters that have been adjusted during this work.

During the ECAP densification, the dispersion of the reinforcement particles within the matrix, occurred during ball milling step. Then the powder was process through the ECAP dies for a controlled number of pass. Different parameters, such as the ball milling time, number of pass, or amount of reinforcement has been adjusted.

During the hydrogenation/dehydrogenation processes (pressureless sintering and hot pressing), the initial composite powders prior densification were the same. The preparation of these powders, from the hydrogenation of the Ti sponge to the dispersion of the reinforcements, allowed controlling the particle size (via ball milling time) and the volume fraction of the reinforcement. Then, each process has its own parameters that have been optimised. The HDH pressureless sintering needed cold compaction prior the densification, and the working temperature and time was adjusted. The HDH hot pressing had its pressure applied, its time and working temperature adjusted.

The different parameters for the processes used were shown to have an influence on the final materials prepared. To anticipate the influence of the different parameters on the properties of the composite, a modelling work has been done.

The model has shown the possibility of improvement in mechanical properties of Ti based nanocomposites offers for the considered reinforcements by the investigated powder metallurgy processes. The theory shows that the different parameters that can be adjusted during the processes (grain size, reinforcement volume fraction, reinforcement nature, size and shape) have an influence on the material's properties and can be optimised. Using reinforcements in the nanometre range allow increasing considerably the yield strength of the composite at very low volume fraction. In this simulation, the yield strength goes from 545 MPa for unreinforced Ti with a grain size of 1 µm to 632 MPa when adding 1% of TiC particles of 40 nm. Using reinforcement with high aspect ratio has an impact on the yield strength and the Young's modulus of the composite materials.

The characterisation done on the produced materials have shown the limitation of the processes used. For the ECAP process, the limitation comes from the ball milling step, to distribute the reinforcement particles within the matrix particles. This process was not efficient for high volume fraction (higher than 1%) and induced contamination to the ball milled samples. For the HDH pressureless sintering, residual porosity was observed on the final material. For the HDH hot pressing, the process did not eliminate all the hydrogen and consequently, the final material has presented a fragile behaviour. Despite that, encouraging results has been observed during the characterisations. The sample produced using ECAP processing does not show any interphase at the TiC/Ti boundary.

The mechanical characterisations done on the ECAP produced sample have shown encouraging results that are in accord with the modelling calculations. Indeed, considering a grain size of 3.5 µm (as measured on the ECAPed samples) and a volume fraction of TiC (40 nm) at 1%, the calculated yield strength is equal to 706 MPa. The measured yield strength for the Ti – 1% TiC ECAPed for 2 and 20 passes was respectively 650 MPa and 670 MPa. Even if the measurements are not sufficient to conclude on the veracity of the model, the fact that the values are in accord is an observation that the model is not out of the range. The characterisations also have shown the possibility of ECAP process to texture the material, using powder metallurgy.

Analysis of the HDH produced material has shown the possibility of this process to uniformly disperse reinforcement without contaminating the composites. Both *in-situ* and *ex-situ* reinforcements are possible to obtain using HDH processes, and no interphase (clean interfaces) has been observed between the reinforcement and the matrix. The grain size of the final material was linked to the TiH_2 size powder (10 times bigger for pressureless sintering and 2 times bigger for hot pressing).

The different processes used during this work have their limitations and were not successful to produce a satisfying sample; nevertheless, encouraging observation has been done in regards of the potential of such techniques, in future works:

- Optimising the green density of the HDH pressureless sintering by using a high pressure cold press would lead to a fully dense composite that could show significant improvement in mechanical properties.
- Using a hot pressing apparatus working under high vacuum could allow obtaining Ti composite with a very low amount of residual hydrogen, and interesting mechanical properties.
- Optimising the ball milling step during the ECAP process, by working in a non-polluting medium (liquid medium or nacre balls and jars) under reducing atmosphere would allow a better dispersion of the reinforcement within the matrix without contaminating the sample or increasing the size of the oxide layer, leading to a well dispersed composite powder.
- Another idea would be to combine the HDH and the ECAP processes. Indeed, using the ball mixing of the HDH process to disperse the reinforcements offers uniform results without contamination. And the ECAP densification process produces fully dense material with the possibility of texturing and refining the grains. The TiH_2 based composite powder should be dehydrogenated prior ECAP densification. This could lead to a uniformly distributed composite with adjustable grain size and texture.

Titre : Elaboration de matériaux composites à matrice de Titane et à nano-renforts TiC et TiB par différents procédés de métallurgie des poudres : frittage par hydruration/déshydruration et densification par déformation plastique sévère (Equal Channel Angular Pressing : ECAP)

Résumé : Les composites à matrice Titane avec des renforts nanométriques présente des améliorations intéressantes quant aux propriétés mécaniques, sans affecter la ductilité du matériau. Ce travail de thèse se concentre sur l'élaboration et la caractérisation de matériaux composites de Titane obtenus par deux différents procédés de métallurgie des poudres : La densification par déformation plastique sévère utilisant l'ECAP (Equal Channel Angular Pressing) et les procédés de frittage par hydrogénation/déshydrogénation (HDH). L'ECAP est un procédé de densification rapide utilisant la déformation plastique des matériaux, se faisant à relativement basse température. Les procédés HDH utilisent la déshydrogénation du titane comme un levier sur les mécanismes de frittage. Les différents nano-renforts utilisés dans ces travaux sont les particules sphériques de TiC et les aiguilles de TiB. Cette étude montre l'influence de la nature et de la forme des renforts, ainsi que du procédé de métallurgie des poudres utilisé, sur les propriétés et la microstructure final des matériaux denses.

Mots clés : Déformation plastique sévère, ECAP, Hydruration, Déshydruration, Composites, Titane, Nano-renforts, EBSD, Microstructures

---

Title: Processing of titanium-based composite materials with nanosized TiC and TiB reinforcements using different powder metallurgy processes: hydrogenation/dehydrogenation sintering, and severe plastic deformation (Equal Channel Angular Pressing: ECAP)

Abstract: Titanium based composites using nano-sized reinforcements are good candidates for the improvement in mechanical properties without affecting ductility. This study is dedicated to fabrication and characterisation of Ti-based composites using two different powder metallurgy processes: Densification using severe plastic deformation via Equal Channel Angular Pressing (ECAP) and Hydrogenation/Dehydrogenation (HDH) sintering processes (pressureless sintering and hot pressing).ECAP is a fast process based on a severe plastic deformation of material at relatively low temperature. HDH processes use the dehydrogenation of Ti as a leverage of the sintering. The different nanosized reinforcements used in this study are the TiC spherical particles and the whisker shaped TiB. This study shows the influence of either the reinforcement nature and type, and the powder metallurgy processes used, on the final microstructure and properties of the dense materials.

Keywords: Severe Plastic Deformation, ECAP, Hydrogenation, Dehydrogenation, Composites, Titanium, Nanoreinforcements, EBSD, Microstructures

---

Unité de recherche

ICMCB, UPR 9048, 87 av. Du Dr. Schweitzer, 33608 PESSAC CEDEX